Nonperturbative Studies of Quantum Field Theories on Noncommutative Spaces

DISSERTATION

zur Erlangung des akademischen Grades
doctor rerum naturalium
(Dr. rer. nat.)
im Fach Physik

eingereicht an der
Mathematisch-Naturwissenschaftlichen Fakultät I
Humboldt-Universität zu Berlin

von
Herr Dipl.-Phys. Jan Volkholz
geboren in Schwerin/Meckl.

Präsident der Humboldt-Universität zu Berlin:
Prof. Dr. Dr. h.c. Christoph Markschies

Dekan der Mathematisch-Naturwissenschaftlichen Fakultät I:
Prof. Dr. Christian Limberg

Gutachter:

1. Prof. Dr. M. Müller-Preußker
2. Prof. Dr. D. O'Connor
3. Dr. H. Dorn

eingereicht am:	26. März 2007
Tag der mündlichen Prüfung:	16. November 2007

Abstract

This work deals with three quantum field theories on spaces with noncommuting position operators. Noncommutative models occur in the study of string theories and quantum gravity. They usually elude treatment beyond the perturbative level. Due to the technique of dimensional reduction, however, we are able to investigate these theories nonperturbatively. This entails translating the action functionals into a matrix language, which is suitable for numerical simulations.

First we explore the $\lambda\phi^4$ model on a noncommutative plane. We investigate the continuum limit at fixed noncommutativity, which is known as the double scaling limit. Here we focus especially on the fate of the striped phase, a phase peculiar to the noncommutative version of the regularized $\lambda\phi^4$ model. We find no evidence for its existence in the double scaling limit.

Next we examine the U(1) gauge theory on a four-dimensional spacetime, where two spatial directions are noncommutative. We examine the phase structure and find a new phase with a spontaneously broken translation symmetry. In addition we demonstrate the existence of a finite double scaling limit which confirms the renormalizability of the theory. Furthermore we investigate the dispersion relation of the photon. In the weak coupling phase our results are consistent with an infrared instability predicted by perturbation theory. If the translational symmetry is broken, however, we find a dispersion relation corresponding to a massless particle.

Finally, we investigate a supersymmetric theory on the fuzzy sphere, which features scalar neutral bosons and Majorana fermions. The supersymmetry is exact in the limit of infinitely large matrices. We investigate the phase structure of the model and find three distinct phases.

Summarizing, we study noncommutative field theories beyond perturbation theory. Moreover, we simulate a supersymmetric theory on the fuzzy sphere, which might provide an alternative to attempted lattice formulations.

Keywords:
noncommutative geometry, quantum field theories, lattice gauge theories, matrix models

Zusammenfassung

Diese Arbeit befasst sich mit Quantenfeldtheorien auf nicht-kommutativen Räumen. Nicht-kommutative Räume zeichnen sich durch nicht-vertauschende Ortsoperatoren aus. Solche Modelle treten im Zusammenhang mit der Stringtheorie und mit der Quantengravitation auf. Ihre nicht-störungstheoretische Behandlung ist üblicherweise schwierig. Hier untersuchen wir jedoch drei nicht-kommutative Quantenfeldtheorien nicht-perturbativ, indem wir die Wirkungsfunktionale in eine äquivalente Matrixformulierung übersetzen. Dies geschieht mit Hilfe der Methode der dimensionellen Reduktion. In der Matrixdarstellung kann die jeweilige Theorie dann numerisch behandelt werden.

Als erstes betrachten wir ein regularisiertes $\lambda\phi^4$ Modell auf der nicht-kommutativen Ebene und untersuchen den Kontinuumslimes bei festgehaltener Nicht-Kommutativität. Dies wird auch als Doppelskalierungslimes bezeichnet. Insbesondere untersuchen wir das Verhalten der gestreiften Phase. Wir finden keinerlei Hinweise auf die Existenz dieser Phase im Doppelskalierungslimes.

Im Anschluss daran betrachten wir eine vier-dimensionale U(1) Eichtheorie. Hierbei sind zwei der räumlichen Richtungen nicht-kommutativ. Wir untersuchen sowohl die Phasenstruktur als auch den Doppelskalierungslimes. Es stellt sich heraus, dass neben den Phasen starker und schwacher Kopplung eine weitere Phase existiert, in welcher die Translationssymmetrie spontan gebrochen ist (die *gebrochene Phase*). Dann bestätigen wir die Existenz eines endlichen Doppelskalierungslimes, und damit die Renormierbarkeit der Theorie. Weiterhin untersuchen wir die Dispersionsrelation des Photons. In der Phase mit schwacher Kopplung stimmen unsere Ergebnisse mit störungstheoretischen Berechnungen überein, die eine Infrarot-Instabilität vorhersagen. Andererseits finden wir in der gebrochenen Phase die Dispersionsrelation, die einem masselosen Teilchen entspricht.

Als dritte Theorie betrachten wir ein einfaches, in seiner Kontinuumsform supersymmetrisches Modell, welches auf der „Fuzzy Sphere“ formuliert wird. Hier wechselwirken neutrale skalare Bosonen mit Majorana-Fermionen. Wir untersuchen die Phasenstruktur dieses Modells, wobei wir drei unterschiedliche Phasen finden.

Insgesamt untersucht diese Arbeit nicht-kommutative Quantenfeldtheorien nicht-störungstheoretisch. Weiterhin simulieren wir eine supersymmetrische Theorie auf der „Fuzzy Sphere“, die in dieser Hinsicht eine Alternative zu den Versuchen einer Gitterformulierung darstellt.

Schlagwörter:
Nichtkommutative Geometrie, Quantenfeldtheorien, Gittereichtheorien, Matrixmodelle

Contents

Chapter 1

Introduction

One of the earliest subjects of human thought was the study of forms and figures. This fascination eventually led to the rise of the field of geometry, still a vibrant and intriguing part of modern mathematics.

An early culmination in this endeavor were Euclid's (325BC?-265BC?) "Elements" Euclid [1956]. Euclid and his predecessors built the entire planar geometry from a set of only five axioms. From these axioms he derived in a logically sound way the geometry of circles, lines and polygons. His version of geometry reigned supreme for the next two millennia. It is the canonical curriculum in schools to this day, for it is based on intuitively comprehensible and familiar concepts.

The by then dogma of Euclidean geometry was shattered by B. Riemann (1826-1866) in 1854 Riemann [1854]. He eliminated the "parallel axiom" from 2000 years before[1] and rid geometry of its shackles. Through this he opened the door to the rich world of Riemannian manifolds. The prize for the newly gained freedom, however, was a seeming alienation from the familiar world around us. In the early 20th century, however, it became apparent that the abstract geometry developed by Riemann was necessary to describe the world on a large scale Einstein [1915].

The last century gave birth to yet another twist in the evolution of geometry, *noncommutative (NC) geometry*. Like in quantum mechanics the points making up the NC manifold are obtained as eigenvalues from position operators which act on states of a Hilbert space. In NC geometries, however, these position operators do not commute.

The first physicist to consider a NC space was probably W. Heisenberg. When he uncovered the uncertainty relation, embodied by the canonical op-

[1]The history of overcoming the "parallel axiom" is actually much more complicated and also involves earlier work by e.g. G. G. Saccheri, C. F. Gauß, J. Bolyai and N. I. Lobachevski. See for example Ref. Struik [1987].

erator algebra[2]

$$[\hat{x}^\mu, \hat{p}_\nu] = \mathrm{i}\,\delta^\mu_\nu,$$

he discovered that the quantum mechanical phase space is noncommutative. However, this was merely considered a remarkable side product, and it was not deemed worth further study in its own right. In any case, a remarkable connection between NC spaces and physics emerged.

Early attempts to formulate quantum field theories (QFTs) were plagued by a multitude of problems. Not the least among them was the appearance of singularities. Here H. S. Snyder used the scheme introduced before by Heisenberg and tried to apply the NC paradigm to spatial coordinates. In this way he hoped to cure the apparently fatal infinities. This hope was founded in the fact that NC coordinates induce a natural cutoff at large momenta Snyder [1947a,b], Yang [1947]. In light of the success of renormalization schemes, though, attempts to further develop NC geometries and incorporate them into physics were mostly abandoned.

This period of slumber ceased in the 1980s when interest in NC geometries was rising again. During this period a sound and rigid mathematical foundation was built. This formalization was generally led by mathematicians, and in particular by A. Connes Connes [1994].

In physics, interest in noncommutative quantum field theories (NCQFTs) reemerged, when the low energy limit of some string theoretic models turned out to be equivalent to NC field theories Veneziano [1986], Gross and Mende [1988], Amati et al. [1989]. Since strings are not point-like objects, string theories are inherently nonlocal, just like NC geometries. NC spaces are also used to investigate different formulations of gravity Connes [1986], Chamsedinne et al. [1993], Landi and Rovelli [1997].

In this work, however, we are investigating NCQFTs in their own right. We employ numerical methods in order to study NCQFTs nonperturbatively. The basics, on which our tools and techniques are founded, will be introduced in Chapter 2.

In particular we will introduce basic features and concepts of NC spacetimes. For technical reasons we will only consider manifolds of even dimensionality. Then we will develop the machinery to handle scalar fields on real NC spaces $\mathbb{R}^D_{\mathrm{NC}}$ as well as on NC tori $\mathbb{T}^D_{\mathrm{NC}}$. We will especially rely on Weyl bases and the star product. Combining these instruments with the Morita equivalence will enable us to use the technique of dimensional reduction. This will allow us to rewrite NCQFTs in the language of matrices, which is

[2] We use natural units $\hbar = c = 1$.

suitable for numerical simulations. We also discuss UV/IR mixing, a feature typical for NCQFTs.

Furthermore we will review the foundations for dealing with fields on a fuzzy sphere. The fuzzy sphere is yet another NC space. It introduces noncommutativity by identifying the position operators with the angular momentum operators. Chapter 2 concludes with a short discussion of experimental data related to a possible noncommutativity in our universe. The bulk of these data stems from astronomical observations and collider experiments.

In Chapter 3 we examine a NC $\lambda\phi^4$ QFT of neutral scalar particles on a plane. First we review the phase structure of the discretized theory, which features three distinct phases, one more than its commutative counterpart. This additional phase is the so-called *striped phase*. Here the translational symmetry is spontaneously broken and field patterns emerge even in the ground state. Then we investigate the *double scaling limit (DSL)*. This is a simultaneous continuum/large volume limit at fixed noncommutativity. We focus especially on the fate of the striped phase in the DSL.

In Chapter 4 we examine the NC U(1) gauge theory. This theory is put on a four-dimensional spacetime, where two spatial directions are noncommutative. This choice was mandated by possible problems, among them a spurious unitarity due to a noncommutative time. We then examine the phase structure of the theory. We find, besides the strong and the weak coupling phase, a new phase, which we denote as the *broken phase*. It is characterized by a spontaneously broken translational symmetry. Subsequently the DSL of this model is investigated. Then results from one-loop perturbative calculations are succinctly quoted. These results hint at an IR instability of the pure U(1) NC gauge theory in the weak coupling phase. We investigate these issues nonperturbatively and gain new insights in this regard.

Chapter 5 deals with a field theory on the fuzzy sphere. The characteristic trait of this theory is its supersymmetry (SUSY). The SUSY model will again be formulated as a matrix model. We remark, however, that this formulation is only supersymmetric in the limit of infinitely large matrices. The bosons are neutral scalars, while the fermions are of Majorana type. In Chapter 5 we present a first investigation of this model's phase structure.

In the final Chapter 6 we draw our conclusions.

In the appendices we elaborate on a few technicalities.

Appendix A shows how NC coordinates can effectively result from an external background field. This is demonstrated with the example of a charged particle in a strong magnetic field.

Appendix B describes technical tools for the algorithm used for simulating NC quantum electrodynamics (QED) in Chapter 4, which speed up

the simulations considerably. Especially the algorithm for coping with the contributions from Wilson loops lying in both the NC and the commutative directions is not straightforward.

Finally Appendix C surveys polarization tensors. These are the matrix equivalents to the spherical harmonics and form a convenient basis for handling fields on the fuzzy sphere. We review basic properties of polarization tensors as well as their explicit formulation. Also the formulation of the SU(2) angular momentum operators, as used in the simulations, is given explicitly.

Chapter 2

Noncommutative Quantum Field Theories

In this chapter we are briefly going to introduce *noncommutative field theories.* Much more detailed reviews are available, such as Refs. Barbón [2001], Douglas and Nekrasov [2001], Szabo [2003].

The term "noncommutative (quantum) field theory" refers to a (quantum) field theory which has been put onto a manifold endowed with a noncommutative geometry. Analogous to quantum mechanics (QM), the real number coordinates x^μ are replaced by Hermitian position operators $\hat{x}^\mu$. Contrary to the usual QM scenario, however, the $\hat{x}^\mu$ do not commute,

$$[\hat{x}^\mu, \hat{x}^\nu] = \mathrm{i}\,\Theta^{\mu\nu}(\hat{x})\,. \tag{2.1}$$

Θ is the real and antisymmetric *NC tensor.* It has the dimension

$$[\Theta^{\mu\nu}] = \text{length}^2. \tag{2.2}$$

Because of relation (2.1) the concept of *points* is discarded. Accordingly, NC geometries are sometimes also called "pointless geometries". Solid mathematical foundations of NC geometries were laid in the 1980s. We refer to Refs. Connes [1994], Connes and Rieffel [1987], Madore [1999] for further details.

There are many possibilities to choose $\Theta(\hat{x})$ in Eq. (2.1). The elements $\Theta^{\mu\nu}(\hat{x})$ can be thought of as "structure functions"[1] of an algebra $\mathcal{A}$. This algebra $\mathcal{A}$ is defined through its generators $\hat{x}^\mu$, and its elements are functions $f(\hat{x}^\mu)$ satisfying certain constraints. Setting $\Theta^{\mu\nu} = 0$ recovers the commutative geometry.

In this work we will focus on three types of NC spaces:

[1] They are an analogue to the structure constants of Lie groups.

- the two-dimensional Euclidean space $\mathbb{R}^2_{\mathrm{NC}}$,
- the two-dimensional torus $\mathbb{T}^2_{\mathrm{NC}}$ and
- the two-dimensional *fuzzy sphere* $\mathbb{S}^2_{\mathrm{F}}$,

while also referring to the general D-dimensional case (D even).

In general, the manifolds $\mathbb{R}^D_{\mathrm{NC}}$ and $\mathbb{T}^D_{\mathrm{NC}}$ are obtained by setting $\Theta^{\mu\nu}(\hat{x}) = \Theta^{\mu\nu} \in \mathbb{R}$, which simplifies Eq. (2.1) to

$$[\hat{x}^\mu, \hat{x}^\nu] = \mathrm{i}\,\Theta^{\mu\nu}, \qquad \mu, \nu \in 1 \dots D. \tag{2.3}$$

If the spectrum of $\hat{x}^\mu$, $\mu \in 1 \dots D$, covers the real line for each μ, we are describing a $\mathbb{R}^D_{\mathrm{NC}}$ space. If the D spectra are periodic, the NC torus $\mathbb{T}^D_{\mathrm{NC}}$ is described instead.

The two-dimensional fuzzy sphere $\mathbb{S}^2_{\mathrm{F}}$ of radius R is the solution of

$$\hat{x}_1^2 + \hat{x}_2^2 + \hat{x}_3^2 = R^2\,\hat{\mathbb{1}} \tag{2.4}$$

in $\mathbb{R}^3$. $\hat{\mathbb{1}}$ here refers to the identity operator. With the choice

$$\hat{x}_\mu = \frac{R}{\sqrt{s\,(s+1)}}\,\hat{L}_\mu, \qquad \mu = 1 \dots 3, \tag{2.5}$$

where the $\hat{L}_\mu$ are the three SU(2) angular momentum operators in the spin s representation, Eq. (2.1) turns into

$$[\hat{x}_\mu, \hat{x}_\nu] = \mathrm{i}\,\frac{R}{\sqrt{s\,(s+1)}}\,\epsilon_{\mu\nu\rho}\,\hat{x}_\rho. \tag{2.6}$$

As long as the spin s representations are finite, the emerging field theory is captured by a discrete set of variables. We can recover a QFT with infinitely many degrees of freedom only in the $s \to \infty$ limit.

2.1 Classical Fields on the NC Plane

Position operators, eigenvalues and commutation relations

As stated before, on a $\mathbb{R}^D_{\mathrm{NC}}$ space the operator commutation relation is given by Eq. (2.3). To start with we restrain ourselves to classical scalar fields ϕ on a 2D plane. The following arguments hold for fields $\phi \in \mathbb{R}$ and $\phi \in \mathbb{C}$.

In the two-dimensional case the NC tensor simplifies to

$$\Theta^{12} = -\Theta^{21} = \theta. \tag{2.7}$$

This way we have encoded the noncommutativity of the plane in a single parameter θ and the commutation relation is

$$\left[\hat{x}^1, \hat{x}^2\right] = \mathrm{i}\,\theta. \tag{2.8}$$

The NC plane is also denoted as the *Moyal plane.*

The eigenvalues x^μ of the position operator $\hat{x}^\mu$ are regarded as the coordinates parametrizing the spacetime. These eigenvalues arise from the application of the position operators $\hat{x}^\mu$ onto states living in a Hilbert space $\mathcal{H}_{\mathrm{NC}}$. The space $\mathcal{H}_{\mathrm{NC}}$ is the "passive arena", on which the dynamics unfold.

As hinted earlier, the relation (2.3) introduces nonlocality into NC manifolds on length scales of order $\mathcal{O}(\sqrt{\theta})$. Equivalent to the minimal cells in QM phase space, there are minimal areas in position space. The coordinate uncertainties obey

$$\Delta x^1\,\Delta x^2 \geq \frac{1}{2}\,|\theta|\,. \tag{2.9}$$

The length scale $\sqrt{\theta}$ provides a physically interesting cutoff, since below this scale locality and possibly Lorentz invariance are broken. This property provides the most remarkable deviation in phenomenology from commutative QFTs, because it should result in deformed dispersion relations at low momenta. This distorted dispersion relation is a quantum effect resulting from the UV/IR mixing to be described in Section 2.3.

Let us now investigate a simple example in the regular QM operator formalism. We consider the wave function $\psi(x)$, which is an element of the Schwartz space of square integrable function $\mathrm{L}^2(\mathbb{R})$. This is synonymous to decreasing sufficiently fast at infinity, meaning that convergence and invertibility of the Fourier transform of $\psi(x)$ are guaranteed. In this example $\mathcal{H}_{\mathrm{NC}}$ is parametrized by a real line $x \in \mathbb{R}$.

Considering

$$\left[\hat{x}^1, \hat{p}_1\right] = \mathrm{i}, \tag{2.10}$$

we see that the choice $\hat{x}^2 = \theta\,\hat{p}_1$ yields the desired commutation relation

$$\left[\hat{x}^1, \hat{x}^2\right] = \mathrm{i}\,\theta. \tag{2.11}$$

Consequently we can write

$$\hat{x}^1\,\psi(x) = x\,\psi(x) \quad \text{and} \quad \hat{x}^2\,\psi(x) = -\mathrm{i}\,\theta\,\psi'(x)\,. \tag{2.12}$$

This results in the operator identity

$$\mathrm{e}^{\mathrm{i}p\hat{x}^2} f\left(\hat{x}^1\right) = f\left(\hat{x}^1 + p\theta\right) \mathrm{e}^{\mathrm{i}p\hat{x}^2}, \tag{2.13}$$

which means that the $\hat{x}^2$ operator generates translations in the eigenvalues of $\hat{x}^1$.

At this point it is convenient to determine the plane wave composition rule, and for this purpose we return to the general D-dimensional space. Application of the Baker-Campbell-Hausdorff formula[2]

$$\exp\Big(\varepsilon\hat{A}\Big)\,\exp\Big(\varepsilon\hat{B}\Big) = \exp\bigg(\varepsilon(\hat{A}+\hat{B}) + \frac{\varepsilon^2}{2}[\hat{A},\hat{B}] + \frac{\varepsilon^3}{12}\Big([\hat{A},[\hat{A},\hat{B}]] + [\hat{B},[\hat{B},\hat{A}]]\Big) + \mathcal{O}\Big(\varepsilon^4\Big)\bigg) \tag{2.14}$$

is much simplified in our case, since $[\hat{x}^\mu,\hat{x}^\nu] \in \mathbb{C}$. This renders all higher order commutators $[\hat{x}^\sigma,[\ldots[\hat{x}^\mu,\hat{x}^\nu]]]$ equal to zero. Applying this leads to

$$\mathrm{e}^{\mathrm{i}\,p_\mu\hat{x}^\mu}\mathrm{e}^{\mathrm{i}\,q_\nu\hat{x}^\nu} = \mathrm{e}^{-\frac{\mathrm{i}}{2}p\wedge q}\,\mathrm{e}^{\mathrm{i}(p_\mu+q_\mu)\hat{x}^\mu}, \tag{2.15}$$

where we have introduced the notation

$$p\wedge q \equiv p_\mu\Theta^{\mu\nu}q_\nu. \tag{2.16}$$

Weyl basis, Weyl mapping and Weyl operators

The next step in "taming" the NC world consists of finding a map between a field $\phi(x)$ defined over commuting coordinates $x=(x_1,x_2,\ldots,x_D)$ and its assigned *Weyl operator* $\hat{\mathcal{W}}[\phi]$, which is an expression in $\hat{x}^1,\hat{x}^2,\ldots,\hat{x}^D$. This is known as the *Weyl mapping*. Because $\hat{x}^\mu$ and x^μ are fundamentally different objects with respect to multiplication, we expect

$$\hat{\mathcal{W}}[\phi\cdot\varphi] \neq \hat{\mathcal{W}}[\phi]\,\hat{\mathcal{W}}[\varphi]\,. \tag{2.17}$$

Once this Weyl map is established, we will be able to work much more intuitively on NC spaces.

Basically, we are going to expand $\hat{\mathcal{W}}[\phi]$ in a basis, which is convenient to work with. Just like one can choose a basis of generators $\{T^i\}$ to span a Lie algebra, we look for a basis that spans the operators $\hat{\mathcal{W}}[\phi]$ acting on $\mathcal{H}_{\mathrm{NC}}$. Because the spectrum of the operators $\hat{x}^\mu$ is continuous, we require an infinite momentum space. Guided by the Fourier transformations

$$\phi(x) = \int\frac{\mathrm{d}^Dk}{(2\pi)^D}\,\tilde{\phi}(k)\,\mathrm{e}^{\mathrm{i}k_\mu x^\mu} \quad\text{and}\quad \tilde{\phi}(k) = \int\mathrm{d}^Dx\,\phi(x)\,\mathrm{e}^{-\mathrm{i}k_\mu x^\mu}, \tag{2.18}$$

[2] An exponential of an operator $\hat{A}$ is to be understood in terms of its power series, $\mathrm{e}^{\hat{A}} = \sum_{n=0}^{\infty}\frac{\hat{A}^n}{n!}$.

we expand $\hat{\mathcal{W}}[\phi]$ in the plane wave operator basis $\exp(\mathrm{i}\, k_\mu \hat{x}^\mu)$, while $\tilde{\phi}(k)$ are the weights. Thus we write

$$\hat{\mathcal{W}}[\phi] = \int \frac{\mathrm{d}^D k}{(2\pi)^D}\, \tilde{\phi}(k)\; \mathrm{e}^{\mathrm{i} k_\mu \hat{x}^\mu}, \tag{2.19}$$

which yields

$$\hat{\mathcal{W}}[\phi] = \int \mathrm{d}^D x\, \phi(x)\; \hat{T}_{\mathbb{R}}(x)\,. \tag{2.20}$$

Here we have used the mixed basis

$$\hat{T}_{\mathbb{R}}(x) = \int \frac{\mathrm{d}^D k}{(2\pi)^D}\, \mathrm{e}^{\mathrm{i} k_\mu \hat{x}^\mu} \mathrm{e}^{-\mathrm{i} k_\mu x^\mu} \tag{2.21}$$

spanning all $\hat{\mathcal{W}}[\phi]$, whereas $\phi(x)$ gives the components ("coordinates") of $\hat{\mathcal{W}}[\phi]$. The set of Hermitian operators $\hat{T}_{\mathbb{R}}(x)$ is called the *Weyl basis*.

The utility of the Weyl mapping stems from the fact that it associates the plane wave function $\exp(\mathrm{i}px)$ with the plane wave operator $\exp(\mathrm{i}p\hat{x})$,

$$\hat{\mathcal{W}}\left[\mathrm{e}^{\mathrm{i} p_\mu x^\mu}\right] = \mathrm{e}^{\mathrm{i} p_\mu \hat{x}^\mu}. \tag{2.22}$$

This mapping can be used to derive the relation

$$\begin{aligned}
&\hat{T}_{\mathbb{R}}(x)\; \hat{T}_{\mathbb{R}}(y) \\
&\quad = \int\int \frac{\mathrm{d}^D k}{(2\pi)^D} \frac{\mathrm{d}^D p}{(2\pi)^D} \int \mathrm{d}^D z\, \mathrm{e}^{\mathrm{i}(k+p)_\mu z^\mu}\; \hat{T}_{\mathbb{R}}(z)\; \mathrm{e}^{-\frac{\mathrm{i}}{2} k \wedge p}\, \mathrm{e}^{-\mathrm{i} k_\mu x^\mu - \mathrm{i} p_\nu y^\nu} \\
&\quad = \frac{1}{\pi^D |\det(\Theta)|} \int \mathrm{d}^D z\, \hat{T}_{\mathbb{R}}(z)\; \mathrm{e}^{2\mathrm{i}(\Theta^{-1})_{\mu\nu}(x^\mu - z^\mu)(y^\nu - z^\nu)}.
\end{aligned} \tag{2.23}$$

This expression requires the invertibility of Θ, which is only possible if we demand D to be even. Thus we will implicitly assume that D is even throughout this work.

In the commutative limit $\Theta \to 0$ the Weyl map simplifies to

$$\lim_{\Theta \to 0} \hat{\mathcal{W}}[\phi] = \phi(\hat{x})\,. \tag{2.24}$$

Integration and derivatives in the Weyl formalism

Some of the most common operations performed on functions defined over $\mathbb{R}^D$ are integrations and derivatives. Therefore it is natural to look for their respective equivalents in the Weyl formalism.

Introducing the defining properties

$$[\hat{\partial}_\mu, \hat{x}^\nu] \equiv \delta_\mu^\nu \quad \text{and} \quad [\hat{\partial}_\mu, \hat{\partial}_\nu] \equiv 0 \tag{2.25}$$

for the antihermitian derivative operator $\hat{\partial}_\mu$, it is easy to show that

$$[\hat{\partial}_\nu,\, \mathrm{e}^{\mathrm{i}k_\mu \hat{x}^\mu}] = \mathrm{i}k_\nu \mathrm{e}^{\mathrm{i}k_\mu \hat{x}^\mu}. \tag{2.26}$$

The operator $\hat{\partial}_\mu$ only acts on $\hat{x}^\mu$, while ∂_μ acts only on x^μ. Therefore we obtain

$$[\hat{\partial}_\mu, \hat{T}_{\mathbb{R}}(x)] = -\partial_\mu \hat{T}_{\mathbb{R}}(x)\,. \tag{2.27}$$

If this is now integrated by parts, we arrive at

$$\left[\hat{\partial}_\mu, \hat{\mathcal{W}}[\phi]\right] = \int \mathrm{d}^D x\ (\partial_\mu \phi(x))\, \hat{T}_{\mathbb{R}}(x) = \hat{\mathcal{W}}[\partial_\mu \phi]\,, \tag{2.28}$$

thus providing a sensible concept of derivatives on NC spaces.

Another property of the derivative operators $\hat{\partial}_\mu$ is that they generate translations in $\hat{T}_{\mathbb{R}}(x)$,

$$\mathrm{e}^{v^\mu \hat{\partial}_\mu}\, \hat{T}_{\mathbb{R}}(x)\, \mathrm{e}^{-v^\nu \hat{\partial}_\nu} = \hat{T}_{\mathbb{R}}(x+v)\,. \tag{2.29}$$

This is a consequence of Eq. (2.27) and it allows for the definition of an operator trace $\mathrm{Tr}_{\mathrm{Op}}\big(\hat{\mathcal{W}}[\phi]\big)$. Because of Eq. (2.29) the trace $\mathrm{Tr}_{\mathrm{Op}}\big(\hat{T}_{\mathbb{R}}(x)\big)$ must be independent of x. We can therefore set the normalization to

$$\mathrm{Tr}_{\mathrm{Op}}\big(\hat{T}_{\mathbb{R}}(x)\big) \equiv 1. \tag{2.30}$$

Combining this convention with definition (2.20), we arrive at

$$\mathrm{Tr}_{\mathrm{Op}}\big(\hat{\mathcal{W}}[\phi]\big) = \int \mathrm{d}^D x\, \phi(x)\,. \tag{2.31}$$

From this reasoning we can also infer another useful trace identity given by

$$\mathrm{Tr}_{\mathrm{Op}}\big(\hat{T}_{\mathbb{R}}(x)\, \hat{T}_{\mathbb{R}}(y)\big) = \delta(x-y)\,. \tag{2.32}$$

The relation (2.20) provides a map from the space of ordinary functions to the operator algebra. With the trace we can state the inverse transformation as

$$\phi(x) = \mathrm{Tr}_{\mathrm{Op}}\big(\hat{\mathcal{W}}[\phi]\, \hat{T}_{\mathbb{R}}(x)\big)\,. \tag{2.33}$$

This completes the construction of the bijective Weyl mapping

$$\text{function } \phi(x) \quad \longleftrightarrow \quad \text{operator } \hat{\mathcal{W}}[\phi]\,. \tag{2.34}$$

The star product

We now return to the multiplication problem from Eq. (2.17). In order to tackle this problem we adapt the notation of the star product[3]

$$\phi(x) \star \varphi(x)\,. \tag{2.35}$$

The defining property of this product is the relation

$$\hat{\mathcal{W}}[\phi]\,\hat{\mathcal{W}}[\varphi] = \hat{\mathcal{W}}[\phi \star \varphi]\,. \tag{2.36}$$

The star product is, just like the Weyl operators, noncommutative, but associative. From the Weyl plane wave map (2.22) one immediately obtains the star product of two plane waves

$$\mathrm{e}^{\mathrm{i}\,p_\mu x^\mu} \star \mathrm{e}^{\mathrm{i}\,q_\nu x^\nu} = \mathrm{e}^{-\frac{\mathrm{i}}{2}p\wedge q}\,\mathrm{e}^{\mathrm{i}(p_\mu+q_\mu)x^\mu}. \tag{2.37}$$

The general form of the star product is obtained from the inverse Weyl map

$$\phi(x)\star\varphi(x) = \mathrm{Tr}_{\mathrm{Op}}\Big(\hat{\mathcal{W}}[\phi\star\varphi]\;\hat{T}_{\mathbb{R}}(x)\Big) = \mathrm{Tr}_{\mathrm{Op}}\Big(\hat{\mathcal{W}}[\phi]\;\hat{\mathcal{W}}[\varphi]\;\hat{T}_{\mathbb{R}}(x)\Big)\,, \tag{2.38}$$

yielding

$$\begin{aligned}\phi(x)\star\varphi(x) &= \phi(x)\cdot\varphi(x) + \sum_{n=1}^{\infty}\Bigg[\left(\frac{\mathrm{i}}{2}\right)^n \frac{1}{n!}\Theta^{\mu_1\nu_1}\ldots\Theta^{\mu_n\nu_n} \\ &\qquad\times\left(\partial_{\mu_1}\ldots\partial_{\mu_n}\phi(x)\right)\left(\partial_{\nu_1}\ldots\partial_{\nu_n}\varphi(x)\right)\Bigg] \\ &= \phi(x)\exp\Big(\frac{\mathrm{i}}{2}\overleftarrow{\partial_\mu}\,\Theta^{\mu\nu}\,\overrightarrow{\partial_\nu}\Big)\,\varphi(x)\,.\end{aligned} \tag{2.39}$$

In Eq. (2.39) one clearly sees that the terms differing from the usual commutative product disappear in the commutative limit $\Theta^{\mu\nu} \to 0$. Thus the regular multiplication is recovered.

The star product has a few peculiar features. First of all the expression

$$\mathrm{Tr}_{\mathrm{Op}}\Big(\hat{\mathcal{W}}[\phi_1]\;\hat{\mathcal{W}}[\phi_2]\;\ldots\;\hat{\mathcal{W}}[\phi_n]\Big) = \int \mathrm{d}^D x\,\phi_1(x)\star\phi_2(x)\star\ldots\star\phi_n(x) \tag{2.40}$$

is invariant under a cyclic permutation of the fields $\phi_i(x)$. Another useful identity is

$$\int \mathrm{d}^D x\,\phi(x)\star\varphi(x) = \int \mathrm{d}^D x\,\phi(x)\cdot\varphi(x)\,, \tag{2.41}$$

[3]The star product is also known under the name *Groenewold-Moyal* product.

which can be reproduced by partial integration. This relies again on the fact that the fields drop sufficiently fast at infinity.

Introducing the star commutator

$$[\phi(x)\,,\varphi(x)]_\star \equiv \phi(x)\star\varphi(x) - \varphi(x)\star\phi(x)\,, \tag{2.42}$$

one can write

$$[x^\mu, \phi(x)]_\star = \mathrm{i}\,\Theta^{\mu\nu}\,\partial_\nu\phi(x)\,. \tag{2.43}$$

It is enlightening to consider the star product of two δ-functions $\delta^{(D)}(x)$,

$$\delta^{(D)}(x)\star\delta^{(D)}(x) = \frac{1}{\pi^D|\det(\Theta)\,|} \qquad \text{for } \det(\Theta)\neq 0. \tag{2.44}$$

Here we can see that the star product regularizes the usually undefined product $\delta^{(D)}(x)\cdot\delta^{(D)}(x)$. Furthermore this equation shows how the star product of two point sources is infinitely nonlocal.

This observation can be generalized. If two fields $\phi(x)$ and $\varphi(x)$ are localized in a region of size $s \ll \sqrt{\|\Theta\|}$, their star product will spread over a possibly much larger region $\sqrt{\|\Theta\|}/s$ Minwalla et al. [2000]. For field theories this means that very low energy processes may have contributions from high-energy virtual particles. On the same footing, imposing a UV momentum cutoff Λ establishes a low momentum cutoff $1/(\|\Theta\|\cdot\Lambda)$ as well.

In summary, we are now able to hide the NC geometry of the underlying space in a deformed algebra of functions defined on a commutative space $\mathbb{R}^D$.

We can either

- use regular products in the NC algebra of Weyl operators $\hat{\mathcal{W}}[\phi]\,\hat{\mathcal{W}}[\varphi]$

or

- deform the regular product of functions $\phi(x)\cdot\varphi(x)$ on the commutative space $\mathbb{R}^D$ to the star product $\phi(x)\star\varphi(x)$.

Differentiation and integration on NC spaces can be handled through Eqs. (2.28) and (2.31).

2.2 Classical Fields on the NC Torus

In order to eventually simulate NCQFTs, it is necessary to reduce the original theory to one with a finite number of degrees of freedom. One possibility to achieve this is to replace the continuous manifold $\mathbb{R}^D_{\mathrm{NC}}$ by the discrete NC torus.

The continuous NC torus

The characteristic property of tori is their periodicity along each of their D directions, i.e. the points x and $x + \Sigma_\nu$ coincide. Σ_ν are the $\nu = 1 \dots D$ translation vectors defining the extent of the torus in each direction ν.

In terms of functions on a torus $\mathbb{T}^D_{\mathrm{NC}}$, the periodicity can be stated as

$$\phi(x + \Sigma_\nu) = \phi(x)\,, \quad \nu = 1 \dots D. \tag{2.45}$$

Besides the vectors Σ_ν it is convenient to employ the matrix Σ, which is defined by

$$\Sigma \equiv (\Sigma_1, \Sigma_2, \dots, \Sigma_D)\,. \tag{2.46}$$

Because of the periodicity property of the torus we cannot build on the general $\hat{x}^\mu$ operators from Eq. (2.3). Instead we are restricted to use a proper subalgebra $\hat{Z}^\mu$, that fulfills the periodicity requirements. A suitable choice are the unitary operators

$$\hat{Z}^\mu = \mathrm{e}^{2\pi \mathrm{i}\,(\Sigma^{-1})^\mu{}_\nu \hat{x}^\nu}, \tag{2.47}$$

which are invariant under the transformations $\hat{x}^\nu \to \hat{x}^\nu + \Sigma^\nu{}_\rho \hat{\mathbb{1}}$. The $\hat{Z}^\mu$ operators generate the *Weyl-'t Hooft algebra*

$$\hat{Z}^\mu \hat{Z}^\nu = \mathrm{e}^{-2\pi \mathrm{i}\,\tilde{\Theta}^{\mu\nu}}\, \hat{Z}^\nu \hat{Z}^\mu \qquad \text{(no summation)}. \tag{2.48}$$

$\tilde{\Theta}^{\mu\nu}$ is the dimensionless version of the NC tensor,

$$\tilde{\Theta}^{\mu\nu} = 2\pi\, (\Sigma^{-1})^\mu{}_\rho\, \Theta^{\rho\sigma}\, (\Sigma^{-1})^\nu{}_\sigma. \tag{2.49}$$

The periodicity of the torus goes along with a discretization of the momentum space. Precisely, the only possible momenta on the torus $\mathbb{T}^D_{\mathrm{NC}}$ are

$$k_\mu = 2\pi\, (\Sigma^{-1})^\nu{}_\mu\, n_\nu, \quad n_\nu \in \mathbb{Z}, \tag{2.50}$$

just like in the case of the commutative torus.

Again it is worthwhile to use the Fourier transformation as a guiding light for finding a suitable basis $\hat{T}_{\mathbb{T}}(x)$ to span the Weyl operators $\hat{\mathcal{W}}[\phi]$. In periodic spaces the original transformation (2.18) is reduced to the Fourier series $\tilde{\phi}_n$,

$$\phi(x) = \sum_{n \in \mathbb{Z}^D} \tilde{\phi}_n\, \mathrm{e}^{2\pi \mathrm{i}\,(\Sigma^{-1})^\nu{}_\mu n_\nu x^\mu} \tag{2.51}$$

and

$$\tilde{\phi}_n = \frac{1}{|\det(\Sigma)|}\int_{\mathbb{T}^D} \mathrm{d}^D x\, \phi(x)\, \mathrm{e}^{-2\pi\mathrm{i}\,(\Sigma^{-1})^{\nu}{}_{\mu} n_\nu x^\mu}. \tag{2.52}$$

Following the same reasoning as in the previous section, the Weyl mapping turns out to be

$$\hat{\mathcal{W}}[\phi] = \int_{\mathbb{T}^D} \mathrm{d}^D x\, \phi(x)\; \hat{T}_{\mathbb{T}}(x)\,, \tag{2.53}$$

where the Weyl basis $\hat{T}_{\mathbb{T}}(x)$ is now

$$\begin{aligned}\hat{T}_{\mathbb{T}}(x) =& \frac{1}{|\det(\Sigma)|}\sum_{n\in\mathbb{Z}^D}\left(\prod_{\mu=1}^{D}(\hat{Z}^\mu)^{n_\mu}\right)\prod_{\mu<\nu}\exp\Big(-\pi\mathrm{i}\, n_\mu\tilde{\Theta}^{\mu\nu}n_\nu\Big)\\ &\times\exp\Big(-2\pi\mathrm{i}\,(\Sigma^{-1})^{\sigma}{}_{\rho}\, n_\sigma x^\rho\Big)\,.\end{aligned} \tag{2.54}$$

$\hat{T}_{\mathbb{T}}(x)$ are periodic field operators,

$$\hat{T}_{\mathbb{T}}(x+\Sigma_\nu) = \hat{T}_{\mathbb{T}}(x)\,, \quad \nu = 1\ldots D. \tag{2.55}$$

As in the case of $\mathbb{R}^D_{\mathrm{NC}}$, a derivative operator can be defined. With

$$[\hat{\partial}_\mu, \hat{Z}^\nu] = 2\pi\mathrm{i}\,(\Sigma^{-1})_\mu{}^\nu\, \hat{Z}^\nu \tag{2.56}$$

one finds for $\hat{T}_{\mathbb{T}}(x)$ from Eq. (2.54)

$$[\hat{\partial}_\mu, \hat{T}_{\mathbb{T}}(x)] = -\partial_\mu \hat{T}_{\mathbb{T}}(x)\,. \tag{2.57}$$

This relation is the analogue to Eq. (2.27).

The discrete NC torus

On the discrete torus the operators $\hat{x}^\mu$ are not only periodic, but they are also restricted to discrete eigenvalues x^μ. If they are evenly spaced, their separation is denoted by[4] a.

The spacing a leads to an upper bound on the independent momenta k_μ,

$$|k_\mu| \leq \frac{\pi}{a}, \tag{2.58}$$

[4]For simplicity we consider isotropic lattices only.

thus the momentum space is compactified to a *Brillouin zone* $-\frac{\pi}{a} < k_\mu \leq \frac{\pi}{a}$. This also implies invariance under a shift of k_μ,

$$k_\mu \to k_\mu + \frac{2\pi}{a}\,\delta_\mu^\nu, \qquad \nu = 1 \dots D, \tag{2.59}$$

from which we infer the operator identity

$$\mathrm{e}^{\mathrm{i}\left(k_\mu + \frac{2\pi}{a}\,\delta_\mu^\nu\right)\hat{x}^\mu} = \mathrm{e}^{\mathrm{i}k_\mu \hat{x}^\mu}, \qquad \nu = 1 \dots D. \tag{2.60}$$

If both sides of this equation are multiplied by $\exp(-\mathrm{i}\,k_\rho \hat{x}^\rho)$ from the left side, we obtain

$$\exp\!\left(\frac{\mathrm{i}\,\pi}{a} k_\rho\,\Theta^{\rho\nu}\right) \exp\!\left(\frac{2\pi\mathrm{i}}{a}\,\hat{x}^\nu\right) = \hat{\mathbb{1}}, \qquad \nu = 1 \dots D. \tag{2.61}$$

In agreement with the usual constraint for lattice theories — the spectrum of the position operator ought to be compatible with the spatial discretization — we find

$$\exp\!\left(\frac{2\pi\mathrm{i}}{a}\,\hat{x}^\mu\right) = \hat{\mathbb{1}}, \qquad \mu = 1 \dots D, \tag{2.62}$$

as well as

$$\frac{\Theta^{\mu\nu} k_\nu}{2a} \in \mathbb{Z}, \quad \mu = 1 \dots D. \tag{2.63}$$

If this equation is combined with the momentum periodicity of Eq. (2.59), we see that $\Theta^{\mu\nu}\pi/a^2$ is an integer for all μ and ν.

Since the spacetime is now discrete, we replace the derivative operator defined in Eqs. (2.56) and (2.57) by the shift operator

$$\hat{D}_\mu = \mathrm{e}^{a\hat{\partial}_\mu}. \tag{2.64}$$

Application of this operator equals translations in lattice units a (cf. Eq. (2.29)),

$$\hat{D}_\mu \hat{Z}^\nu \hat{D}_\mu^\dagger = \mathrm{e}^{2\pi\mathrm{i}a\,(\Sigma^{-1})_\mu{}^\nu}\,\hat{Z}^\nu. \tag{2.65}$$

The Weyl basis on the lattice reads

$$\begin{aligned}\hat{T}_{\mathbb{T}_{\mathrm{dis}}}(x) =& \frac{1}{|\det\!\left(\frac{1}{a}\Sigma\right)|} \sum_{n\in\mathbb{Z}^D} \left(\prod_{\mu=1}^{D} (\hat{Z}^\mu)^{n_\mu}\right) \left(\prod_{\mu<\nu} \mathrm{e}^{-\pi\mathrm{i}\,n_\mu \tilde{\Theta}^{\mu\nu} n_\nu}\right) \\ & \times \exp\!\left(-2\pi\mathrm{i}(\Sigma^{-1})_\rho{}^\mu\, n_\mu\, x^\rho\right), \end{aligned} \tag{2.66}$$

where $x \in a\mathbb{Z}^D$. The Weyl map now turns into

$$\hat{\mathcal{W}}[\phi] = \sum_x \phi(x)\ \hat{T}_{\mathbb{T}_{\text{dis}}}(x)\,, \tag{2.67}$$

while its inverse is given by

$$\phi(x) = \text{Tr}_{\text{Op}}\Big(\hat{\mathcal{W}}[\phi]\ \hat{T}_{\mathbb{T}_{\text{dis}}}(x)\Big)\,. \tag{2.68}$$

Again, the "integration" equivalent is obtained by taking the trace,

$$\text{Tr}_{\text{Op}}\Big(\hat{\mathcal{W}}[\phi]\Big) = \sum_x \phi(x)\,. \tag{2.69}$$

Here we made use of the normalization

$$\text{Tr}_{\text{Op}}\Big(\hat{T}_{\mathbb{T}_{\text{dis}}}(x)\Big) = 1, \tag{2.70}$$

which is analogous to Eq. (2.30). Tying all of the above together yields

$$\begin{aligned}\phi(x) \star \varphi(x) &= \text{Tr}_{\text{Op}}\Big(\hat{\mathcal{W}}[\phi]\ \hat{\mathcal{W}}[\varphi]\ \hat{T}_{\mathbb{T}_{\text{dis}}}(x)\Big) \\ &= \frac{1}{|\det(\frac{1}{a}\Sigma)|}\sum_{y,z} \mathrm{e}^{-2\mathrm{i}(\Theta^{-1})_{\mu\nu}\, y^\mu z^\nu}\, \phi(x+y)\,\varphi(x+z)\,. \end{aligned} \tag{2.71}$$

Overall we have two equivalent descriptions of a NC discrete torus. Both have been carried over from the $\mathbb{R}^D_{\text{NC}}$ space. By choosing suitable Weyl bases $\hat{T}_{\mathbb{T}}(x)$ and $\hat{T}_{\mathbb{T}_{\text{dis}}}(x)$ on the torus we can now rely on the same formalisms as before. Thus we can either use the formalism of Weyl operators $\hat{\mathcal{W}}[\phi]$, or we use functions $\phi(x)$ on $x \in a\mathbb{Z}^D$ with a deformed product.

2.3 Perturbation Theory and UV/IR Mixing

When investigating NCQFTs in the framework of perturbation theory, a new effect, called *UV/IR mixing* occurs. There is no equivalent in the context of field theories on commutative spacetimes, so this provides a most remarkable deviation from the commutative field theories. We will explain this effect with the example of a scalar field theory. In particular, we are going to sketch the one-loop mass renormalization of the scalar $\lambda\phi^4$ model[5].

The action of this Euclidean four-dimensional model in the language of Weyl operators is given by

$$S\Big[\hat{\mathcal{W}}[\phi]\Big] = \text{Tr}_{\text{Op}}\left(\frac{1}{2}\,\Big[\hat{\partial}_\mu, \hat{\mathcal{W}}[\phi]\Big]^2 + \frac{m^2}{2}\,\hat{\mathcal{W}}^2[\phi] + \frac{\lambda}{4}\,\hat{\mathcal{W}}^4[\phi]\right), \tag{2.72}$$

[5]This section follows Refs. Szabo [2003], Minwalla et al. [2000].

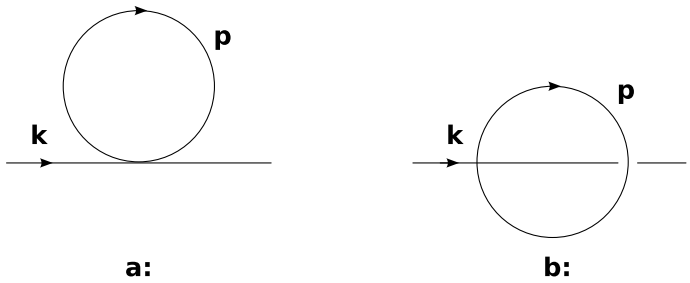

Figure 2.1: *The one-loop planar (left, figure a.) and nonplanar (right, figure b.) irreducible Feynman diagrams. They contribute to the two-point function in the NC $\lambda\phi^4$ theory.*

whereas it reads

$$S[\phi] = \int \mathrm{d}^4x \left[\frac{1}{2}\,\partial_\mu\phi(x)\,\partial_\mu\phi(x) + \frac{m^2}{2}\,\phi^2(x) + \frac{\lambda}{4}\phi(x)\star\phi(x)\star\phi(x)\star\phi(x)\right] \tag{2.73}$$

in the framework of the star product and fields $\phi(x)$ defined on commuting coordinates. Because of Eq. (2.41) the difference between the NC field theory and the commutative field theory arises only from the $\lambda\phi^4$ interaction term.

In order to investigate the UV/IR mixing in perturbation theory, we consider the one particle irreducible two-point function

$$\Gamma(k) = \langle\tilde{\phi}(k)\,\tilde{\phi}(-k)\rangle_{1\mathrm{PI}} = \sum_{n=0}^{\infty}\lambda^n\Gamma^{(n)}(k)\,. \tag{2.74}$$

The lowest order term in the perturbative expansion of the above two-point function $\Gamma(k)$ is

$$\Gamma^{(0)}(k) = k^2 + m^2. \tag{2.75}$$

The next order contribution already splits into two parts, the *planar* one, and the *nonplanar* one (cf. Fig. 2.1). The planar contribution is given by

$$\Gamma^{(1)}_{\mathrm{planar}} = \frac{1}{3}\int\frac{\mathrm{d}^4p}{(2\pi)^4}\,\frac{1}{p^2+m^2}, \tag{2.76}$$

whereas the nonplanar contribution amounts to

$$\Gamma^{(1)}_{\mathrm{nonplanar}}(k) = \frac{1}{6}\int\frac{\mathrm{d}^4p}{(2\pi)^4}\,\frac{\exp(\mathrm{i}\,p\wedge k)}{p^2+m^2}. \tag{2.77}$$

Note that in perturbation theory the exponential $\exp(\mathrm{i}\, p \wedge k)\,|_{k\neq 0}$ dies out in the $\Theta^{\mu\nu} \to \infty$ limit due to the rapid oscillations of the phase. Thus we recover the commutative perturbation theory in the strong NC limit.

The term "planar" comes from the fact that the corresponding diagrams can be drawn on a plane. For the nonplanar diagrams this is not the case. The planar contribution (2.76) is relatively easy to handle, since it is proportional to the perturbative contribution of its commutative field theory equivalent Minwalla et al. [2000], Filk [1996]. The proportionality constant can be absorbed in the bare parameters of the theory, thus the planar contributions can be handled straightforwardly. The commutative theory, in order to carry out this program, must be renormalizable, of course. Therefore the discussion of field theories on NC spaces still requires renormalization schemes.

Nonplanar diagrams

The nonplanar contribution (2.77) can be dealt with by using the Schwinger parametrization

$$\frac{1}{p^2+m^2} = \int_0^\infty \mathrm{d}\alpha\, \mathrm{e}^{-\alpha(p^2+m^2)}. \tag{2.78}$$

If we insert this into Eq. (2.77) and carry out the Gaussian momentum integration, as well as the integration over the Schwinger parameter α, we obtain Szabo [2003]

$$\begin{aligned}\Gamma^{(1)}_{\text{nonplanar}}(k) =& \frac{m^{\frac{D-2}{2}}}{6(2\pi)^{\frac{D}{2}}} \left(\frac{4}{\Lambda^2} - k_\mu(\Theta^2)^{\mu\nu}k_\nu\right)^{\frac{D-2}{2}} \\ & \times\, K_{\frac{D-2}{2}}\left(m\sqrt{\frac{4}{\Lambda^2} - k_\mu(\Theta^2)^{\mu\nu}k_\nu}\right).\end{aligned} \tag{2.79}$$

Here we have given the D-dimensional version. $K_n(x)$ is the modified Bessel function of order n. Λ is the momentum cutoff due to multiplying the integrand in Eq. (2.77) with a Pauli-Villars regulator $\exp(-1/(\Lambda^2\alpha))$. In $D = 4$ the divergences are[6]

$$\Gamma^{(1)}_{\text{nonplanar}}(k) = \frac{1}{96\pi^2}\left(\Lambda^2_{\text{eff}} - m^2 \ln\left(\frac{\Lambda_{\text{eff}}}{m^2}\right)\right) + \mathcal{O}(1)\,, \tag{2.80}$$

where the effective cutoff is given by

$$\Lambda^2_{\text{eff}} = \frac{1}{\frac{1}{\Lambda^2} + k_\mu(\Theta^2)^{\mu\nu}k_\nu}. \tag{2.81}$$

[6] This is due to the limit $\lim_{x\to 0} K_n(x) = 2^{n-1}\Gamma(n)\, x^{-n} + \ldots, \quad n \neq 0.$

Remarkably, this two-point function $\Gamma^{(1)}_{\text{nonplanar}}(k)$ remains finite in the $\Lambda \to \infty$ limit, because it is effectively regulated by the NC spacetime.

On the other hand, for the commutative limit $\Theta \to 0$ or the infrared limit $k \to 0$ we can see that $\Lambda_{\text{eff}} \to \Lambda$, so the commutative theory with its UV divergence is restored. In the infrared limit $k \to 0$, when Λ is taken to be still finite, we also retrieve the standard mass renormalization

$$m^2_{\text{ren}} = m^2 + \frac{1}{32}\frac{\lambda\Lambda^2}{\pi^2} - \frac{1}{32}\frac{\lambda m^2}{\pi^2}\ln\left(\frac{\Lambda^2}{m^2}\right) + \mathcal{O}\left(\lambda^2\right). \tag{2.82}$$

Finally we have arrived at the complete first order two-point function (up to first order in perturbation theory). It reads

$$\Gamma(k) = k^2 + m^2 + 2\lambda\Gamma^{(1)}_{\text{nonplanar}}(0) + \lambda\Gamma^{(1)}_{\text{nonplanar}}(k) + \mathcal{O}\left(\lambda^2\right). \tag{2.83}$$

In this formulation we have made use of

$$\Gamma^{(1)}_{\text{planar}} = 2\Gamma^{(1)}_{\text{nonplanar}}(0). \tag{2.84}$$

Limits and UV/IR mixing

Since the first order term in the perturbation expansion of the two-point function (2.83) is essentially described by the nonplanar contribution (2.80), we investigate that expression in different limits.

In particular, the UV limit $\lim_{\Lambda\to\infty}\Gamma^{(1)}_{\text{nonplanar}}(k)$ does not commute with the IR limit $\lim_{k\to 0}\Gamma^{(1)}_{\text{nonplanar}}(k)$, nor with the commutative limit $\Theta \to 0$. This can be seen in Eq. (2.80), where Λ_{eff} from the different limits,

$$\lim_{k\to 0}\Lambda^2_{\text{eff}} = \Lambda^2 \quad \text{and} \quad \lim_{\Lambda\to\infty}\Lambda^2_{\text{eff}} = \frac{1}{k_\mu(\Theta^2)^{\mu\nu}k_\nu}, \tag{2.85}$$

inflicts different singularities.

If we first take the $k \to 0$ limit of Eq. (2.83), yielding

$$\Gamma(0) = m^2 + 3\lambda\Gamma^{(1)}_{\text{nonplanar}}(0) + \mathcal{O}\left(\lambda^2\right), \tag{2.86}$$

we can go on as usual by subsequently sending the cutoff to infinity. We obtain e.g. Eq. (2.82).

If the limits are taken the other way around, namely first the UV limit and subsequently the low momentum limit, the intermediate effective cutoff $(k_\mu(\Theta^2)^{\mu\nu}k_\nu)^{-1}$ causes the result to assume a complicated, nonlocal form.

The crucial observation here is that the renormalized propagator (2.83) contains a zero momentum pole as well as a logarithmic singularity. Therefore the IR limit $k \to 0$ and the UV limit $\Lambda \to \infty$ do not commute. This

phenomenon is called *UV/IR mixing,* and it is a characteristic of NCQFTs. The pole at $k = 0$ in the propagator actually arises in the high momentum regions (cf. left hand side of Eq. (2.85)). This effect from high energy (large k) dynamics leads to long range correlations in position space for low wavelength particles Minwalla et al. [2000]. Another consequence is that, unlike in the commutative case, the correlation functions decay polynomially at weak coupling λ and provided that Θ is of maximal rank. Minwalla et al. [2000]. In the commutative case the decay for particles with mass $m > 0$ is generally exponential.

Roughly speaking, a particle having momentum k can induce effects at a distance $|\Theta^{\nu\mu}k_\mu|$. Therefore the behavior of NCQFTs on distances less than the NC scale Eq. (2.9) is completely different from commutative QFTs. This is further discussed in Section 4.2.

2.4 Lattice Formulation and the Morita Equivalence

The numerical implementation of the star product is tremendously resource demanding, since it involves coupling every lattice site to every other site. In order to ease the CPU effort in numerical simulations, we deploy a technique known as *dimensional reduction* based on the so-called *Morita equivalence* Connes [1994], Madore [1999], Landi [1997], Gracia-Bondía et al. [2000]. This equivalence establishes a bijective correspondence between complex-valued functions and matrix models.

Thus we rewrite the above discussed technology in terms of matrices.

The Weyl operator formalism on the two-dimensional discrete torus

We finish the discussion of the D-dimensional case now and turn to an explicit formulation suitable for the two-dimensional NC planes encountered in Chapters 3 and 4.

In two dimensions the periodicity matrix Σ of the discrete torus $\mathbb{T}^2_{\mathrm{NC}}$ can be chosen as

$$\Sigma = \begin{pmatrix} Na & 0 \\ 0 & Na \end{pmatrix}. \tag{2.87}$$

The number N here describes the number of lattice sites in each of the two directions, while a is the lattice spacing. Now the periodic coordinate

operator (2.47) turns into

$$\hat{Z}^\mu = \exp\Big(\frac{2\pi \mathrm{i}}{aN}\,\hat{x}^\mu\Big)\,, \tag{2.88}$$

and the dimensionless noncommutativity tensor $\tilde{\Theta}^{\mu\nu}$ from Eq. (2.49) is given by

$$\tilde{\Theta}^{\mu\nu} = \frac{2\pi}{a^2N^2}\,\Theta^{\mu\nu}. \tag{2.89}$$

The momentum discretization (2.50) simplifies to

$$k_\mu = \frac{2\pi}{aN}\,n_\mu, \qquad n_\mu \in \mathbb{Z}. \tag{2.90}$$

Along with Eq. (2.63) we find the noncommutativity parameter ($\theta = \Theta^{12}$)

$$\theta = \frac{1}{\pi}\,Na^2. \tag{2.91}$$

The algebra (2.48) also needs to be rewritten, resulting in

$$\hat{Z}^\mu \hat{Z}^\nu = \exp\Big(-\frac{4\pi \mathrm{i}}{N}\epsilon^{\mu\nu}\Big)\,\hat{Z}^\nu \hat{Z}^\mu, \qquad \mu,\nu = 1,2, \qquad \text{(no summation)} \tag{2.92}$$

and

$$\hat{D}^\mu \hat{Z}^\nu \hat{D}^{\mu\dagger} = \exp\Big(\frac{2\pi \mathrm{i}}{N}\,\delta^{\mu\nu}\Big)\,\hat{Z}^\nu. \tag{2.93}$$

The symbol $\epsilon^{\mu\nu}$ denotes the totally antisymmetric unit tensor (Levi-Civita symbol).

Dimensional reduction

The crucial step in formulating NC theories as matrix models, justified by the Morita equivalence, is to represent the above coordinate operators $\hat{Z}^\mu$ and shift operators $\hat{D}^\mu$ by suitable $N \times N$ matrices. For odd N there are simple building blocks (in the 2D case), which we will employ to construct the required objects. These building blocks are the so-called *twist eaters*, which are denoted by $\hat{\Gamma}_1$ and $\hat{\Gamma}_2$.

Explicitly $\hat{\Gamma}_1$ is given by

$$\hat{\Gamma}_1 = \begin{pmatrix} 0 & 1 & & & 0 \\ & 0 & 1 & & \\ & & \ddots & \ddots & \\ & & & \ddots & 1 \\ 1 & & & & 0 \end{pmatrix}, \tag{2.94}$$

which is called the *shift matrix*. The other matrix $\hat{\Gamma}_2$, which is also known as the *clock matrix*, reads

$$\hat{\Gamma}_2 = \begin{pmatrix} 1 & & & & \\ & \mathcal{Z}_{12}^* & & & \\ & & (\mathcal{Z}_{12}^*)^2 & & \\ & & & \ddots & \\ & & & & (\mathcal{Z}_{12}^*)^{N-1} \end{pmatrix}. \tag{2.95}$$

Here we have introduced the *twist* $\mathcal{Z}_{12} \in \mathbb{C}$. It obeys $\mathcal{Z}_{12}^N = 1$ and $\mathcal{Z}_{21} = \mathcal{Z}_{12}^*$. The twist will show up frequently in Chapter 4.

These $\hat{\Gamma}_\mu$ matrices are just one possible (albeit convenient) choice. For extensions and other possibilities cf. Refs. Ambjørn et al. [2000a, 1999], van Baal and van Geemen [1986].

In any case, these two unitary matrices fulfill

$$\hat{\Gamma}_1^N = \hat{\Gamma}_2^N = \mathbb{1}_N, \quad N \text{ odd}, \tag{2.96}$$

($\mathbb{1}_N$ denotes the unit matrix) as well as

$$\hat{\Gamma}_1 \hat{\Gamma}_2 = \mathcal{Z}_{12}\, \hat{\Gamma}_2 \hat{\Gamma}_1 \quad \text{and} \quad \hat{\Gamma}_1^\dagger \hat{\Gamma}_2 = \mathcal{Z}_{12}^*\, \hat{\Gamma}_2 \hat{\Gamma}_1^\dagger. \tag{2.97}$$

The twist eaters $\hat{\Gamma}_1$ and $\hat{\Gamma}_2$ in turn allow us to build up the $\hat{Z}^\mu$ operators

$$\hat{Z}^1 = (\hat{\Gamma}_2)^{\frac{N+1}{2}} \quad \text{and} \quad \hat{Z}^2 = (\hat{\Gamma}_1^\dagger)^{\frac{N+1}{2}}, \quad N \text{ odd}. \tag{2.98}$$

Using all the above with the explicit form of the star product (2.71), we can now represent the operators $\hat{T}_{\mathbb{T}_{\text{dis}}}(x)$ from Eq. (2.66) as $N \times N$ matrices,

$$\hat{T}_{\mathbb{T}_{\text{dis}}}(x) = \sum_{n_1,n_2} (\hat{Z}^1)^{n_1} (\hat{Z}^2)^{n_2} \mathrm{e}^{-2\pi \mathrm{i}\, n_1 n_2/N} \mathrm{e}^{-2\pi \mathrm{i}\, n_\mu x^\mu/N}, \quad n_1, n_2 \in \mathbb{Z}. \tag{2.99}$$

From now on we drop the $\mathbb{T}_{\text{dis}}$ subscript in the Weyl basis $\hat{T}_{\mathbb{T}_{\text{dis}}}(x)$, because we will only deal with $\hat{T}(x)$ matrices Morita equivalent to the Weyl basis on the discrete torus.

The above expression gives a new invertible mapping between some real function $\phi(x)$ and its assigned Hermitian $N \times N$ matrix $\hat{\phi}$ in terms of the $\hat{T}(x)$ matrices, namely

$$\hat{\phi} = \frac{1}{N^2} \sum_x \phi(x)\; \hat{T}(x) \quad \text{and} \quad \phi(x) = \frac{1}{N} \operatorname{Tr}_N\Big(\hat{\phi}\; \hat{T}(x)\Big). \tag{2.100}$$

We use the symbol $\hat{\phi}$ now, which is to stress the matrix nature of $\hat{\phi}$ compared to the previous Weyl operators $\hat{\mathcal{W}}[\phi]$. The trace Tr_N here refers to the matrix trace of $N \times N$ matrices.

The scalar field on the $N \times N$ lattice, which has N^2 degrees of freedom, is now mapped to a single $N \times N$ matrix, hence preserving the N^2 degrees of freedom. The two-dimensional torus has been reduced to a single entity, namely the matrix $\hat{\phi}$. This technique is called *dimensional reduction*. It reduces the spacetime on which the field lives, but preserves all degrees of freedom.

It is convenient to introduce the $N \times N$ unitary matrices $\hat{J}(n)$,

$$\hat{J}(n) = (\hat{Z}^1)^{n_1} (\hat{Z}^2)^{n_2} \mathrm{e}^{-2\pi \mathrm{i} n_1 n_2 / N}, \quad n_1, n_2 \in \mathbb{Z}, \tag{2.101}$$

which fulfill

$$\hat{J}(-n) = \hat{J}^\dagger(n)\,. \tag{2.102}$$

The Fourier series

$$\tilde{\phi}(n) = \frac{1}{N} \sum_x \phi(x)\ \mathrm{e}^{-2\pi \mathrm{i} n_\mu x^\mu / N} \tag{2.103}$$

can now be written as

$$\tilde{\phi}(n) = \frac{1}{N} \mathrm{Tr}_N \big(\hat{\phi}\, \hat{J}^\dagger(n) \big)\,. \tag{2.104}$$

Similarly, the $\hat{J}$ matrices can be used to compactly restate the left side of Eq. (2.100) in terms of the Fourier transform,

$$\hat{\phi} = \frac{1}{N} \sum_n \tilde{\phi}(n)\, \hat{J}(n)\,. \tag{2.105}$$

By using the Morita equivalence, we are now able to formulate fields on a NC lattice in terms of finite N matrices. Also all previous machinery can be formulated in terms of matrices.

In the following chapters we will apply these results in order to formulate various field theories on NC lattices. A most wanted effect of reducing fields on NC spaces into single matrices is that these matrix models are well suited for numerical simulations.

2.5 Continuum Limits of NC Field Theories

The numerical simulation of field theories necessarily entails some form of discretization. One possibility for this is the introduction of a spacetime

lattice. Ultimately, however, one is usually interested in the continuum limit and the large volume limit of a theory.

In Chapters 3 and 4 we consider spaces involving a NC plane. In the lattice formulation these are reduced to two-dimensional discrete tori $\mathbb{T}^2_{\mathrm{NC}}$. Therefore Eq. (2.91) is applicable, which we repeat here for convenience,

$$\theta = \frac{1}{\pi} N a^2.$$

When dealing with lattice field theories on a two-dimensional NC torus $\mathbb{T}^2_{\mathrm{NC}}$, two different limits are considered in the literature.

The planar limit

The planar limit is characterized by sending $N \to \infty$ while keeping the gauge coupling fixed. The name of this limit is derived from the fact that the nonplanar diagrams in perturbation theory turn into planar contributions. From Eq. (2.91) one can see that the limit $N \to \infty$ at fixed a corresponds to sending $\theta \to \infty$. As can be seen e.g. in Eq. (2.77), the nonplanar perturbative contributions assume planar characteristics in the planar limit, so on the perturbative level commutativity is restored. However, since perturbation theory does not encompass all aspects of the full theory, not all commutative aspects reemerge.

The double scaling limit

In this work, though, we are mainly interested in a continuum limit of a NC theory. Thus, as we decrease the lattice spacing a, we simultaneously increase N such that the NC parameter θ remains fixed. This limit is referred to as the *double scaling limit (DSL)*. From Eq. (2.91) we find

$$N \propto \frac{1}{a^2}$$

as the necessary condition. The existence of a finite DSL is a necessary condition for the renormalizability of a NC theory.

2.6 Classical Fields on the Fuzzy Sphere

We are now going to discuss scalar fields ϕ on the fuzzy sphere $\mathbb{S}^2_{\mathrm{F}}$. It is the original and simplest example of a fuzzy space. The fuzzy sphere was introduced as a NC deformation of the two-dimensional sphere $\mathbb{S}^2$ Madore

[1992]. Fuzzy formulations can be developed for a number of compact even-dimensional manifolds Balachandran et al. [2005], Nair [2005]. Besides being used in string theory for the description of brane fluctuations, they also appear in the research of quantum gravity Chamsedinne and Connes [1997].

A fuzzy space is a sequence of finite-dimensional approximations to the algebra of functions on a smooth manifold $\mathbb{M}$. For instance, a function $\phi(x) \in \mathbb{C}$ defined over $x \in \mathbb{S}^2$ can be expanded like

$$\phi(x) = \phi_0 + \phi_\mu\, x_\mu + \frac{1}{2!}\phi_{\mu\nu}\, x_\mu x_\nu + \frac{1}{3!}\phi_{\mu\nu\rho}\, x_\mu x_\nu x_\rho + \ldots, \quad \mu, \nu, \rho \ldots = 1, 2, 3. \tag{2.106}$$

If there is a cutoff at some large power of x, we obtain a fuzzy space formulation. This formulation can be represented by a finite-dimensional matrix model. The matrix formulation can also be utilized to carry out numerical simulations. A decisive difference to spatial lattices is that the fuzzy space formulations preserve continuum symmetries exactly.

The reformulation of $\phi(x)$ as a matrix, which we denote by $\hat{\phi}$, implies a recasting of all operators, such as coordinate operators (Eq. (2.5)), the derivative operator $\hat{\partial}_\mu$ or the Laplace-Beltrami operator $\hat{\partial}_\mu\hat{\partial}_\mu$ into a finite matrix representation. In order to do this we stick to the simplest of all fuzzy spaces, the fuzzy sphere $\mathbb{S}^2_{\mathrm{F}}$ from Eqs. (2.4) and (2.5).

First we reformulate the position operator (2.5). This is straightforward, since we can simply use the canonical matrix representation of the SU(2) angular momentum operators $\hat{L}_\mu$. Their explicit form is reviewed in Appendix C. The derivative operators are built from the $\hat{L}_\mu$ operators as well Balachandran et al. [2005],

$$\hat{\partial}_\mu\, \hat{\phi} = [\hat{L}_\mu, \hat{\phi}]. \tag{2.107}$$

From this the Laplace-Beltrami operator $\hat{\partial}_\mu\hat{\partial}_\mu$ is easily obtained,

$$\hat{\partial}_\mu\hat{\partial}_\mu\, \hat{\phi} = \sum_{\mu=1}^{3} [\hat{L}_\mu, [\hat{L}_\mu, \hat{\phi}]]. \tag{2.108}$$

As stated before, $\hat{\phi}$ here marks the finite matrix equivalent of the continuous field $\phi(x)$. In the theory investigated in Chapter 5, $\phi(x)$ represents scalar neutral bosons. In this case $\hat{\phi}$ is a $N \times N$ Hermitian matrix.

The equivalent of the integral

$$\int_{\mathbb{S}^2} \mathrm{d}\Omega\, \phi(x) \tag{2.109}$$

is

$$\frac{4\pi}{N}\,\mathrm{Tr}_N\big(\hat{\phi}\big)\,. \tag{2.110}$$

We now want to elaborate a little more on the relation between the function $\phi(x)$ and the corresponding matrix $\hat{\phi}$. The spherical harmonics $\mathcal{Y}^{lm}(x)$, which are the eigenfunctions of the angular momentum operators $\hat{L}_3$ and $\hat{L}^2$ in the continuum, form a complete function basis. Thus any function $\phi(x)$ can be expanded in the basis of $\mathcal{Y}^{lm}(x)$,

$$\phi(x) = \sum_{l=0}^{\infty}\sum_{m=-l}^{l} c_{lm}\,\mathcal{Y}^{lm}(x)\,. \tag{2.111}$$

Similarly, the matrices $\hat{\phi}$ can be expanded in the basis of the *polarization tensors*[7] $\hat{Y}^{lm}$, which are eigenmatrices with respect to the finite N angular momentum operators $\hat{L}_3$ and $\hat{L}^2$. Thus the expansion in terms of polarization tensors takes the form

$$\hat{\phi} = \sum_{l=0}^{N-1}\sum_{m=-l}^{l} c_{lm}\,\hat{Y}^{lm}. \tag{2.112}$$

Note that a matrix size N implies an angular momentum cutoff at $\hat{L}^2 = N(N-1)$. This prescription is not unique, of course. Other bases are possible as well Balachandran et al. [2005]. In any case, through the coefficients c_{lm} we are able to relate

$$\phi(x) \quad \longleftrightarrow \quad \hat{\phi}. \tag{2.113}$$

Limits

Here we briefly mention two interesting limits. The first is the planar limit $N \to \infty$ describing a theory on a commutative spacetime. The other is the $R \to \infty$ limit, which describes a NC plane (at finite N).

In light of Eq. (2.5) one can see, why $N \to \infty$ describes a theory in which the coordinate operators $\hat{x}^\mu$ commute, since $s = N - 1$.

The other limit worth considering is $R \to \infty$. Since the curvature of the sphere approaches zero with increasing radius R, this limit recovers the two-dimensional plane.

Overall, taking the $N \to \infty$ limit as well as the $R \to \infty$ limit recovers the two-dimensional commutative plane. It is not clear yet, however, how far QFT observables on the fuzzy sphere can be extrapolated to these limits.

[7] A review of basic properties of the polarization tensors as well as their explicit construction can be found in Appendix C.

2.7 Noncommutativity and Phenomenology

Experimental data related to a possible noncommutativity of nature are scarce. First there are the so-called *gamma ray bursts (GRB)* and *threshold anomalies* observed in astrophysics. GRBs are a means to search for a distorted dispersion relation of the photon, while threshold anomalies in the observation of high energy cosmic rays could be explained by a broken Lorentz invariance. Furthermore, like in the case of the $\lambda\phi^4$ perturbation expansion, a nonvanishing noncommutativity leaves its trace in the terms of the perturbation series, which in turn could be manifest in particle scattering experiments. These topics are briefly reviewed now.

Time shift analysis in gamma ray bursts

GRBs are short (0.1 s ... 100 s) and intense burst of high energy photons ($E_\gamma > 10^5$ eV). They are the biggest explosions in the universe since the big bang and are observed about once a day.

GRBs are of extra galactic origin and travel over large distances (about 3×10^9 pc) before arriving on earth. If there were a deformed dispersion relation (which entails a broken Lorentz invariance), photons emitted in a GRB would reach the detector with different time spreads depending on their energy. The long travel makes them particularly sensitive to such distortions.

GRBs cannot be observed directly on earth because they cannot pass through the atmosphere. Therefore they are usually detected from satellites. Examples are the "Compton Gamma Ray Observatory" (CGRO) (1991-2000) with its instrument "Burst and Transient Source Experiment" (BATSE), the "High Energy Transient Explorer" (HETE) satellite[8] (since 2000) or the "Swift Gamma-Ray Burst Mission" satellite (since 2004).

There are several analyses carried out with the data obtained by these experiments Amelino-Camelia et al. [1998], Ellis et al. [2006], Boggs et al. [2004]. Unfortunately, all collaborations have to cope with sparse data and many systematic errors. Not surprisingly, none of them finds conclusive evidence for a deformed dispersion relation.

Threshold anomalies

One of the most puzzling phenomena in current astrophysics is the observation of *ultra high energy cosmic rays (UHECR)*. They contain protons carrying energies of $E_\mathrm{p} > 10^8$ TeV.

[8] This is actually HETE-2. The original HETE satellite was launched successfully into orbit in 1994 but failed within a day due to lack of solar power.

The UHECRs are observed by detecting the particle showers resulting from their interaction with the earth's atmosphere. These events are rather difficult to investigate. One expects about one particle of $E > 10^8$ TeV per km^2 and century. Therefore the observatories for UHECRs usually cover quite a large area.

The main experiments devoted to the investigation of UHECRs are the "Akeno Giant Air Shower Array" (AGASA) experiment, and its successor, the "Pierre Auger" observatory. AGASA, located in Akeno, Japan, covers an area of about $100\,\mathrm{km}^2$ and consists of 111 detectors on the ground (surface detectors) and 27 detectors underground absorbers (muon detectors). It was in operation from 1990 to 2003.

The *Pierre Auger observatory* is still under construction. The Argentinian part of the installation is to be finished some time in 2007 and has an area of about 3000 km^2. An installation of similar size is planned in Colorado, USA. The Auger observatory should be able to deliver much better data and statistics than its predecessor, the AGASA experiment.

AGASA found in its 14 years of operation about 1000 UHECRs with $E > 10^7$ TeV, including eleven events with $E > 10^8$ TeV Shinozaki [2006]. This poses questions regarding the origin and the propagation of these particles Stecker [2003]. Greisen Greisen [1966] and Zatsepin and Kuzmin Zatsepin and Kuzmin [1966] showed that high energy particles, such as protons traveling through space, should interact with the microwave background according to

$$p + \gamma \to p + \pi. \tag{2.114}$$

The threshold for this reaction is called *Greisen-Zatsepin-Kuzmin (GZK) threshold*. It is about $E \approx 5 \times 10^7$ TeV Greisen [1966], Zatsepin and Kuzmin [1966]. This threshold ensures absorption within about 50 Mpc for cosmic rays (such as the above mentioned protons) above the GZK threshold

$$E_{\mathrm{GKZ}} = \frac{(m_{\mathrm{p}} + m_\pi)^2 - m_{\mathrm{p}}^2}{4k}, \tag{2.115}$$

where k is the energy of universal background photons, $k \approx 10^{-1}$ eV Protheroe and Meyer [2000]. The GZK threshold is sensitive to the Lorentz invariance, so the observation of particles beyond this threshold could be due to a broken Lorentz invariance. This in turn might be the result of some noncommutativity in nature.

The AGASA experiment saw an excess of $E > 10^7$ TeV particles, thus somewhat supporting a broken Lorentz invariance. However, these analyses have to deal with poor statistics as well, so hopefully the Auger observatory will improve this situation.

In a similar vein one sees bursts of photons emitted from blazars (highly active galactic nuclei), such as Markarian 421 or Markarian 501, that have energies of $E_\gamma \approx 20$ TeV. According to Refs. Nikishov [1961], Goldreich and Morrison [1963], the dominant absorption process for high-energy γ-rays in intergalactic space is pair creation through collisions with low energy photons (microwave background),

$$\gamma + \gamma \to e^+ + e^-. \tag{2.116}$$

The threshold for this reaction is about $E_\gamma \approx 1$ TeV Greisen [1966], Stecker and de Jager [1993]. The source Markarian 501 is about 157 Mpc away from earth, which is much longer than the free path for photons from the blazar through the IR background radiation photons. Again, for a small deformation in the Lorentz kinematics these thresholds might be increased, thus allowing for the observation of such high energy photons Amelino-Camelia et al. [1998], Coleman and Glashow [1999], Amelino-Camelia and Piran [2001], Aloisio et al. [2005].

Scattering experiments

We have seen in Section 2.3 how some terms pick up a phase factor $\exp(\mathrm{i}\, p \wedge k)$ in the one-loop expansion (cf. Eq. (2.77)). Similarly, in NCQED e.g. the extraction of the magnetic dipole coupling in the $ee\gamma$ vertex function picks up a kinetic phase factor $\exp(\mathrm{i}\, p \wedge k)$, where p and k are the electron momenta Hayakawa [2000]. Therefore some NC effects could show up in collider experiments Hewett et al. [2001], Mathews [2001]. From results of these experiments some bounds on θ could be extracted.

One possible way to detect NC effects is to reconsider the Lamb shift, as has been done by Chaichian *et al.* in Ref. Chaichian et al. [2001]. NC effects in the $2P_{1/2} \to 2S_{1/2}$ transition occur already on the tree level and thus are accessible by NC perturbation theory. Results from collider experiments allow for an estimate of the NC parameter θ. Chaichian *et al.* found

$$\theta \lesssim (10 \text{ TeV})^{-2}. \tag{2.117}$$

Another limit has been obtained from Aharonov-Bohm effect investigations in Ref. Falomir et al. [2002]. There Falomir *et al.* showed how the holonomy receives a nontrivial kinematic θ-correction that leads to a different differential cross section. Essentially they found that differential cross sections for small angles are suitable for detecting a possible noncommutativity. When applying their findings to experimental data, they obtained again the θ bound (2.117).

A third estimate has been obtained from "clock comparisons" in Ref. Carroll et al. [2001]. Clock comparisons monitor the difference between two atomic hyperfine or Zeeman transition frequencies and look for variations as the earth rotates Prestage et al. [1985], Lamoreaux et al. [1986]. Based on this technique they obtained once more the result from Eq. (2.117).

Finally we want to cite Ref. Alboteanu et al. [2006], which investigated what bounds on θ might be obtained from $q + \bar{q} \to e^+ + e^- + \gamma$ processes in future LHC and Tevatron experiments. More precisely, they studied the azimuthal dependence of the cross section to be measured in these experiments. They anticipate bounds of

$$\theta \lesssim (1.2 \text{ TeV})^{-2} \quad \text{resp.} \quad \theta \lesssim (1 \text{ TeV})^{-2}, \tag{2.118}$$

where the first number is a bound on the temporal noncommutativity and the second one refers to spatial noncommutativity. These numbers correspond to a somewhat larger NC parameter θ than the ones from Eq. (2.117).

All bounds derived from experimental data coincide. If we take Eq. (2.117) as a basis, the spacetime cells have a linear extent of at most 1.4×10^{-20} m. Therefore, the NC regime would be barely probable by todays machines. Thus, none of the authors states to have found evidence for a nonvanishing noncommutativity θ.

In summary, no conclusive evidence for a noncommutative universe has been found so far. There are some bounds on θ from collider experiments, most of which have the drawback of being due to perturbative reasonings, which often are even limited to the tree level. There are also some hints at a broken Lorentz invariance from astronomical observations, but overall noncommutativity has yet to be observed in nature.

Chapter 3

The 2D NC Scalar Theory

3.1 The Action on a NC Spacetime

In the previous chapter we sketched how to deal with a scalar function on a discrete torus $\mathbb{T}^D_{\mathrm{NC}}$. In the following we are interested in simulating the $\lambda\phi^4$ model on a two-dimensional NC plane. The action of its commutative, continuous counterpart is given by

$$S_{\mathrm{comm}}[\phi] = \int \mathrm{d}^2x \left[\frac{1}{2}\left(\partial^\mu\phi\right)\left(\partial_\mu\phi\right) - \frac{m^2}{2}\,\phi^2 - \frac{\lambda}{4}\,\phi^4\right]. \tag{3.1}$$

Here $\phi(x)$ is a neutral scalar field, $\phi \in \mathbb{R}$.

First of all we perform the Wick rotation, thereby transforming the Minkowski type space into a Euclidean one. The validity of this procedure is guaranteed by the Osterwalder-Schrader axioms Osterwalder and Schrader [1972].

Secondly we reformulate the theory on a NC space. This can be achieved in two ways: either by using Weyl operators

$$S\Big[\hat{\mathcal{W}}[\phi]\Big] = \mathrm{Tr}_{\mathrm{Op}}\left(\frac{1}{2}\left[\hat{\partial}_\mu, \hat{\mathcal{W}}[\phi]\right]^2 + \frac{m^2}{2}\,\hat{\mathcal{W}}^2[\phi] + \frac{\lambda}{4}\,\hat{\mathcal{W}}^4[\phi]\right), \tag{3.2}$$

or by employing the star product

$$S[\phi] = \int \mathrm{d}^2x \left[\frac{1}{2}\left(\partial_\mu\phi\right)(\partial_\mu\phi) + \frac{m^2}{2}\,\phi^2 + \frac{\lambda}{4}\,\phi\star\phi\star\phi\star\phi\right]. \tag{3.3}$$

As we remarked in Section 2.3, this theory differs from its commutative equivalent only in the interaction term.

The matrix model

Since we want to investigate the model numerically, we replace the underlying manifold in Eq. (3.3) by the discrete torus $\mathbb{T}^2_{\mathrm{NC}}$. This lattice formulation is subsequently translated into the language of matrices via the technique of dimensional reduction (cf. Section 2.4). Thus we effectively associate a Hermitian matrix $\hat{\phi}$ with the field $\phi(x)$ through the Morita equivalence

$$\phi(x) \quad \longleftrightarrow \quad \hat{\phi} \in \mathrm{Mat}_{N\times N}, \qquad \hat{\phi} = \hat{\phi}^\dagger. \tag{3.4}$$

The number N refers to the number of lattice points per direction as well as to the size of the matrix $\hat{\phi}$, since the number of degrees of freedom (N^2) must be identical in either case. The hat notation was chosen in order to stress the matrix nature of $\hat{\phi}$.

Overall, the Morita equivalence leads to the matrix model

$$S[\hat{\phi}] = N \,\mathrm{Tr}_N \left(\frac{1}{2} \sum_\mu \left(\hat{\Gamma}_\mu \hat{\phi} \, \hat{\Gamma}_\mu^\dagger - \hat{\phi} \right)^2 + \frac{m^2}{2} \, \hat{\phi}^2 + \frac{\lambda}{4} \, \hat{\phi}^4 \right). \tag{3.5}$$

Here the twist eaters $\hat{\Gamma}_\mu$ from Eqs. (2.94) and (2.95) provide a shift by a in the μ-direction,

$$\hat{\Gamma}_\mu \hat{\phi} \, \hat{\Gamma}_\mu^\dagger \quad \longleftrightarrow \quad \phi(x + a\hat{\mu}) \, . \tag{3.6}$$

The symbol $\hat{\mu}$ refers to the unit vector in the μ-direction. Thus the term $\hat{\Gamma}_\mu \hat{\phi} \, \hat{\Gamma}_\mu^\dagger - \hat{\phi}$ in Eq. (3.5) is the matrix model's discretized equivalent of a derivative.

3.2 The Phase Structure

The NC specific phenomenon of UV/IR mixing leaves its mark on the phase diagram as well. Compared to the phase diagram of the commutative $\lambda\phi^4$ theory, new phenomena occur. In particular the IR singularity gives rise to new effects. Usually phase transitions are related to modes that minimize the two-point function $\Gamma(k)$ (see Eq. (2.74)). Thus in the NC case, at large λ resp. θ, we would not expect zero modes to drive phase transitions.

The phase structure of the NC $\lambda\phi^4$ theory has been investigated by S. S. Gubser and S. L. Sondhi Gubser and Sondhi [2001], where they have used an effective action due to S. A. Brazovskii Brazovskii [1975].

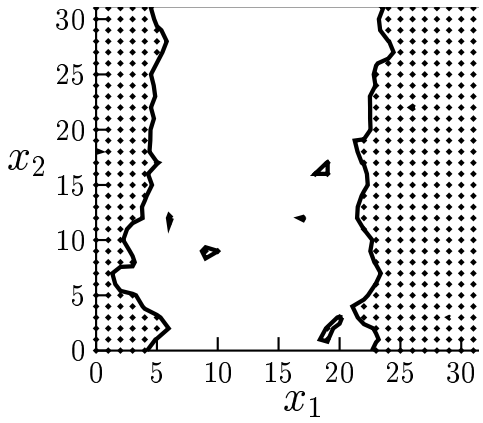

Figure 3.1: *A sample configuration from the striped phase illustrating a pattern dominated by the condensation of a nonzero mode. This is a configuration from simulations at $N = 35$. The dotted region refers to $\phi(x) > 0$, while the blank area represents $\phi(x) < 0$.*

The phase structure

At small values of the NC parameter θ, Gubser and Sondhi conjectured an *Ising type* phase, at which the expectation value of the scalar field is nonzero[1], $\langle\phi\rangle \neq 0$. This phase will be labeled as the *uniform phase.* The transition from the disordered phase to the uniform phase in $D = 3$ is of second order Hofheinz [2004], Bietenholz et al. [2004a].

At sufficiently large θ the minimum of the two-point function $\Gamma(p)$ does not occur at $p = 0$ anymore. In this case the dominant low energy configurations are characterized by a spatially varying $\phi(x)$, so the symmetry due to translation invariance is spontaneously broken. This implies a ground state featuring some nonuniform $\phi(x)$ pattern. Such patterns have been observed in 2D in Refs. Hofheinz [2004], Bietenholz et al. [2004a], Ambjørn and Catterall [2002] and extensively in 3D in Refs. Hofheinz [2004], Bietenholz et al. [2004a]. In both cases these patterns were manifest as stripes. Therefore this phase is customarily called the *striped phase*, even though any periodic structure may occur. The exact pattern depends on the momenta driving the phase transition. A typical example configuration in $D = 2$ from Ref. Hofheinz [2004] is shown in Fig. 3.1.

Gubser and Sondhi worked with the Brazovskiian form of the action.

[1]This corresponds to the spontaneous symmetry breaking in a ferromagnet, where a nonvanishing magnetization can be triggered by an external magnetic field. This persists, even when the external field has been driven to zero. Typical configurations in this phase deviate strongly from the rotational symmetry, even when there is no external field at all.

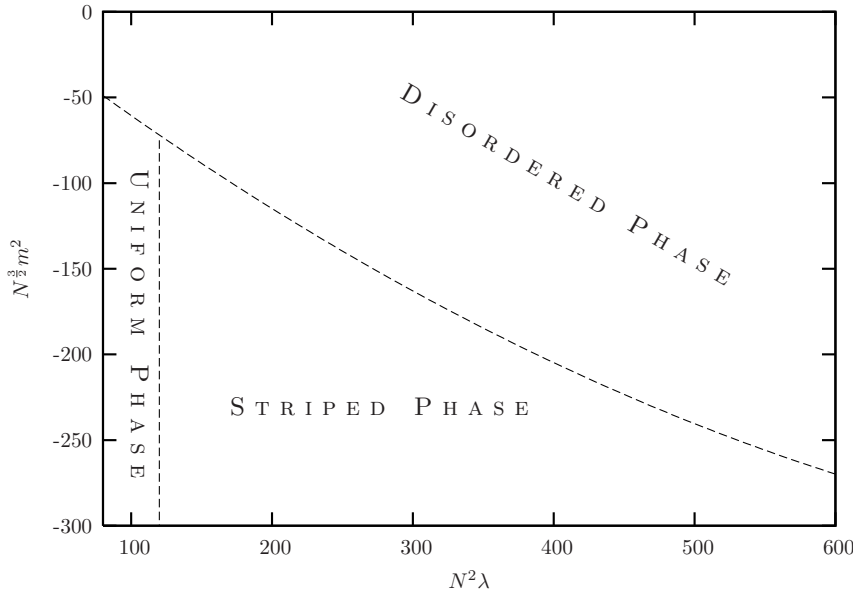

Figure 3.2: *The phase diagram of the NC 2D $\lambda\phi^4$ theory on a discrete torus, as provided by Refs. Hofheinz [2004], Bietenholz et al. [2004a]. There are three phases: the disordered phase, the striped phase and the uniform phase. The diagram is shown in the $N^{\frac{3}{2}}\lambda$ – N^2m^2 plane. This choice is mandated to obtain stable phase transition lines valid for weak and intermediate coupling strengths λ.*

They suggested a generalization of the reasoning of the *Mermin Wagner theorem* Mermin and Wagner [1966], Hohenberg [1967], Coleman [1973]. It states that a spontaneous breakdown of a continuous symmetry is impossible in $D \leq 2$ local theories. Their generalization extended its applicability to the Brazovskiian NC $\lambda\phi^4$ model, even though it is nonlocal. As mentioned before, the striped phase with its patterns constitutes a spontaneous breakdown of a continuous symmetry, namely of the translational invariance. Thus the considerations by Gubser and Sondhi suggest that the striped phase should disappear in the continuum limit and might merely be a lattice artifact.

In the third phase, the *disordered phase*, the relation $\langle\phi\rangle = 0$ holds as well. However, neither translation invariance nor the symmetry

$$\phi(x) \to -\phi(x) \tag{3.7}$$

are broken. In the disordered phase periodic patterns do not occur.

The phase diagram of the theory is plotted in Fig. 3.2 in the $N^{\frac{3}{2}}\lambda$ – N^2m^2 plane. It is due to Refs. Hofheinz [2004], Bietenholz et al. [2004a] and reproduced here for convenience.

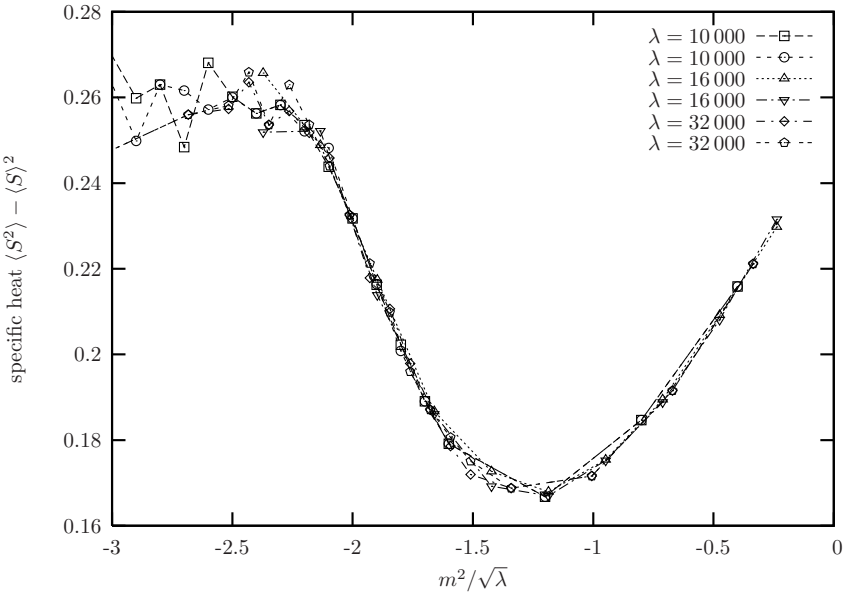

Figure 3.3: *The specific heat as a function of* $m^2/\sqrt{\lambda}$ *at strong self-couplings* λ*. The behavior changes at about* $m^2/\sqrt{\lambda} = -2$*, which agrees with the prediction (3.8). These results have been obtained with matrices of the size* $N = 15$*.*

Results for the phase structure at large λ values

The phase structure shown in Fig. 3.2 has been obtained at weak and intermediate coupling strengths λ. In the large λ limit, where the kinetic term becomes negligible, the critical m_c^2 can be computed from 1-matrix considerations Brezin et al. [1978]. The result is

$$m_c^2 = -2\sqrt{\lambda} \qquad \text{for } \lambda \to \infty. \tag{3.8}$$

We verified numerically the behavior described by Eq. (3.8). In order to determine the phase transition in the large λ regime, we measured the specific heat, which corresponds to the variance of the action in the Monte Carlo history. This is a well known technique for detecting second order phase transitions.

The result is shown in Fig. 3.3. We can see that the specific heat changes its behavior noticeably around $m^2/\sqrt{\lambda} = -2$. This agrees quite well with the prediction from Eq. (3.8). The same behavior has been observed in Ref. Garcia Flores et al. [2006], where the $\lambda\phi^4$ model was regularized by the fuzzy sphere $\mathbb{S}_F^2$. For detailed numerical studies of that model we refer to Refs. Martin [2004], Panero [2006].

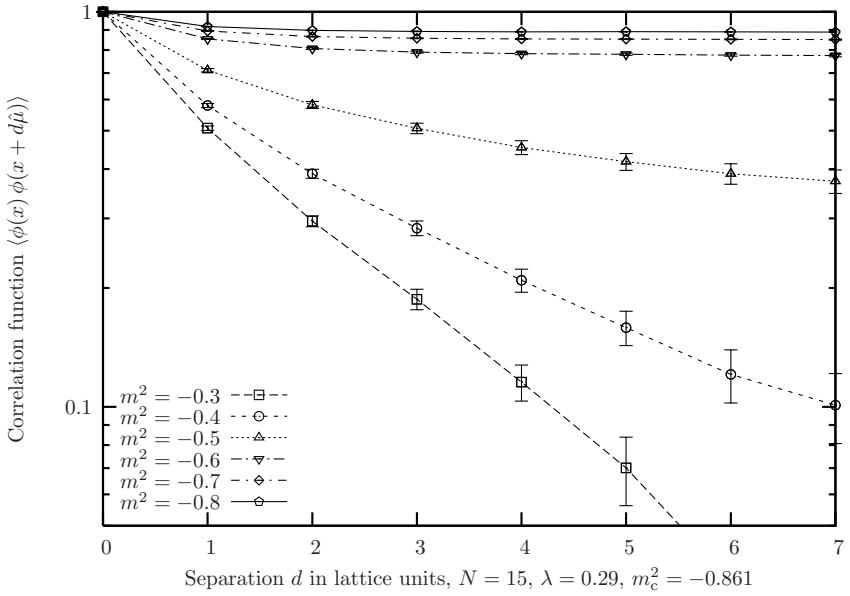

Figure 3.4: *Here we show examples of the two-point function (3.9). One can clearly see how the function gets more and more flat as* m^2 *approaches the critical value* $m_c^2 = -0.861$. *The flatness of the correlation function is equivalent to a diverging correlation length. This indicates that the phase transition from the disordered phase to the striped phase is of second order. Another feature of NC theories, namely nonexponential correlation functions at small couplings* λ, *is clearly displayed. These results were obtained at* $N = 15$ *and* $\lambda = 0.29$.

3.3 Lattice Spacing and Scaling

In order to study how the theory scales for different matrix sizes N, we consider the two-point function

$$C(x) = \left\langle \frac{1}{N^2} \sum_y \phi(x+y)\ \phi(y) \right\rangle. \tag{3.9}$$

When approaching m_c^2 from above (at fixed N and λ), these correlations become more and more flat.

In Fig. 3.4 we show some examples of the two-point function (3.9). They display a feature peculiar to NC spaces, namely a nonexponential decay (cf. Section 2.3). At low couplings λ this is expected for a $\lambda\phi^4$ theory situated on a NC spacetime Minwalla et al. [2000].

We now investigate, how the difference $m^2 - m_c^2$ translates into the lattice spacing a. We are studying this issue in the disordered phase, since the finite

size effects are rather harmless in the $m^2 > m_c^2$ regime. First we need to set a scale. We arbitrarily chose the lattice spacing to be

$$a = 1 \qquad \text{at } N = 45. \tag{3.10}$$

This holds at any fixed coupling λ.

In order to fix the NC parameter θ, we combine the above convention with Eq. (2.91). This leads to a lattice spacing

$$a(N) = \sqrt{\frac{45}{N}} \quad \longleftrightarrow \quad \theta = 14.32. \tag{3.11}$$

To obtain the DSL, we fine-tune the m^2 parameter at fixed λ, but different N such that the two-point functions $C(|x|a)$ coincide when plotted over the physical distance. The parameters are chosen such that we always remain in the vicinity of the striped phase. The various values m^2_{scaling} obtained from this tuning in turn allow us to determine the critical exponent σ from

$$Na^2 = N(m^2 - m_c^2)^\sigma. \tag{3.12}$$

If the striped phase still exists in the DSL, the values for σ should agree for different N and λ.

In order to determine m^2_{scaling}, we chose the matrix sizes $N = 13$, 15, 19 and 25, because the measurement of the correlation functions $C(|x|a)$, especially for larger separations $|x|a$, is very resource demanding. Furthermore the autocorrelation needs to be overcome. For instance, in the $N = 25$ case, in order to obtain 200 well thermalized and decently decorrelated correlation function data points (at the largest separation $|x_\mu| = 12a$), 1.5×10^9 configurations had to be generated. Of these 5×10^8 were necessary to overcome thermalization. We tried to apply the overrelaxation procedure suggested by Ref. Panero [2006], however it proved unsuitable for our model.

In practice we first evaluated a decay at $N = 25$ and two different λ values, $\lambda = 0.24$ and $\lambda = 0.29$. Then we fine-tuned the m^2 values as described above. This has been done at $N = 13$, 15 and 19. The results are shown in Fig. 3.5. Even though we tuned $N = 15$ for scaling, it might be too close to $N = 19$ for determining the critical exponent σ. Thus $N = 13$ was chosen, although it is quite small. The precise simulation parameters are listed in Tab. 3.1. The errors in this table are conservative estimates. Since we take the $N = 25$ data as the base for the comparison, we do not attach an error to these numbers.

With the m^2_{scaling} values from the tuning, we can now determine the critical exponent σ in Eq. (3.12). The errors on σ have been obtained by using the

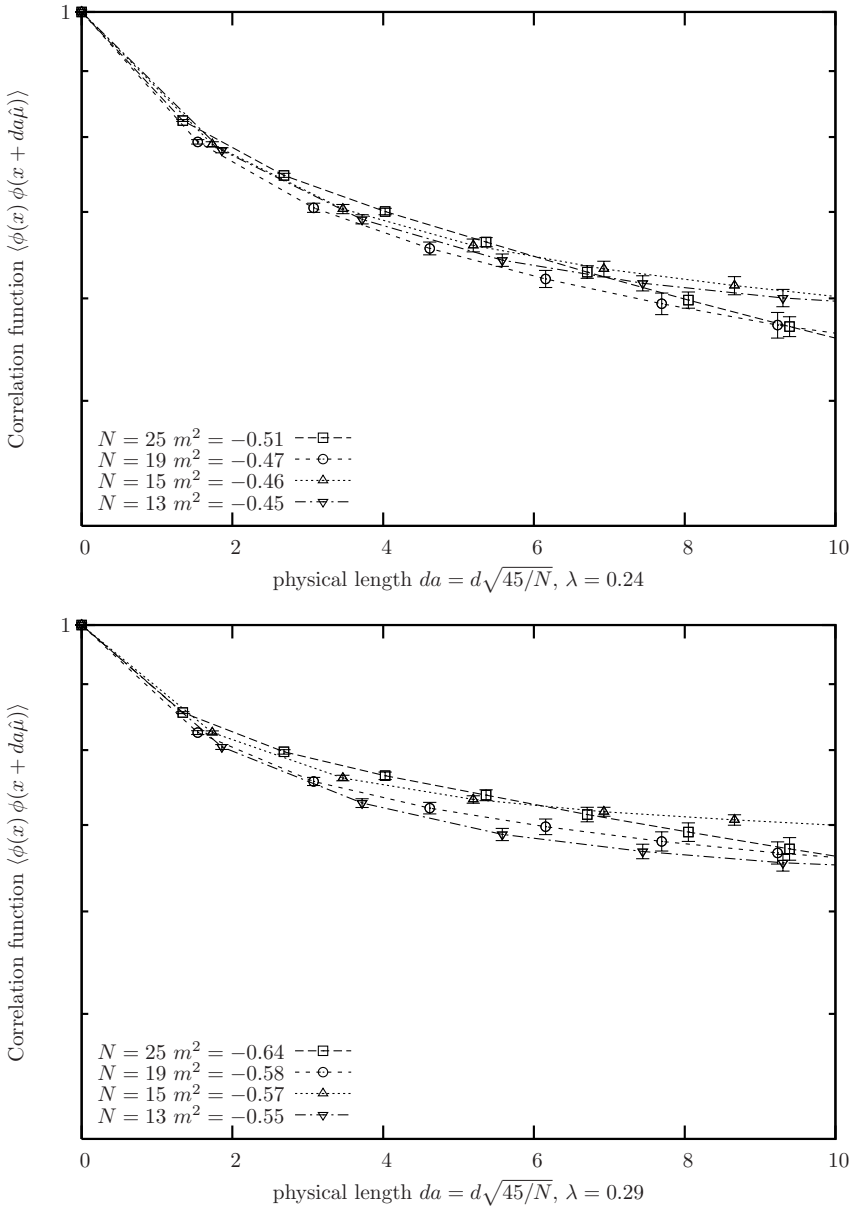

Figure 3.5: *The scaling of the correlation functions at* $\lambda = 0.24$ *(top) and* $\lambda = 0.29$ *(bottom).*

	$\lambda = 0.24$		$\lambda = 0.29$	
N	m_c^2	m^2_{scaling}	m_c^2	m^2_{scaling}
$N = 25$	-0.757	-0.51	-0.878	-0.64
$N = 19$	-0.707	$-0.470(5)$	-0.916	$-0.580(5)$
$N = 15$	-0.602	$-0.46(1)$	-0.861	$-0.57(1)$
$N = 13$	-0.736	$-0.45(1)$	-0.883	$-0.55(1)$

Table 3.1: *The values of m^2_{scaling} and the critical m_c^2 at $\lambda = 0.24$ and at $\lambda = 0.29$. The errors are conservative estimates. These values were used to determine the critical exponent σ from Eq. (3.12), see Tab. 3.2.*

λ	$N = 25, 19$	$N = 25, 15$	$N = 25, 13$
0.24	-6.64 ± 3.39	-0.92 ± 0.12	4.46 ± 1.06
0.29	0.80 ± 0.03	2.54 ± 0.43	1.95 ± 0.17

Table 3.2: *The critical exponents σ. These numbers were obtained by using the respective N pairs from the top line of this table. The errors are due to the uncertainties in the m^2_{scaling} and computed according to the Gauß error propagation law. If the striped phase would survive in the DSL, all σ values (cf. Eq. (3.12)) should agree.*

Gaussian error propagation law. The resulting critical exponents σ are listed in Tab. 3.2.

Since σ in Tab. 3.2 varies strongly and even takes on negative values, we are tempted to conclude that for the two-dimensional $\lambda\phi^4$ theory the striped phase is merely a lattice artifact. We cannot find a DSL while being in the vicinity of the striped phase and thus this phase does not seem to survive the continuum limit. Maybe larger N than ours ought to be considered to make a definite statement. However, as stated before, this is very resource demanding, since the correlations at large separations are extremely inert.

Chapter 4

The 4D U(1) Gauge Theory

4.1 Pure NC U(N) Gauge Theory

In the following we review some properties of unitary NC gauge theories. Just like in the last chapter, we will work on a Euclidean spacetime.

U(N) and SU(N) groups

In order to investigate NC gauge theories, we consider U(N) gauge fields $A_\mu(x)\,, \mu = 1 \dots D$ on $\mathbb{R}^D_{\mathrm{NC}}$.

In general, group elements $U \in \mathrm{U}(N)$ can be represented (in the fundamental representation) by $N \times N$ unitary matrices. U(N) is a N^2-dimensional Lie group which can be spanned by Hermitian generators T^a, $a = 1 \dots N^2$ that fulfill $\mathrm{Tr}_N\Big(T^a\, T^b\Big) = \delta^{ab}$. These also form a basis for expanding the unitary gauge field $A_\mu(x)$,

$$A_\mu(x) = A^a_\mu(x)\, T^a. \tag{4.1}$$

Let us now consider the *star unitary* U(N) element $U(x)$ on $\mathbb{R}^D_{\mathrm{NC}}$,

$$U^\dagger(x) \star U(x) = \mathbb{1}_N. \tag{4.2}$$

From Eq. (2.39) one can see how this expression reduces to the conventional unitarity definition for a vanishing NC tensor $\Theta \to 0$.

If we consider two star unitary U(N) gauge fields $U(x)$ and $V(x)$, we can see from

$$(U(x) \star V(x))^\dagger = V^\dagger(x) \star U^\dagger(x)\,, \quad U(x)\,, V(x) \in \mathrm{U}(N) \tag{4.3}$$

that the star product of two star unitary matrix fields is star unitary again, $U(x) \star V(x) \in \mathrm{U}(N)$. Therefore the U($N$) group is closed under the star product.

We now consider two SU(N) group elements $W(x)$ and $X(x)$. They can be expanded as in Eq. (4.1), where

$$\mathrm{Tr}_N(T^a) = 0 \tag{4.4}$$

holds for the SU(N) group. Due to the identity $\mathrm{Tr}_N\Big([T^a, T^b]\Big) = 0$ the algebra closes under regular multiplication. If the group multiplication is the star product, we have

$$[W^a\, T_a, X^b\, T_b]_\star = \frac{1}{2}[W^a, X^b]_\star(T_aT_b+T_bT_a)+\frac{1}{2}\{W^a, X^b\}_\star(T_aT_b-T_bT_a). \tag{4.5}$$

Since we have in general $\mathrm{Tr}_N(T_aT_b + T_bT_a) \neq 0$, the algebra does not close. Therefore we must conclude that the SU(N) group is not closed under the star product, $W(x) \star X(x) \notin \mathrm{SU}(N)$.

We are therefore unable to formulate a SU(N) gauge theory on a NC space[1]. Thus we will only consider U(N) NC gauge theories in general, and the U(1) NC gauge theory in particular.

The pure U(1) gauge theory

In order to formulate the NC U(1) gauge theory, it is again convenient to use the Weyl mapping between the Weyl operators $\hat{\mathcal{W}}_\mu[A]$ and some functions $A_\mu(x)$ on commuting coordinates but with star product multiplication,

$$\hat{\mathcal{W}}_\mu[A] = \int \mathrm{d}^D x\, \hat{T}_{\mathbb{R}}(x) \otimes A_\mu(x)\,. \tag{4.6}$$

The noncommutativity of the star product implies that even the U(1) gauge fields do not commute, i.e. $A_\mu(x) \star A_\nu(x) \neq A_\nu(x) \star A_\mu(x)$.

Applying straightforwardly the methods from Chapter 2, we write the Euclidean action as

$$S = \frac{1}{4}\,\mathrm{Tr}_{\mathrm{Op}} \otimes \mathrm{Tr}_N\Big(\Big(\Big[\hat{\partial}_\mu, \hat{\mathcal{W}}_\nu[A]\Big] - \Big[\hat{\partial}_\nu, \hat{\mathcal{W}}_\mu[A]\Big] + \mathrm{i}g\,\Big[\hat{\mathcal{W}}_\mu[A]\,, \hat{\mathcal{W}}_\nu[A]\Big]\Big)^2\Big)\,. \tag{4.7}$$

The coupling constant is denoted by g.

In the language of the star product the action is

$$S[A] = \frac{1}{4}\int \mathrm{d}^D x\, \mathrm{Tr}_N(F_{\mu\nu}(x) \star F_{\mu\nu}(x))\,, \tag{4.8}$$

[1] NC SU(N) gauge theories are still discussed in the literature. There the SU(N) are embedded into some higher groups Jurco et al. [2001], Carlson et al. [2001], Calmet et al. [2002].

with the field strength tensor

$$F_{\mu\nu} = \partial_\mu A_\nu - \partial_\nu A_\mu + \mathrm{i}g[A_\mu, A_\nu]_\star. \tag{4.9}$$

The NC U(1) gauge theory therefore is a Yang-Mills theory. It shares some properties with other nonabelian theories, e.g. a negative β-function. In fact, the one-loop β-function after renormalization can be computed as Martín and Sanchez-Ruiz [1999]

$$\beta\big(g^2\big) = \frac{\partial g^2}{\partial \ln(\Lambda)} = -\frac{11}{3}\frac{g^4}{4\pi^2}. \tag{4.10}$$

Λ denotes the momentum cutoff. We see that even the NC U(1) gauge theory is asymptotically free; the effective coupling decreases at very short distances.

It is also conjectured that the NC photons form bound states Fatollahi and Jafari [2003], similarly to *glueballs* in Quantum Chromodynamics.

4.2 Observables and Star Gauge Invariance

Star gauge invariance

The defining feature of a U(N) gauge theory is its invariance under a U(N) transformation of the field(s). For this purpose we introduce a U(N) field $G(x)$. In the language of Weyl operators the unitarity is expressed as

$$\hat{\mathcal{W}}[G]\,\hat{\mathcal{W}}^\dagger[G] = \hat{\mathcal{W}}^\dagger[G]\,\hat{\mathcal{W}}[G] = \hat{\mathbb{1}} \otimes \mathbb{1}_N, \tag{4.11}$$

while the corresponding expression in the language of the star product is

$$G(x) \star G^\dagger(x) = G^\dagger(x) \star G(x) = \mathbb{1}_N. \tag{4.12}$$

From the expression (4.7) one can see that the action is invariant under

$$\hat{\mathcal{W}}_\mu[A] \to \hat{\mathcal{W}}[G]\ \hat{\mathcal{W}}_\mu[A]\ \hat{\mathcal{W}}^\dagger[G] + \mathrm{i}\,\hat{\mathcal{W}}[G]\left[\hat{\partial}_\mu, \hat{\mathcal{W}}^\dagger[G]\right]. \tag{4.13}$$

We can express this symmetry with the star product as

$$A_\mu(x) \to G(x) \star A_\mu(x) \star G^\dagger(x) + \mathrm{i}\,G(x) \star \partial_\mu G^\dagger(x)\,, \tag{4.14}$$

where $G(x)$ is now a star unitary matrix field.

Summarizing, the gauge transformation formalism can readily be translated to the NC world. A NC U(N) gauge theory is a theory invariant under the U(N) star gauge transformation (4.14).

Star gauge invariant observables

To investigate star gauge invariant observables, we first consider some arbitrary smooth contour $\mathcal{C}_v$ connecting two points x and $x+v$. The contour $\mathcal{C}_v$ is parametrized by $t \in [0,1]$, $\xi(t) : [0,1] \to \mathbb{R}^D$ with $\xi(0) = 0$ and $\xi(1) = v$.

The parallel transporter $\mathcal{U}$ over the contour $\mathcal{C}_v$ is given by

$$\mathcal{U}(x, \mathcal{C}_v) = \hat{\mathrm{P}} \exp_\star \left(\mathrm{i} \int_{\mathcal{C}_v} \mathrm{d}\xi_\mu \, A_\mu(x+\xi) \right). \tag{4.15}$$

In this formula $\hat{\mathrm{P}}$ is the path ordering operator. The function $\exp_\star$ is to be understood such that in the Taylor expansion the regular products are replaced by the star product. $\mathcal{U}(x, \mathcal{C}_v)$ is a $N \times N$ star unitary matrix. It transforms under the star gauge transformation as

$$\mathcal{U}(x, \mathcal{C}_v) \to G(x) \star \mathcal{U}(x, \mathcal{C}_v) \star G^\dagger(x+v) \,. \tag{4.16}$$

It is worth pointing out again that plane waves $\mathrm{e}^{\mathrm{i}k_\mu x_\mu}$ generate translations on a NC spacetime

$$\phi(x+v) = \mathrm{e}^{\mathrm{i}k_\mu x_\mu} \star \phi(x) \star \mathrm{e}^{-\mathrm{i}k_\rho x_\rho}, \qquad k_\mu = (\Theta^{-1})_{\mu\nu} v_\nu, \tag{4.17}$$

where Θ has to be invertible. This property can be derived from

$$\mathrm{e}^{\mathrm{i}k_\mu x_\mu} \star \mathrm{e}^{\mathrm{i}p_\nu x_\nu} \star \mathrm{e}^{-\mathrm{i}k_\rho x_\rho} = \mathrm{e}^{\mathrm{i}\, p_\mu (x_\mu + \Theta_{\mu\nu} k_\nu)}, \tag{4.18}$$

which in turn is a consequence of the star unitarity of plane waves and Eq. (2.15). From this expression one can see that the translation group is a subgroup of the star gauge group (for a NC gauge theory).

Having now defined the NC parallel transporter, we can associate any contour $\mathcal{C}_v$ with a star gauge invariant observable $\mathcal{O}$ by

$$\mathcal{O}(\mathcal{C}_v) = \int \mathrm{d}^D x \, \mathrm{Tr}_N \Big(\mathcal{U}(x, \mathcal{C}_v) \star \mathrm{e}^{\mathrm{i}k_\mu x_\mu} \Big) \,. \tag{4.19}$$

The star gauge invariance follows from Eqs. (4.14), (4.17) and the cyclicity of the trace over the star product.

There is a decisive difference to commutative gauge theories. In commutative gauge theories only closed contours make gauge invariant observables. In the NC case, however, even open contours correspond to gauge invariant observables. We will call these open contour observables *Polyakov lines.*

Since momentum operators induce translation, it is natural to associate the line parameter k in Eq. (4.17) with a momentum. In fact, k gives the total momentum of the observable $\mathcal{O}(\mathcal{C}_v)$. This peculiarity is closely related

to the UV/IR mixing introduced in Section 2.3. If the momentum component k_μ increases, the length of the associated contour in the ν-direction increases proportionally to $\Theta_{\mu\nu}k_\mu$. In the commutative limit $\Theta \to 0$ we have $v \to 0$, so no gauge invariant observable is associated with open lines in the commutative space.

Of course, we can employ Eq. (4.19) in the case of closed contours $\mathcal{C}_0$, too. They are associated with a vanishing momentum, $\exp(\mathrm{i}k_\mu x_\mu) = 1$. Therefore the dynamics of the closed Wilson loops is much more restricted when compared to the commutative case. For the commutative limit $\Theta \to 0$ we gain the freedom to plug any function $\phi(x)$ into the kernel of (4.19), since the total momentum of a commutative closed Wilson loop is unrestricted. If we choose $\phi(x)$ to be a δ-function at some specific spacetime point x, we recover the usual gauge invariant Wilson loop of gauge theories.

A remarkable property of the closed NC Wilson loops is that they are complex valued. This is due to the broken parity on a NC space, caused by the NC tensor Θ.

4.3 Lattice Gauge Theories and the Twisted Eguchi-Kawai Model

The Eguchi-Kawai equivalence

In 1982 T. Eguchi and H. Kawai conjectured that commutative (Euclidean) U(N) and SU(N) lattice gauge theories in the large N limit would be equivalent to their dimensionally reduced ($D = 0$) model Eguchi and Kawai [1982]. The reduced model, called the *Eguchi-Kawai (EK) model,* is obtained by replacing all U(N) (resp. SU(N)) matrix link variables lying in the μ-direction with one unitary $N \times N$ matrix U_μ.

The Eguchi-Kawai model has the action

$$S_{\mathrm{EK}}[U] = -\beta \sum_{\mu \neq \nu} \mathrm{Tr}_N \left(U_\mu \, U_\nu \, U_\mu^\dagger \, U_\nu^\dagger \right), \quad \mu, \nu = 1 \ldots D \tag{4.20}$$

$$\text{with} \quad \beta = \frac{1}{g^2}. \tag{4.21}$$

If the $\mathrm{U}^D(1)$ center symmetry is not spontaneously broken, the above theory obeys the same *Schwinger-Dyson equations* as the U(N) lattice gauge theory (for $N \to \infty$), thus it obeys the same relations as Wilson loops on the lattice. This $\mathrm{U}^D(1)$ symmetry is unbroken for $D = 2$. However, for $D > 2$ the *Eguchi Kawai equivalence* does not hold anymore in general. It is valid in the strong

coupling sector only, since there the $\mathrm{U}^D(1)$ symmetry is unbroken Bhanot et al. [1982].

The twisted Eguchi-Kawai model

Shortly afterward A. González-Arroyo and M. Okawa found a way around this restriction by replacing periodic boundary conditions with *twisted boundary conditions* González-Arroyo and Okawa [1983]. The twisted boundary conditions significantly alter the model's behavior at weak coupling by preventing the $\mathrm{U}^D(1)$ symmetry breaking.

The first step in constructing the *twisted Eguchi-Kawai (TEK)* model consists of transforming the lattice link variables in the Wilson gauge action

$$S_{\mathrm{Wilson}}[U] = -\beta \sum_{x,\mu\neq\nu} \mathrm{Tr}_N\Big(U_\mu(x)\; U_\nu(x+a\hat{\mu})\; U_\mu^\dagger(x+a\hat{\nu})\; U_\nu^\dagger(x)\Big) \quad (4.22)$$

according to

$$U_\mu(x) \to \mathcal{Z}_\mu(x)\; U_\mu(x)\,, \quad \mathcal{Z}_\mu(x) \in \mathrm{Z}_N. \quad (4.23)$$

This transformation leaves the integration measure invariant. Carrying out this procedure yields

$$S[U] = -\beta \sum_{x,\mu\neq\nu} \mathcal{Z}_{\mu\nu}\, \mathrm{Tr}_N\Big(U_\mu(x)\; U_\nu(x+a\hat{\mu})\; U_\mu^\dagger(x+a\hat{\nu})\; U_\nu^\dagger(x)\Big)\,. \quad (4.24)$$

This expression differs from Eq. (4.22) only in the *twist* $\mathcal{Z}_{\mu\nu}$, which we have encountered before in Section 2.4. If we now apply the Eguchi-Kawai equivalence to the twisted Wilson action, we arrive at the TEK model with the action

$$S_{\mathrm{TEK}}[U] = -\beta \sum_{\mu\neq\nu} \mathcal{Z}_{\mu\nu}\, \mathrm{Tr}_N\Big(U_\mu\, U_\nu\, U_\mu^\dagger\, U_\nu^\dagger\Big)\,, \quad \mathcal{Z}_{\mu\nu} \in \mathrm{Z}_N. \quad (4.25)$$

The twist $\mathcal{Z}_{\mu\nu}$ can be described by an integer valued $D \times D$ antisymmetric matrix $n_{\mu\nu}$, resulting in

$$\mathcal{Z}_{\mu\nu} = \mathcal{Z}_{\nu\mu}^* = \mathrm{e}^{2\pi\mathrm{i}\, n_{\mu\nu}/N}, \quad n_{\mu\nu} \in \mathbb{Z}. \quad (4.26)$$

The Eguchi-Kawai equivalence also allows translating arbitrary shapes on the lattice into their matrix model equivalent. If we e.g. consider an $I \times J$ Wilson loop in the μ-ν plane, denoted by $W_{\mu\nu}^{(I\times J)}$, we find the matrix model equivalent

$$W_{\mu\nu}^{(I\times J)} = \mathcal{Z}_{\mu\nu}^{IJ}\, \mathrm{Tr}_N\Big(U_\mu^I\, U_\nu^J\, U_\mu^{\dagger I}\, U_\nu^{\dagger J}\Big)\,. \quad (4.27)$$

In Ref. González-Arroyo and Korthals Altes [1983] it is shown that the TEK model (4.25) is again equivalent to commutative U(N) and SU(N) lattice models in the $N \to \infty$ limit. Due to the previously mentioned improved symmetry properties this equivalence extends to gauge theories with $D > 2$ at weak coupling.

Since the $D = 2$ case could be handled with the EK model already, there seemed to be little value in considering a two-dimensional TEK model. This was even more true since D. J. Gross and E. Witten had succeeded in solving the 2D U(N) and SU(N) lattice gauge theories in the planar large N limit analytically Gross and Witten [1980].

The TEK model as a NC U(n) gauge theory

The missing incentive was provided by the insight that the TEK model (4.25) is not only related to commutative lattice gauge theories. In Ref. Aoki et al. [2000] H. Aoki *et al.* showed that TEK models at $N \to \infty$ are equivalent to NC U(n) , $n = 1, 2, \ldots$ gauge theories on infinite lattices as well[2]. They embedded the (dynamically generated) coordinates and momenta of the TEK model into matrices. These matrices are Morita equivalent to functions of commuting coordinates. However, upon the mapping the product transforms into the star product, while the trace turns into integrals, just like in the Weyl mapping. In the end one recovers the action (4.8).

Later on Refs. Ambjørn et al. [2000a, 1999, 2000b] showed that even the TEK model with finite matrices could be interpreted as a NC U(n) lattice gauge theory.

We now consider the most elementary scenario, namely a two-dimensional U(1) gauge theory. Translating the pure lattice ($\mathbb{T}^2_{\mathrm{NC}}$) gauge theory with compact link variables into gauge unitary Weyl operators $\hat{\mathcal{W}}_\mu[U]$, we obtain

$$S = -\beta \sum_{\mu \neq \nu} \mathrm{Tr}_{\mathrm{Op}} \Big(\hat{\mathcal{W}}_\mu[U] \left(\hat{D}_\mu \hat{\mathcal{W}}_\nu[U] \, \hat{D}_\mu^\dagger \right) \left(\hat{D}_\nu \hat{\mathcal{W}}_\mu^\dagger[U] \, \hat{D}_\nu^\dagger \right) \hat{\mathcal{W}}_\nu^\dagger[U] \Big) \,, \quad (4.28)$$

where $\hat{D}_\mu$ is the shift operator from Eq. (2.65). If we now apply the technique of dimensional reduction from Section 2.4, we arrive at

$$S = -\beta \sum_{\mu \neq \nu} \mathrm{Tr}_N \Big(\hat{U}_\mu \left(\hat{\Gamma}_\mu \hat{U}_\nu \hat{\Gamma}_\mu^\dagger \right) \left(\hat{\Gamma}_\nu \hat{U}_\mu^\dagger \hat{\Gamma}_\nu^\dagger \right) \hat{U}_\nu^\dagger \Big) \,. \quad (4.29)$$

Here the shifts between the lattice sites are implemented by employing the twist eaters $\hat{\Gamma}_\mu$ from Eqs. (2.94) and (2.95). The Weyl operators $\hat{\mathcal{W}}_\mu[U]$ have

[2] In the following n is to refer to the rank of the gauge group U(n), while N refers to the size of the U_μ unitary matrices in the reduced model.

become unitary $N \times N$ matrices $\hat{U}_\mu$. Since the twist eaters obey the Weyl-'t Hooft commutation relation (2.97), we can upon redefinition of the "gauge fields" $\hat{U}_\mu$

$$\hat{V}_\mu = \hat{U}_\mu \hat{\Gamma}_\mu, \qquad \mu = 1, 2 \tag{4.30}$$

express Eq. (4.29) as

$$S[\hat{V}] = -\beta \sum_{\mu \neq \nu} \mathcal{Z}_{\mu\nu} \operatorname{Tr}_N \left(\hat{V}_\mu \hat{V}_\nu \hat{V}_\mu^\dagger \hat{V}_\nu^\dagger \right).$$

This is again the TEK model from Eq. (4.25).

In summary, the TEK model has a very rich structure. It can represent commutative U(N) and SU(N) lattice gauge theories in the planar limit $N \to \infty$. However, it is also equivalent to NC U(n) lattice gauge theories, both for finite and infinite N.

4.4 NC 4D U(1) Gauge Theory

We now want to describe the four-dimensional theory we have actually simulated. The underlying manifold is a hybrid of two NC directions and two commutative directions. We still work on a Euclidean manifold. Not choosing all directions to be noncommutative avoids conceptual difficulties such as a spurious unitarity or broken causality due to a NC time Bahns et al. [2002]. We chose a two-dimensional NC subspace, since we require the NC tensor Θ to be invertible. In our convention the 1- and 2-directions form a NC plane, while the 3- and 4-directions are commutative. x_4 represents the (Euclidean) time.

This means that the NC tensor Θ, which we still assume to be constant across the spacetime, can be condensed to one NC parameter θ,

$$\Theta_{12} = -\Theta_{21} = \theta, \qquad \text{all other } \Theta_{\mu\nu} = 0. \tag{4.31}$$

The construction of the 4D manifold

In practice we use a 2D commutative and discrete torus $\mathbb{T}^2$ to represent the 3-4 plane. Both directions have an extent of La, where a is again the lattice spacing.

We now need to add the missing degrees of freedom from a 4D NC gauge theory. This is achieved by attaching four unitary $N \times N$ matrices $\hat{V}_\mu$, $\mu = 1 \ldots 4$ to each point (x_3, x_4). Due to the equivalence of the TEK model to a NC $N \times N$ lattice gauge theory, each unitary matrix $\hat{V}_\mu$ can represent a

U(1) gauge field on a NC plane. In our case this lattice constitutes a 2D NC discrete torus as described in Section 2.2, hence the NC parameter is given by Eq. (2.91).

We want to repeat that the previously developed NC machinery only works for odd N (cf. Section 2.4). Often one strives for lattices with equal extent in each direction. Here we chose $L = N \pm 1$, such that L is a multiple of 4 (cf. Tab. 4.1). For sufficiently big N and L this difference becomes negligible. We chose L this way in order to parallelize the simulations more easily. In our simulations we divided the commutative plane into 8 patches, and thus simulated on 8 processors.

Because we attach $\hat{V}_\mu$ to each point (x_3, x_4), we are dealing with a field theory on a four-dimensional discrete manifold,

$$U_\mu(x_1, x_2, x_3, x_4) \quad \longleftrightarrow \quad \hat{V}_\mu(x_3, x_4)\,. \tag{4.32}$$

The star product maps to the matrix product,

$$U_\mu(x_1, x_2, x_3, x_4) \star U_\nu(x_1, x_2, x_3, x_4) \quad \longleftrightarrow \quad \hat{V}_\mu(x_3, x_4)\, \hat{V}_\nu(x_3, x_4)\,. \tag{4.33}$$

Translation on our hybrid world is handled by

$$\begin{aligned} U_\mu\Big(x_1 + m\,a\,\hat{1}, x_2 + n\,a\,\hat{2}, x_3, x_4\Big) \quad &\longleftrightarrow \quad \hat{\Gamma}_2{}^n\, \hat{\Gamma}_1{}^m\, \hat{V}_\mu(x_3, x_4)\, \hat{\Gamma}_1^{\dagger m}\, \hat{\Gamma}_2^{\dagger n}, \\ U_\mu\Big(x_1, x_2, x_3 + m\,a\,\hat{3}, x_4 + n\,a\,\hat{4}\Big) \quad &\longleftrightarrow \quad \hat{V}_\mu\Big(x_3 + m\,a\,\hat{3}, x_4 + n\,a\,\hat{4}\Big)\,, \end{aligned} \tag{4.34}$$

where $\hat{\mu}$ is again the unit vector in the μ-direction. Summation over the NC plane is easily achieved through

$$\frac{1}{N^2} \sum_{x_1, x_2} U_\mu(x_1, x_2, x_3, x_4) \quad \longleftrightarrow \quad \frac{1}{N}\, \mathrm{Tr}_N\Big(\hat{V}_\mu(x_3, x_4)\Big)\,. \tag{4.35}$$

The action of the matrix model

Constructing the 4D manifold from both a NC and a commutative plane naturally splits the action into three different parts,

$$S = S_{\mathrm{NC}} + S_{\mathrm{mixed}} + S_{\mathrm{comm}}. \tag{4.36}$$

As we have seen in Section 4.3, the contribution of the action S_{NC} of Wilson loops lying in the NC plane is given by the TEK model

$$S_{\mathrm{NC}} = -N\beta\mathcal{Z}_{12} \sum_{x_3, x_4} \mathrm{Tr}_N\Big(\hat{V}_1(x_3, x_4)\; \hat{V}_2(x_3, x_4)\; \hat{V}_1^\dagger(x_3, x_4)\; \hat{V}_2^\dagger(x_3, x_4)\Big) + \text{c.c.}$$

(4.37)

In the numerical simulations the twist was set to

$$\mathcal{Z}_{12} = \mathcal{Z}_{21}^{*} = \exp\left(\frac{\pi \mathrm{i}\,(N+1)}{N}\right), \quad N \text{ odd.} \tag{4.38}$$

The contribution S_{mixed} arises from the loops lying partially in the NC plane and partially in the commutative planes,

$$\begin{aligned} S_{\text{mixed}} = &- N\beta \sum_{x_3,x_4} \sum_{\mu=1}^{2} \sum_{\nu=3}^{4} \mathrm{Tr}_N \Big(\hat{V}_\mu(x_3,x_4)\; \hat{V}_\nu(x_3,x_4) \\ &\hat{V}_\mu^\dagger((x_3,x_4)+a\hat{\nu})\, \hat{V}_\nu^\dagger(x_3,x_4) \Big) + \text{c.c.} \end{aligned} \tag{4.39}$$

Finally, the part of the action due to loops lying in the commutative plane is

$$\begin{aligned} S_{\text{comm}} = &- N\beta \sum_{x_3,x_4} \mathrm{Tr}_N \Big(\hat{V}_3(x_3,x_4)\; \hat{V}_4\Big(x_3 + a\hat{3}, x_4\Big) \\ &\hat{V}_3^\dagger(x_3, x_4 + a\hat{4}) \hat{V}_4^\dagger(x_3,x_4) \Big) + \text{c.c.} \end{aligned} \tag{4.40}$$

Symmetries in the matrix model

The symmetry that the action of a U(1) gauge theory should first and foremost respect, is of course the U(1) symmetry. The U(1) gauge transformation leaving the action invariant is given by

$$\hat{V}_\mu(x_3,x_4) \to \begin{cases} \hat{G}(x_3,x_4)\; \hat{V}_\mu(x_3,x_4)\; \hat{G}^\dagger(x_3,x_4) & \text{for } \mu = 1,2, \\ \hat{G}(x_3,x_4)\; \hat{V}_\mu(x_3,x_4)\; \hat{G}^\dagger((x_3,x_4)+a\hat{\mu}) & \text{for } \mu = 3,4. \end{cases} \tag{4.41}$$

Remembering from Section 4.3 that the Eguchi-Kawai equivalence holds only for an unbroken $\mathrm{U}^2(1)$ symmetry, it is worth keeping an eye on this particular symmetry. A $\mathrm{U}^2(1)$ transformation of the $\hat{V}_\mu(x_3,x_4)$ fields is given by the global phase shift

$$\hat{V}_\mu(x_3,x_4) \to \mathrm{e}^{\mathrm{i}\alpha_\mu} \hat{V}_\mu(x_3,x_4)\,, \quad \mu = 1,2, \tag{4.42}$$

where the α_μ are arbitrary phases. We will see below that this symmetry is respected only at strong and weak coupling.

Remember from Section 4.2 that the translation group is a subgroup of the U(1) gauge group. In fact, in this model the translational group (in

the NC directions) is a subgroup of $\mathrm{U}^2(1)$ (up to a star gauge transformation) Bietenholz et al. [2004b]. In case of a spontaneously broken translation invariance, momentum conservation is spontaneously broken, too.

The order parameter for this symmetry is the Polyakov line $P_{\mu,l}$, which will be presented in Eq. (4.51). An expectation value $\langle |P_{\mu,l}| \rangle$ well above zero indicates a broken $\mathrm{U}^2(1)$ symmetry.

From the specific setup of our 4D model, a mix of NC and commutative lattices, we see that the theory is invariant under the exchange of the two commutative directions 3 and 4. Furthermore it is invariant under

$$\begin{cases} \hat{V}_1(x_3, x_4) & \to & \hat{V}_2(x_3, x_4) \\ \hat{V}_2(x_3, x_4) & \to & \hat{V}_1^\dagger(x_3, x_4) \end{cases} . \tag{4.43}$$

Observables in the matrix model

As we have seen in Section 4.2, in NC $\mathrm{U}(N)$ gauge theories open and closed contours are associated with star gauge invariant observables.

We first consider the closed $I \times J$ Wilson loops lying in the μ-ν plane, denoted by $W_{\mu\nu}^{(I\times J)}$. The symbol $W_{\mu\nu}$ represents the 1×1 Wilson plaquette. In order to discuss Wilson loops, it is convenient to introduce the parallel transporter

$$\begin{aligned} \hat{\mathcal{V}}_\mu(x_3, x_4, n) \equiv \hat{V}_\mu(x_3, x_4)\ \hat{V}_\mu((x_3, x_4) + a\hat{\mu}) \\ \dots \hat{V}_\mu((x_3, x_4) + (n-1)a\hat{\mu})\,. \end{aligned} \tag{4.44}$$

The Wilson loops are now given by

$$\begin{aligned} W_{12}^{(I\times J)} = \mathcal{Z}_{12}^{IJ} \frac{1}{NL^2} \sum_{x_3,x_4} \mathrm{Tr}_N \Big(\hat{V}_1^I(x_3, x_4)\, \hat{V}_2^J(x_3, x_4) \\ \hat{V}_1^{\dagger I}(x_3, x_4)\ \hat{V}_2^{\dagger J}(x_3, x_4) \Big), \end{aligned} \tag{4.45}$$

$$\begin{aligned} W_{\mu\nu}^{(I\times J)} = \frac{1}{NL^2} \sum_{x_3,x_4} \mathrm{Tr}_N \Big(\hat{V}_\mu^I(x_3, x_4)\ \hat{\mathcal{V}}_\nu(x_3, x_4, J) \\ \hat{V}_\mu^{\dagger I}((x_3, x_4) + Ia\hat{\nu})\ \hat{\mathcal{V}}_\nu^\dagger(x_3, x_4, J) \Big), \qquad \mu = 1, 2 \quad \nu = 3, 4, \end{aligned} \tag{4.46}$$

$$\begin{aligned} W_{34}^{(I\times J)} = \frac{1}{NL^2} \sum_{x_3,x_4} \mathrm{Tr}_N \Big(\hat{\mathcal{V}}_3(x_3, x_4, I)\ \hat{\mathcal{V}}_4\Big(x_3 + Ia\,\hat{3}, x_4, J\Big) \\ \hat{\mathcal{V}}_3^\dagger\Big(x_3, x_4 + Ja\,\hat{4}, I\Big)\ \hat{\mathcal{V}}_4^\dagger(x_3, x_4, J) \Big). \end{aligned} \tag{4.47}$$

From these expressions we see that $I \times I$ square Wilson loops obey

$$W_{\mu\nu}^{(I\times I)} = (W_{\nu\mu}^{(I\times I)})^*, \quad \mu, \nu = 1 \ldots 4. \tag{4.48}$$

In the following we will focus on square shaped Wilson loops, since it was found in numerical simulations in $D = 2$ that these converge the fastest Gross and Witten [1980].

From the symmetries of the action one can infer that all four mixed Wilson loops have the same real expectation value,

$$\langle W_{1\nu} \rangle = \langle W_{2\nu} \rangle \in \mathbb{R}, \quad \nu = 3, 4. \tag{4.49}$$

The commutative Wilson loops are always real,

$$W_{34} \in \mathbb{R}. \tag{4.50}$$

As we have seen, a closed contour on a NC spacetime does not carry any momentum. This corresponds to the fact that $W_{\mu\nu}^{(I\times I)}$ is invariant under a $\mathrm{U}^2(1)$ transformation.

In the same manner as above we can build any (closed) contour on our 4D lattice.

On the NC lattice open contours make good (star gauge invariant) observables as well. In the matrix model the Polyakov line $P_{\mu,l}$ of length l is given by

$$P_{\mu,l} = \frac{1}{NL^2} \sum_{x_3,x_4} \mathrm{Tr}_N\left(\hat{V}_\mu^l(x_3, x_4)\right), \qquad \mu = 1, 2. \tag{4.51}$$

The Polyakov lines $P_{\mu,l}$ carry a momentum with the absolute value Bietenholz et al. [2002, 2006]

$$p = \frac{2\pi n}{Na}, \qquad n = \begin{cases} \frac{l}{2} & \text{for even } l, \\ \frac{l+N}{2} & \text{for odd } l. \end{cases} \tag{4.52}$$

We see that the lowest momenta p are associated with $P_{\mu,2}$, $P_{\mu,4}$, $P_{\mu,6}$ …, which is an effect of the twisted boundary conditions. The Polyakov lines $P_{\mu,l}$ with odd l carry a momentum of the cutoff order, so they do not couple to excitations surviving in the continuum limit. Therefore we focus on the $P_{\mu,l}$ with even l.

We have hinted before that $P_{\mu,l}$ serves as an order parameter. It detects the spontaneous breaking of the $\mathrm{U}^2(1)$ symmetry, cf. Eq. (4.42).

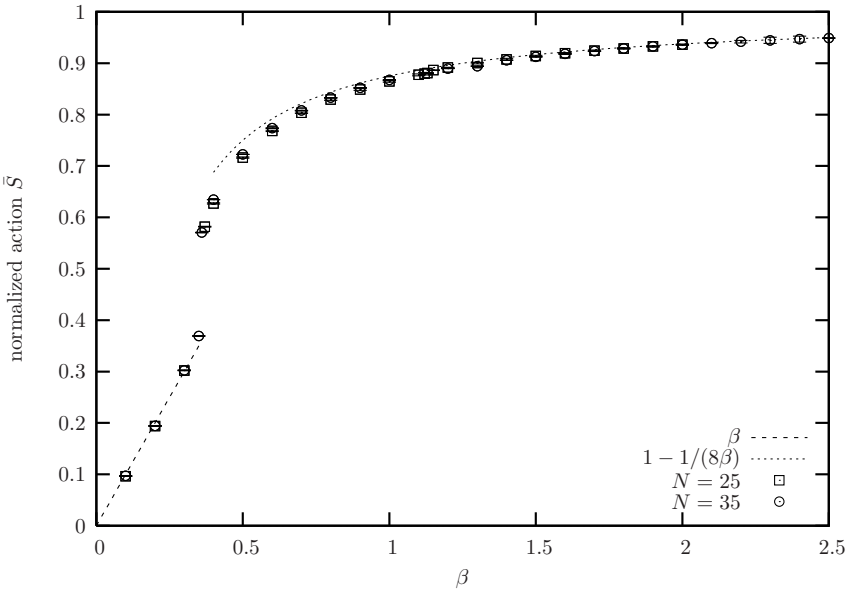

Figure 4.1: *The normalized action $\bar{S}$ from Eq. (4.53) as a function of β. The dotted lines show the prediction for the strong coupling limit, $\bar{S}_{\text{strong}} = \beta$, resp. the weak coupling limit prediction, $\bar{S}_{\text{weak}} = 1 - 1/(8\beta)$. They are due to strong and weak coupling expansions. The numerical results were obtained at $N = 25$ and $N = 35$.*

4.5 The Phase Diagram

The strong, intermediate and weak coupling phases

The first step in investigating the lattice model (4.36) is to determine its phase structure. To this end we measure the normalized action

$$\bar{S} = -\frac{1}{12N^2\beta}\langle S\rangle \tag{4.53}$$

as a function of $\beta = 1/g^2$ (see Eq. (4.21)). S denotes the lattice action (4.36).

The result is shown in Fig. 4.1. We can see that the measurements of the normalized action agree well with the predictions from weak and strong coupling expansions,

$$\bar{S}_{\text{weak}} = 1 - \frac{1}{8\beta} \quad \text{and} \quad \bar{S}_{\text{strong}} = \beta. \tag{4.54}$$

We also found a new phase at intermediate coupling, which we call the *broken phase.* It is characterized by a spontaneously broken $\mathrm{U}^2(1)$ symmetry.

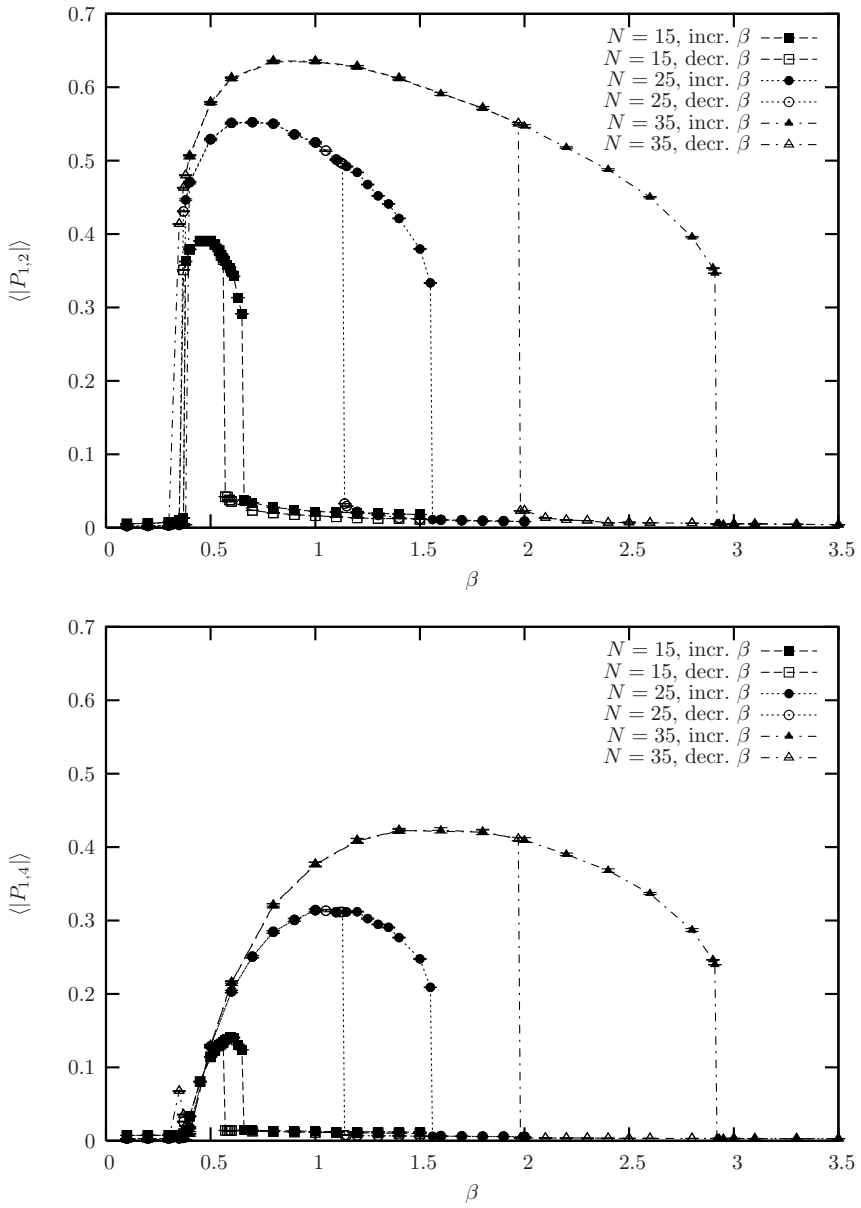

Figure 4.2: *The order parameters* $\langle |P_{\mu,2}| \rangle$ *(top) and* $\langle |P_{\mu,4}| \rangle$ *(bottom) for* $N = 15, 25$ *and* 35*. Regardless of* N *the transition between the strong coupling and the broken phase occurs at about* $\beta \approx 0.35$*. The transition between the broken phase and the weak coupling phase is* N*-dependent. It is characterized by a hysteresis typical for a first order transition, since the transition point depends on whether* β *increases or decreases.*

The $U^2(1)$ group contains the translational group as a subgroup. This causes the translational invariance and momentum conservation to be spontaneously broken. The order parameter signaling the spontaneous breaking of the $U^2(1)$ symmetry is the Polyakov line $P_{\mu,l}$ from Eq. (4.51). A value of $\langle|P_{\mu,l}|\rangle$ well larger than zero indicates the broken symmetry.

In Fig. 4.2 we plot this expectation value for Polyakov lines with length $l = 2$ and $l = 4$ in dependence of β. Since the results for $\langle|P_{1,l}|\rangle$ and $\langle|P_{2,l}|\rangle$ are the same[3] within errors, we plot the average of both directions in order to increase statistics.

For Polyakov lines of odd length l, on the other hand, the spontaneous symmetry breaking is barely visible; the values of $\langle|P_{\mu,l}|\rangle$ are close to zero. In the broken phase the $U(1)^2$ symmetry is broken down to a $(Z_2)^2$ symmetry. That the symmetry is restored for large β values as well as for small β values can be understood from the weak coupling expansion resp. the strong coupling expansion.

The phase transitions

We found that the phase transition from the strong coupling phase to the broken phase always occurs at $\beta \approx 0.35$. This phase transition is independent of the matrix size N, as can be seen in Figs. 4.1 and 4.2. Simulations of similar models found that this phase transition is of first order González-Arroyo and Okawa [1983], Creutz [1981].

From Fig. 4.2 one can see that the transition from the broken phase to the weak coupling phase shows a hysteresis. The β value at which the transition occurs, clearly depends on whether β is increased or decreased. Due to the hysteresis behavior this transition must be of first order.

We want to label that critical β-value by β_c. To be precise, β_c is to refer to the lower of the two β-values. Our simulations found β_c to be compatible with

$$\beta_c \propto N^2. \tag{4.55}$$

The corresponding fits for the critical β are shown in Fig. 4.3.

A consequence is that one ends up in the broken phase for the planar limit ($N \to \infty$ at fixed β), provided $\beta > 0.35$. In the planar limit the NC parameter θ goes to infinity. In perturbation theory around the trivial point this means that commutativity is restored. This is not necessarily true in the present case of spontaneous symmetry breaking, though Bietenholz et al. [2004b].

[3] If the $U^2(1)$ symmetry were only broken down to $U(1)$, $|P_{1,l}|$ and $|P_{2,l}|$ would be very different for a typical configuration. We observe, however, that this is not the case.

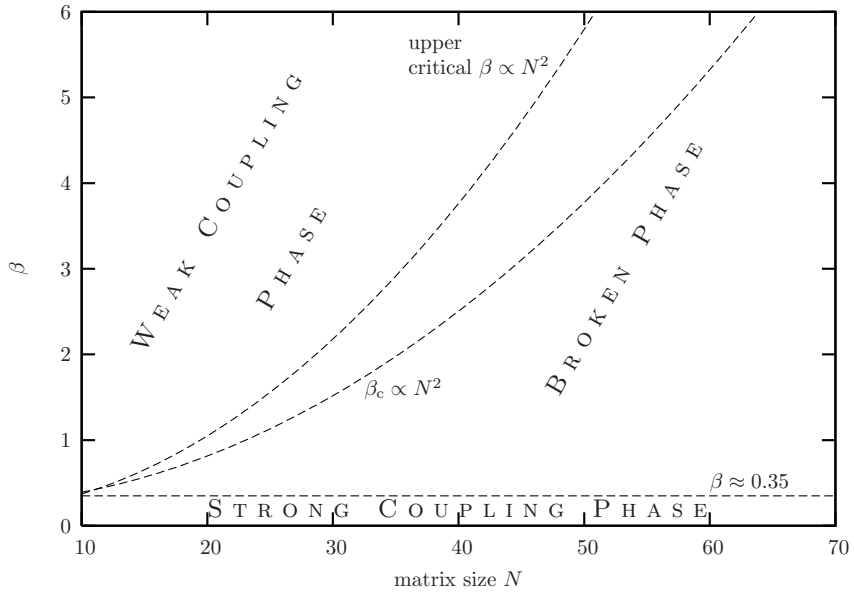

Figure 4.3: *This plot shows schematically the phase structure of the theory in the N-β plane. At low β we are always in the strong coupling phase. As β increases, a new phase, the broken phase, appears. If β is increased even further, the weak coupling phase is reached. Since there is a hysteresis, we show the fits for both critical lines.*

4.6 The Double Scaling Limit

In order to extract physical information from numerical simulations of QFTs, it is necessary to investigate the continuum limit of the theory. Here we are interested in the continuum limit at a fixed NC parameter θ. As discussed in Section 2.5, the limit providing just that is the DSL. The existence of a finite DSL is required for the renormalizability of the theory.

The strategy for investigating a possible DSL was to fine-tune β at different matrix sizes N so that the observables, such as Wilson loops of different sizes, coincide over physical areas. For the fine-tuning we concentrated at first on the decay of the square Wilson loops over their physical side length Ia in the commutative directions, since they show the strongest decay. Because of this feature they are the most suitable Wilson loops for searching for an overlap at different matrix sizes N. In Tab. 4.1 we show the parameters at which we found the best scaling of several observables over the range from $N = 25$ up to $N = 65$.

Tab. 4.1 gives the lattice spacing for each (N, β) set. These spacings refer

N	β	a
25	0.92	1.34
35	1.20	1.13
45	1.50	1.00
55	1.74	0.90
65	2.00	0.83

Table 4.1: *At these parameters we found the best scaling of various observables over the range $N = 25$ up to $N = 65$.*

to an arbitrary scale, where

$$a = 1 \qquad \text{at } N = 45 \text{ and } \beta = 1.5. \tag{4.56}$$

This is equivalent to fixing the NC parameter at (see Eq. (2.91))

$$\theta = \frac{45}{\pi} \approx 14.32. \tag{4.57}$$

The scaling of the Wilson loops in the commutative directions

We have used the Wilson loops lying in the commutative plane for tuning β at the various N such that the scaling is optimal. With the parameters from Tab. 4.1 we obtained the expectation values $\langle W_{34}^{(I\times I)}\rangle$ shown in Fig. 4.4.

We can see that the scaling up to physical lengths of about 10 is excellent for all considered matrix sizes N. Even for larger Wilson loops the scaling becomes good for increasing matrix sizes N. This is in agreement with the expectation that for large lattice resp. matrix sizes finite size effects become negligible.

The vertical axis in Fig. 4.4 is logarithmic. When the expectation value of the $I \times I$ Wilson loops is plotted against the length Ia, one notices a linear behavior. Therefore we conclude that the Wilson loops lying completely in the commutative plane obey a perimeter law. Thus in this phase the theory is nonconfining in the commutative directions.

The fine-tuning of the scaling for one observable is a first hint that a DSL might actually exist for this theory. We now investigate other observables in order to see whether the DSL is really viable.

The scaling of the Wilson loops in the NC directions

As we have seen in Eqs. (4.49) and (4.50), only the Wilson loops lying in the NC plane are truly complex. We are going to look at the real part, the absolute value and the phase of these Wilson loops.

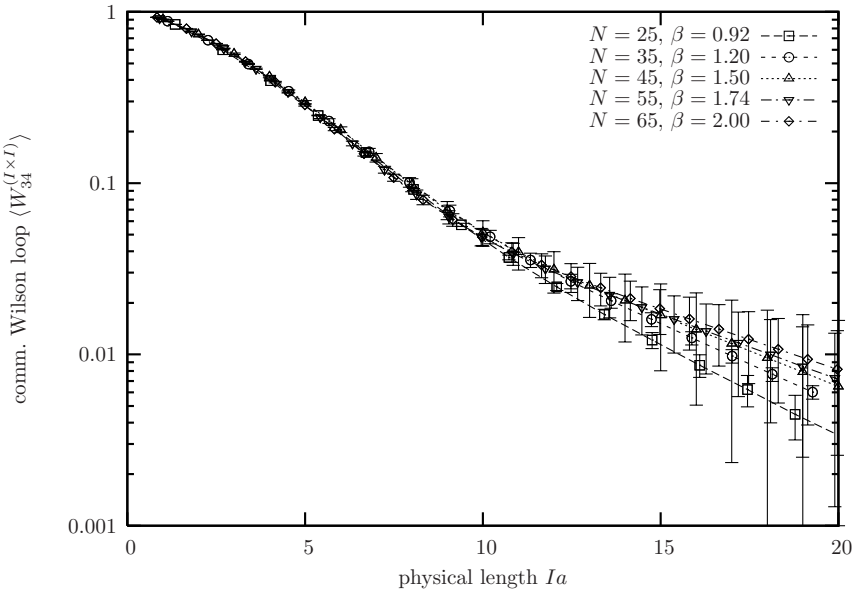

Figure 4.4: *The double scaling of the square Wilson loops lying in the commutative plane. The horizontal axis shows the side length of the Wilson loop in physical units as defined in Eq. (4.56).*

In Fig. 4.5 we show the real part of the Wilson loops lying in the NC plane. The simulations were again run with the parameters from Tab. 4.1. We can see that the scaling is excellent. The only exception one could possibly find are a few $N = 25$ data points. However, the DSL is an asymptotic limit, so we only require the scaling to set in at large N. This is indeed confirmed by our results.

The upper plot in Fig. 4.5 shows another feature of gauge theories on NC spaces as well. The real part first decreases steeply, passes through zero and then begins to oscillate around zero. This oscillation is damped and eventually ceases to exist.

The bottom plot in Fig. 4.5 shows that the decay of $\mathrm{Re}\,\langle W_{12}^{(I\times I)} \rangle$ is exponential at small surrounded areas $(Ia)^2$. Since this behavior occurs at small $(Ia)^2$ only, we cannot infer confinement in the NC directions in general, though.

Apart from this, the real part of Wilson loops lying in the NC plane displays an oscillating dependence at larger sizes. Such oscillations have already been observed in the 2D NC U(1) gauge theory Bietenholz et al. [2002]. Since this feature persists even in the 2+2-dimensional version of the model, we see that the mixing of the NC and the commutative directions

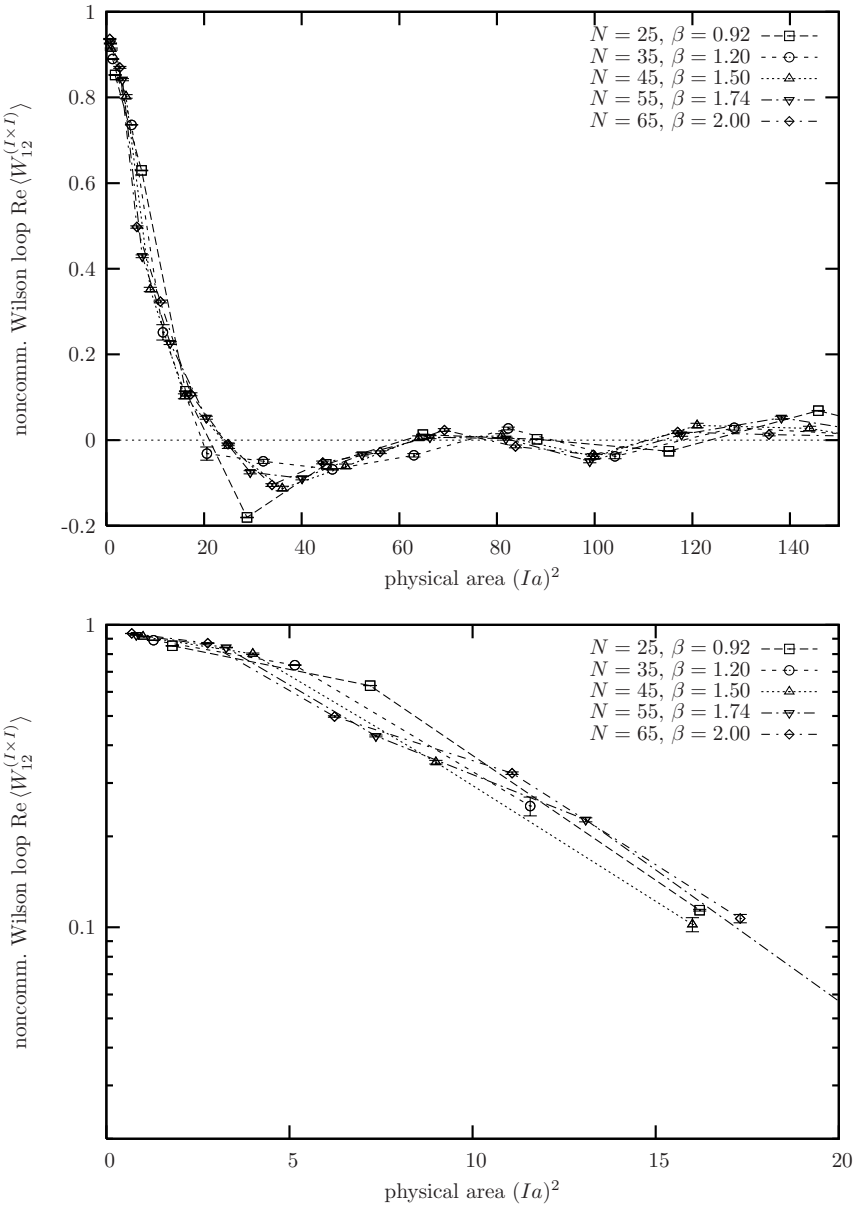

Figure 4.5: *Both plots show the real part of the square Wilson loops lying in the NC plane. The horizontal axis is the area in physical units* $(Ia)^2$*. The lower plot is a zoom into the small area region. In this regime of low areas one can observe a linear behavior indicating an area law. As the area increases the area law gives way to oscillations. In any case, the data at different matrix sizes* N *scale very well.*

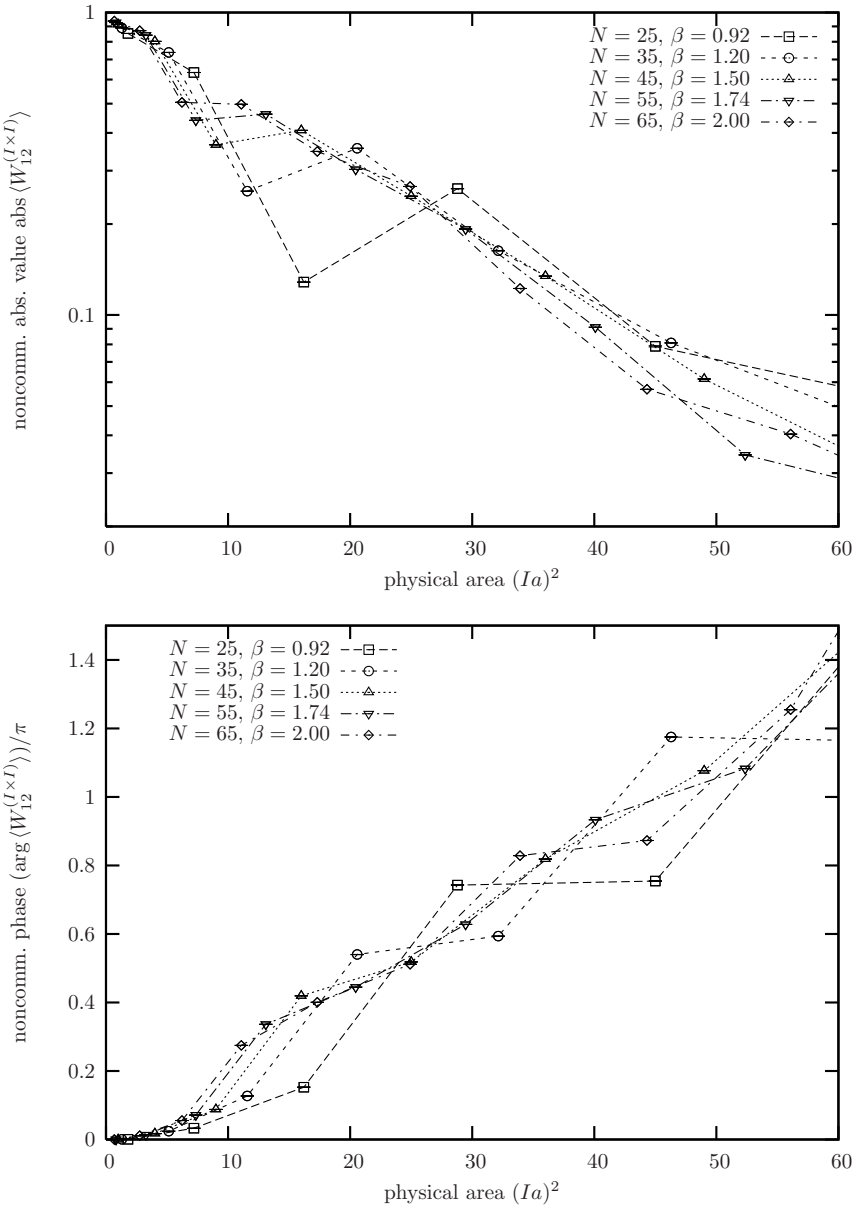

Figure 4.6: *The upper plot shows the absolute values of the NC Wilson loops in dependence of the physical area $(Ia)^2$. We see that their expectation values scale decently, at least for large N. In the bottom plot the phase of the NC Wilson loops is shown. Its behavior is reminiscent of the U(1) gauge theory on a NC plane. For small areas $(Ia)^2$ we see an oscillating behavior, which then gives way to a linear rise. This linear behavior is reminiscent of the Aharonov-Bohm effect.*

does not alter this property qualitatively.

Other instructive observables derived from the NC Wilson loops are their absolute values and their phases. In the upper plot of Fig. 4.6 we show the absolute values of the NC Wilson loops in dependence of the physical area $(Ia)^2$. We can see again that the data follow an area law in the NC directions. The scaling of these values improves significantly as the matrix size N increases.

The bottom plot of Fig. 4.6 displays the phase of the NC Wilson loops in dependence of their physical area $(Ia)^2$. Again we can see that the scaling improves as the matrix size N increases. We also note that this observable shows something akin to oscillations at small areas, which then fade away into a straight line. The phase $\arg \langle W_{12}^{(I\times I)} \rangle$ grows according to

$$\arg \langle W_{12}^{(I\times I)} \rangle = \frac{(Ia)^2}{\theta}. \tag{4.58}$$

This behavior is related to the Aharonov-Bohm effect, if one introduces a (symbolic) magnetic field

$$B = \theta^{-1} \tag{4.59}$$

across the NC plane. This identification is known from open strings Seiberg and Witten [1999]. The same behavior has been seen on the NC plane by Ref. Bietenholz et al. [2002]. Again, the coupling between the NC and the commutative directions does not alter the qualitative behavior of the NC directions when compared to the NC U(1) gauge theory in $D = 2$.

The scaling of the mixed Wilson loops

The expectation values of the Wilson loops lying in the mixed planes are real, just like the ones lying in the commutative plane (cf. Eq. (4.49)).

In Fig. 4.7 we show as a representative how the Wilson loops lying in the 1-3 plane scale as N increases. Their behavior is somewhat intermediate between the NC Wilson loops and the commutative Wilson loops. The initial decay is still reminiscent of a perimeter law, which was observed in the commutative directions. On the other hand, we can still see a faint echo of the oscillating behavior, so some NC characteristics still shine through.

Overall this is another observable that scales excellently and underscores the existence of a finite DSL for this theory.

The scaling of the eigenvalues

Another observable we have investigated in order to demonstrate the existence of the DSL for this theory is the density of eigenvalues of the unitary

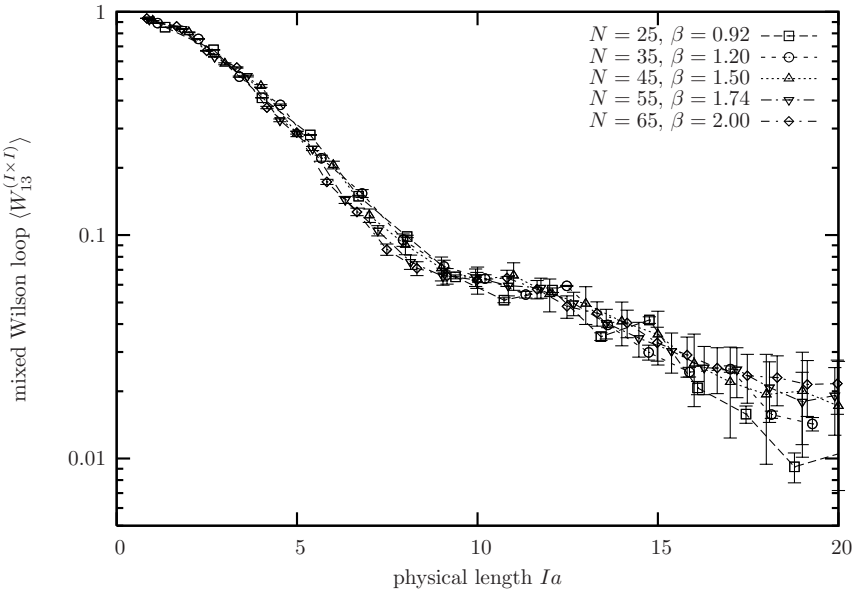

Figure 4.7: *The real part of the Wilson loops lying in the mixed* 1-3 *plane. They clearly confirm the DSL. For small Wilson loops there seems to be a perimeter law, which eventually is superimposed by some oscillating behavior.*

matrices $\hat{V}_\mu(x_3, x_4)$, $\mu = 1, 2$. Such eigenvalues represent a physical observable in related theories. Specifically, they are the coordinates of a dynamically generated space Kawai et al. [2002], Aoki et al. [1998]. Furthermore, they can be interpreted in string theory as the density distribution of D-branes van Raamsdonk [2001].

Since we here consider unitary $N \times N$ matrices, we can represent these eigenvalues by

$$\mathrm{e}^{\mathrm{i}\vartheta_{\mu,i}(x_3,x_4)}, \quad i = 1, \dots N, \quad -\pi < \vartheta_{\mu,i}(x_3, x_4) \leq \pi. \tag{4.60}$$

The Polyakov lines from Eq. (4.51) can be reformulated in terms of $\vartheta_{\mu,i}(x_3, x_4)$,

$$P_{\mu,l} = \frac{1}{NL^2} \sum_{x_3,x_4} \sum_{i=1}^{N} \mathrm{e}^{\mathrm{i}\, l\vartheta_{\mu,i}(x_3,x_4)}. \tag{4.61}$$

Because a $\mathrm{U}^2(1)$ transformation shifts all phases $\vartheta_{\mu,i}$ by a constant α_μ, see Eq. (4.42), the eigenvalue distribution should be flat (uniform) in either unbroken phase, resulting in $\langle P_{\mu,l}\rangle = 0$.

If on the other hand this symmetry is broken, the eigenvalues are clustered into two Z_2 symmetric lumps, yielding $\langle P_{\mu,l}\rangle \neq 0$. For this reason the Polyakov lines $P_{\mu,l}$ can serve as an order parameter for the $\mathrm{U}^2(1)$ symmetry.

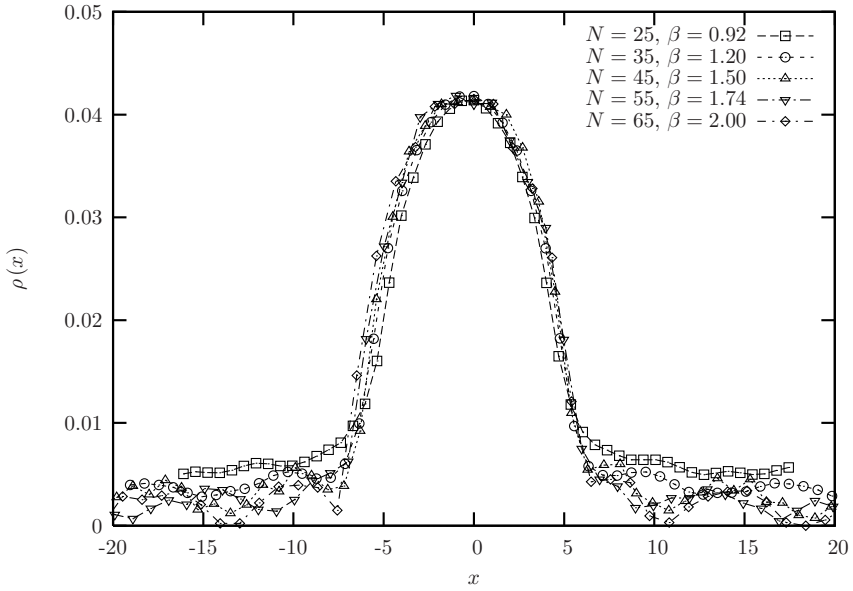

Figure 4.8: *The scaling of the eigenvalue density $\rho(x)$. The definition of the eigenvalue density $\rho(x)$ is given in Eq. (4.62).*

We now give the definition of the spectral density $\rho(x_1, x_2)$ plotted in Fig. 4.8,

$$\rho(x_1, x_2) = \frac{1}{2NL^2} \sum_{x_3,x_4} \sum_{\mu=1}^{2} \sum_{i=1}^{N} \left\langle \delta\Big(x - \frac{Na}{\pi}\vartheta_{\mu,i}(x_3, x_4)\Big)\right\rangle . \tag{4.62}$$

The coefficient in front of $\vartheta_{\mu,i}(x_3, x_4)$ is due to matching the relation (4.52) for even l. In Fig. 4.8 we have used the average over the two NC directions in order to increase statistics.

In practice, before extracting the eigenvalues, we rotate each configuration by a $\mathrm{U}^2(1)$ transformation (4.42) such that $\sum_{x_3,x_4} \mathrm{Tr}_N\Big(U_\mu^2(x_3, x_4)\Big)$ becomes real positive. By fixing the angle in this way we have averaged out the ambiguity due to the Z_2 symmetry. Furthermore, because of Eq. (4.60), we can restrict the plot to the fundamental domain $|x| \leq \frac{Na}{2}$.

In Fig. 4.8 we show the result for $\rho(x_1, x_2)$ over a range of matrix sizes $N = 25 \ldots 65$. Clearly, the eigenvalue densities scale excellently for all N. The pronounced peak indicates that we are in the broken phase.

The phase structure in the continuum theory

We have seen in Section 4.5 that the critical β_c, which corresponds to the transition from the broken phase to the weak coupling phase, grows according

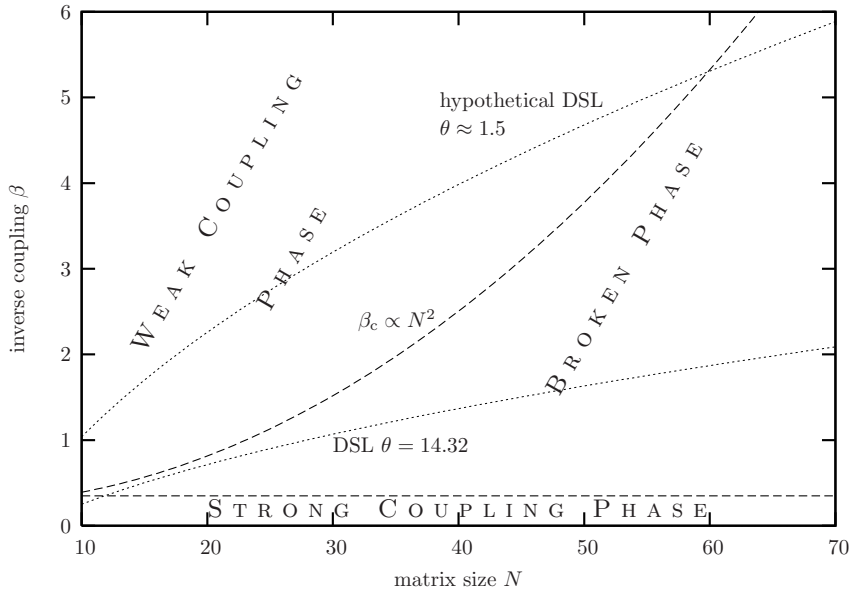

Figure 4.9: *Here we revisit the phase diagram of the* U(1) *gauge theory. In addition to Fig. 4.3 we insert two lines corresponding to a fixed noncommutativity θ. For large matrix sizes N one always ends up in the broken phase.*

to $\beta_c \propto N^2$. On the other hand, if we approach the continuum through the DSL at fixed θ, the required $\beta(N)$ grows much more modestly. The $\beta(N)$ dependence can be approximated by $\beta \propto \sqrt{N}$ and is shown in Fig. 4.9.

Therefore we can conclude that the NC continuum theory will always be in the broken phase.

4.7 Dispersion relation and IR instability

Perturbative analysis of the IR instability

Several authors, when studying U(1) gauge theories on NC spaces perturbatively, found hints at an IR instability, provided the NC theory has less fermionic degrees of freedom than bosonic ones Landsteiner et al. [2000], Martín and Ruiz Ruiz [2001], Ruiz Ruiz [2001], Landsteiner et al. [2001], Bassetto et al. [2001].

Since we here deal with a pure gauge theory, we clearly fulfill the above criterion and thus should observe an IR instability. This result is founded on a first order perturbative analysis only, though.

The perturbative treatment of the pure U(1) gauge theory for the one-loop effective gauge field action yields the quadratic term

$$\Gamma^{(1)} = -\frac{g^2}{\pi^2} \int \frac{\mathrm{d}^4 p}{(2\pi)^4} A_\mu(p) A_\nu(-p) \frac{\tilde{p_\mu} \tilde{p_\nu}}{|\tilde{p}|^4} + \ldots, \tag{4.63}$$

where

$$\tilde{p_\mu} = \Theta_{\mu\nu} p_\nu. \tag{4.64}$$

We remark that the result (4.63) is set on a Euclidean spacetime. The above expression arises from nonplanar contributions and is an effect of the UV/IR mixing. As can be seen, the effective potential involves a negative quadratic term, thus we are dealing with an IR instability.

The quadratic term occurring in Eq. (4.63) is star gauge invariant only in the leading order of the gauge field A_μ. By including higher order terms it is possible to render the expression (4.63) star gauge invariant, as has been done in the supersymmetric case Liu and Michelson [2001], Armoni and Lopez [2002].

In the star gauge invariant effective action the term most singular at small momenta p is van Raamsdonk [2001], Armoni and Lopez [2002]

$$\Gamma^{(1)} = -\frac{1}{\pi^2} \int \frac{\mathrm{d}^4 p}{(2\pi)^4} \bar{P}(p) \bar{P}(-p) \frac{1}{|\tilde{p}|^4}. \tag{4.65}$$

Here $\bar{P}(p)$ stands for the manifestly star gauge invariant Polyakov line Ishibashi et al. [2000]

$$\bar{P}(p) = \int \mathrm{d}^D x \, \mathrm{e}^{\mathrm{i}p\cdot x} \hat{P} \exp_\star\left(\mathrm{i}\, g \int_x^{x+\tilde{p}} \mathrm{d}\xi_\mu \, A_\mu(\xi)\right). \tag{4.66}$$

Again, $\hat{P}$ represents the path ordering operator (cf. Eq. (4.15)). The path for the line integral over ξ is the straight line connecting the points x and $x + \tilde{p}$.

If Eq. (4.65) is expanded in terms of the gauge field A_μ, one again obtains Eq. (4.63), up to some irrelevant constant term.

We need to keep in mind that the above reasoning is based on a one-loop perturbation theory calculation only. To come to a definitive conclusion it is necessary to investigate this issue nonperturbatively.

The dispersion relation in the weak coupling phase

First we are going to investigate the dispersion relation in the weak coupling phase. To this end we are using Polyakov lines $P_{\mu,l}$ from Eq. (4.51) at some

fixed Euclidean time x_4,

$$P_{\mu,l}(x_4) \equiv \frac{1}{NL} \sum_{x_3} \mathrm{Tr}_N\Big(\hat{V}^l_\mu(x_3, x_4)\Big) \quad \text{for } \mu = 1, 2. \tag{4.67}$$

This quantity has zero momentum in the 3-direction. In the NC directions the momentum can be nonzero, depending on the length l.

With the two-point function

$$C_l(\tau) \equiv \frac{1}{2L} \sum_{\mu=1}^{2} \sum_{x_4} \langle P^*_{\mu,l}(x_4)\, P_{\mu,l}(x_4 + \tau)\rangle \tag{4.68}$$

we are able to investigate the dispersion relation. The results for this two-point function in the symmetric phase at $N = 35$ and $\beta = 2$ are shown in Fig. 4.10. In these plots we have actually included the correlations over the 3-direction in order to increase statistics.

In this figure one can see a sharp discrepancy between the correlations of Polyakov lines of even length and Polyakov lines of odd length. Again, this is due to the fact that Polyakov lines of odd length are associated with much higher momenta (cf. Eq. (4.52)), thus decaying much faster. This suggests that the energy as well as the momentum are at the cutoff scale.

These correlations decay exponentially, resp. with a cosh dependence, as is common in commutative theories. This exponential behavior is the key for obtaining the dispersion relation $E(p)$. As stated in Eq. (4.52), the momentum associated with the Polyakov line of even length l is

$$p = \frac{\pi}{Na}\, l.$$

The exponential decay of the normalized two-point functions encodes the energy through the relation

$$\frac{C_l(\tau)}{C_l(0)} \propto \mathrm{e}^{-Ea\tau}. \tag{4.69}$$

For determining the dispersion relation in the symmetric phase we have chosen the (N, β) sets listed in Tab. 4.2. With this choice of parameters we obtain the dispersion relation shown in Fig. 4.11. The one-loop calculations mentioned earlier expected a dispersion relation of the form

$$E^2 = p^2 - \frac{c}{(\theta p)^2}, \qquad c = \text{const.} \tag{4.70}$$

To be precise, this dispersion relation has been obtained from calculations of the vacuum polarization Landsteiner et al. [2000], Martín and Ruiz Ruiz

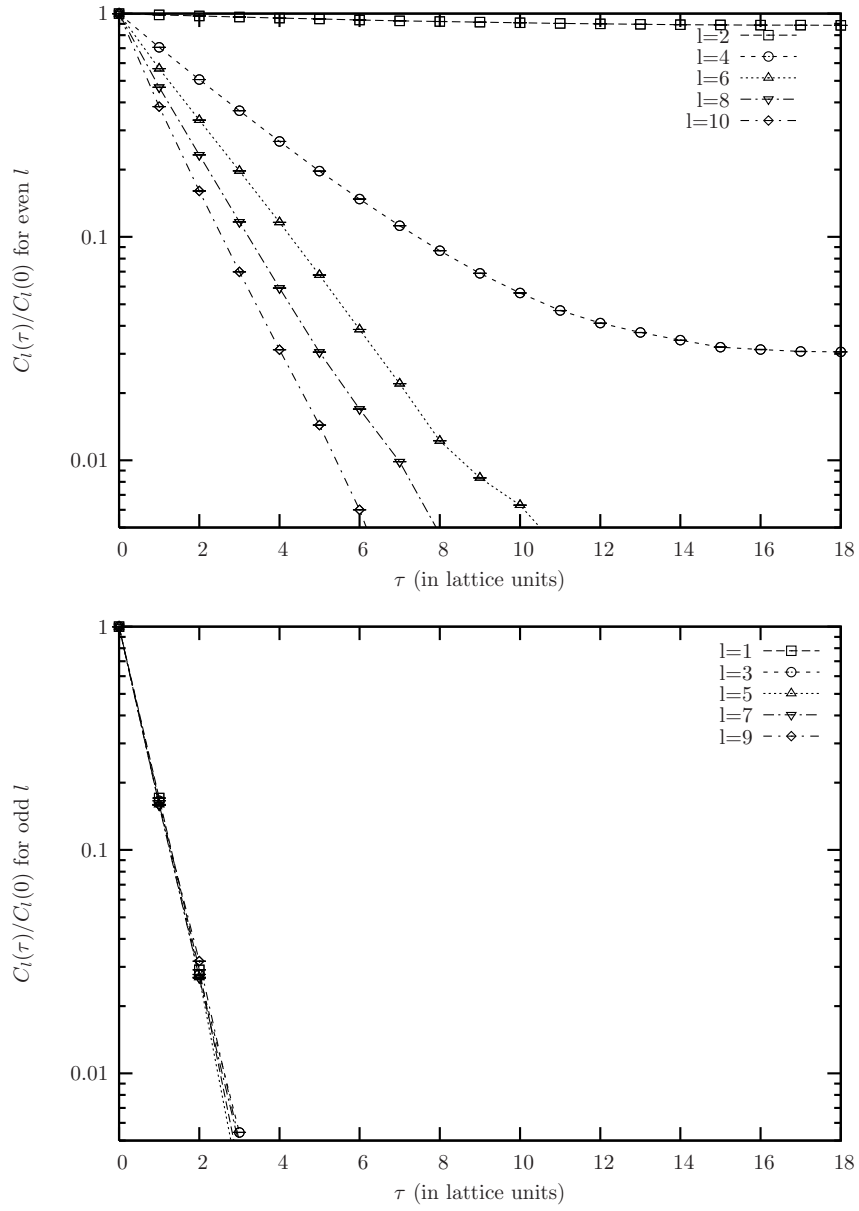

Figure 4.10: *The two-point function for even length Polyakov lines (top) and odd length Polyakov lines (bottom) in the symmetric (weak coupling) phase. These values were obtained at* $N = 35$ *and* $\beta = 2$.

N	β	a
15	1.29	1.73
25	1.69	1.32
35	2.00	1.13

Table 4.2: *We have simulated the 4D U(1) theory at the above parameters. With these parameters we are always in the symmetric (weak coupling) phase. The lattice spacing a can be determined from the convention (4.56).*

[2001], Ruiz Ruiz [2001], Landsteiner et al. [2001], Bassetto et al. [2001], Matusis et al. [2000]. As can be seen from the fit in Fig. 4.11, our results match this prediction very well. The parameter c in Eq. (4.70) is identified as

$$c \approx 0.13. \tag{4.71}$$

The positive sign of c causes the dispersion relation in Fig. 4.11 to bend down. For finite N the lattice acts as a regulator. The smallest possible nonzero momentum $p_{\min}$ on the lattice is associated with the Polyakov line of length $l = 2$,

$$p_{\min} = \frac{2\pi}{Na} \propto \frac{1}{\sqrt{N}}. \tag{4.72}$$

If N increases, smaller and smaller nonzero momenta are possible. This is also visible in Fig. 4.11.

So for large N and β in the broken phase we expect to effectively be lead to an IR instability. This means that the theory, when considered in the symmetric phase only, is in effect ill-defined. It is unable to find a stable ground state.

As we noted before, when taking the DSL we always end up in the broken phase. Therefore the IR instability can be considered a lattice artifact.

The dispersion relation in the broken phase

In the broken phase the situation turns out to be quite different, when compared to the symmetric phase. In the broken phase the energy in the NC directions is not visible anymore, because the two-point function does not decay exponentially. This however is not true for the commutative directions.

Therefore we use the Polyakov line (cf. Eq. (4.67))

$$\tilde{P}_\mu(p_3, x_4) \equiv \frac{1}{NL} \sum_{x_3} \mathrm{e}^{-\mathrm{i}p_3 x_3} \operatorname{Tr}_N\left(\hat{V}_\mu^2(x_3, x_4)\right), \quad \mu = 1, 2. \tag{4.73}$$

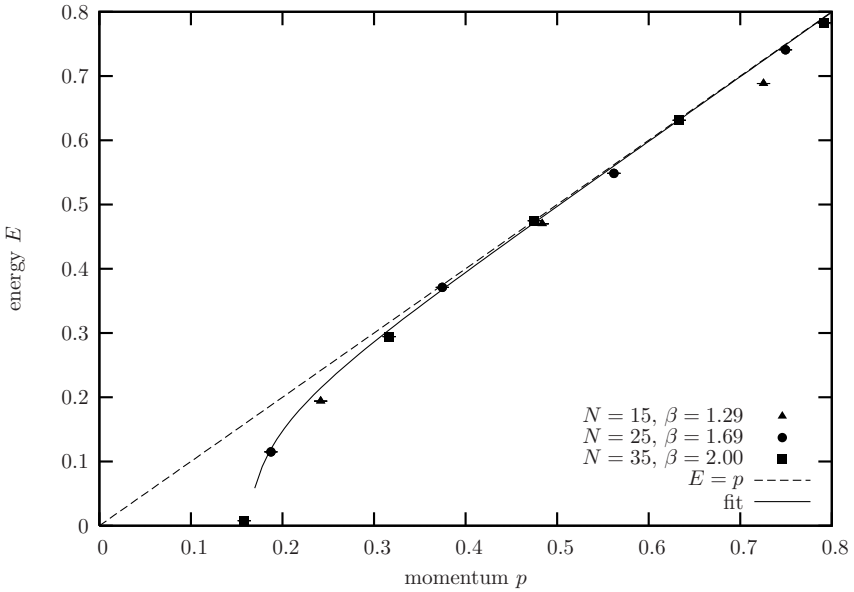

Figure 4.11: *The dispersion relation in the symmetric phase. As the momentum decreases, the potential seems to be unbound from below. This has been conjectured by one-loop perturbation theory calculations van Raamsdonk [2001]. The plot is compatible with the predicted infrared instability of the form (4.70).*

This version of the Polyakov line carries the momentum p_3 in the commutative 3-direction.

If we now use this Polyakov line in the calculation of the two-point function, we obtain

$$\tilde{C}_p(\tau) \equiv \frac{1}{2} \sum_{\mu=1}^{2} \sum_{x_4} \langle \tilde{P}^*_\mu(p_3, x_4)\, \tilde{P}_\mu(p_3, x_4 + \tau) \rangle. \tag{4.74}$$

For the actual evaluation of these two-point functions we also used the correlations across the 3-direction in order to increase statistics, just like we did in the symmetric case.

Since we consider $p_1 = p_2 = 0$, these correlation functions enable us to determine the respective energy $E(p_3)$ for the Polyakov line $\tilde{P}(p_3, x_4)$ of momentum p_3. This can be done again by measuring the slope of the exponential decay of the two-point function $\tilde{C}_p(\tau)\,/\tilde{C}_p(0) \propto \exp(-E(p_3)\, a\tau)$.

The resulting dispersion relation $E(p_3)$ in the broken phase is shown in Fig. 4.12. The data in this plot were obtained with the same parameters as the ones used for identifying the DSL. They are listed in Tab. 4.1.

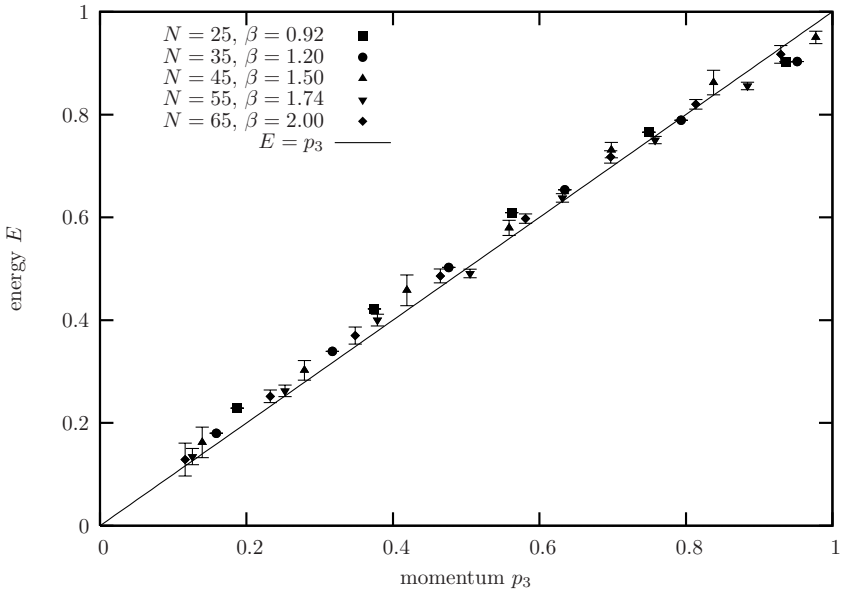

Figure 4.12: *Here we consider the dispersion relation in the broken phase. This is the phase one always ends up when going to the continuum/large volume limit at a fixed NC parameter θ. Down to the smallest probed momenta p_3 we clearly see a linear dispersion relation $E(p_3)$. In contrast to the weak coupling phase no IR instability is observed.*

One can clearly see that the dispersion relation resembles that of a regular massless photon, at least down to the energy-momentum values probed. We find

$$E(p_3) \cong p_3. \tag{4.75}$$

We see that the theory in the broken phase is viable and that approaching the continuum via the DSL leads to a well-defined and sensible theory.

Chapter 5

A SUSY Theory on the Fuzzy Sphere

In Section 2.6 we have briefly discussed how a real scalar field can be put onto a fuzzy sphere $\mathbb{S}_{\mathrm{F}}^2$. In the following section we are going to describe a Wess Zumino type model first discussed by P. Di Vecchia and S. Ferrara Di Vecchia and Ferrara [1977]. We put this model on a fuzzy sphere, thus the number of degrees of freedom is truncated according to Eq. (2.106). This yields a matrix model which is suitable for numerical treatment.

5.1 The Di Vecchia-Ferrara Model on the Fuzzy Sphere

We here briefly describe the model introduced by Di Vecchia and Ferrara in Ref. Di Vecchia and Ferrara [1977]. They investigated a supersymmetric model on a two-dimensional Minkowski type space, which we here translate to the Euclidean setting.

The model on a Euclidean plane

Being supersymmetric, the model features both a bosonic and a fermionic field. The scalar neutral bosons will be denoted by $\phi(x)$, while the spinor field $\psi(x)$ represents Majorana fermions.

For convenience we consider a bosonic potential of the form $\frac{1}{2}\left[V'(\phi)\right]^2$. The action of the Di Vecchia-Ferrara model reads

$$S[\phi,\psi] = \int \mathrm{d}^2x \, \left[\frac{1}{2}(\partial_\mu\phi)(\partial_\mu\phi) + \frac{1}{2}\bar{\psi}\,\gamma_\nu\,\partial_\nu\psi + \frac{1}{2}[V'(\phi)]^2 + \frac{1}{2}\,\bar{\psi}\psi\,Z(\phi)\right]. \quad (5.1)$$

The interaction between bosons and fermions is encoded in $Z(\phi)$. Choosing

$$Z(\phi) = V''(\phi) \tag{5.2}$$

yields a supersymmetric theory; it is symmetric under the SUSY transformation

$$\begin{cases} \delta\phi &= \bar{\epsilon}\,\psi, \\ \delta\psi &= [\gamma^\mu \partial_\mu \phi - V'(\phi)]\,\epsilon, \end{cases} \qquad \begin{cases} \delta\bar{\psi} &= \bar{\epsilon}\,[-\gamma^\mu \partial_\mu \phi - V'(\phi)]. \end{cases} \tag{5.3}$$

The symbol ϵ denotes a constant Graßmann spinor field. If the Lagrangian in Eq. (5.1) is subjected to these transformations, its variation turns out to be a total divergence. Thus the transformation (5.3) describes a symmetry of this theory.

The model with a $\lambda\phi^4$ potential on a sphere

We now want to reformulate the SUSY model on a sphere $\mathbb{S}^2$. The radius (cf. Eq. (2.4)) is chosen as $R = 1$. The γ matrices fulfill

$$\{\gamma_\mu, \gamma_\nu\} = 2\,\delta_{\mu\nu} \mathbb{1}_2, \quad \mu, \nu = 1, 2. \tag{5.4}$$

Thus they can be represented by the Pauli matrices,

$$\gamma_1 = \sigma_1, \quad \text{and} \quad \gamma_2 = \sigma_2. \tag{5.5}$$

Now we put the model on a sphere,

$$\begin{aligned} S[\phi, \psi] = \int_{\mathbb{S}^2} \mathrm{d}^3x \Big[\frac{1}{2}\,(\partial_\mu \phi)\,(\partial_\mu \phi) + \frac{1}{2}\,\bar{\psi}\,(\sigma_\mu \partial_\mu + 1)\,\psi + \frac{1}{2}\,[V'(\phi)]^2 \\ + \frac{1}{2}\,\bar{\psi}\,V''(\phi)\,\psi \Big]\,\delta\Big(\vec{x}^{\,2} - 1\Big), \quad \mu = 1, 2, 3. \end{aligned} \tag{5.6}$$

The formulation on the sphere yields an additive constant 1 in the purely fermionic term. This is a curvature term, which in general amounts to $1/R$. Thus the regular Dirac operator is recovered in the $R \to \infty$ limit Balachandran et al. [2005].

We now specify the potential as

$$V(\phi) = \sqrt{\frac{\lambda}{108}}\,\phi^3 + \frac{m}{2}\,\phi^2, \tag{5.7}$$

which leads to a $\lambda\phi^4$ type bosonic potential

$$\frac{1}{2}\,[V'(\phi)]^2 = \frac{\lambda}{4!}\,\phi^4 + m\sqrt{\frac{\lambda}{12}}\,\phi^3 + \frac{m^2}{2}\,\phi^2 \tag{5.8}$$

and to a linear boson-fermion interaction term with

$$V''(\phi) = \sqrt{\frac{\lambda}{3}}\,\phi + m. \tag{5.9}$$

The potential $[V'(\phi)]^2/2$ is symmetric under

$$\phi \to -\phi - \frac{6m}{\sqrt{3\lambda}}. \tag{5.10}$$

This transformation entails

$$\begin{cases} V'(\phi) & \to & V'(\phi) \\ V''(\phi) & \to & -V''(\phi) \end{cases}. \tag{5.11}$$

Both the bosons and the fermions have the mass

$$m_{\text{boson}} = m_{\text{fermion}} = |m|. \tag{5.12}$$

Fuzzy sphere formulation and implementation

We now translate the model to the fuzzy sphere. This means we truncate according to Eq. (2.106), which yields a matrix model. Such a formulation can then be used to investigate the model numerically. An unfortunate side effect of this truncation is that it breaks the SUSY. If the matrix size is denoted by N, supersymmetry is restored only in the $N \to \infty$ limit. However, in light of previous attempts to formulate SUSY theories on a lattice and their difficulties (a few examples are Bietenholz [1999], Aoyama and Kikukawa [1999], Catterall and Karamov [2002], Kaplan et al. [2003], Harada and Pinsky [2003], Sugino [2004], Catterall and Ghadab [2004], Bonini and Feo [2004], D'Adda et al. [2006]), we consider it worthwhile to explore this alternative approach.

The bosonic contributions can be translated to the matrix formulation right away by using the techniques from Section 2.6. Thus the bosonic field $\phi(x)$ becomes a Hermitian matrix $\hat{\phi}$ in the finite N matrix formulation.

From Eq. (2.107) we see that we need to implement the derivative commutator

$$\hat{\partial}_\mu\,\hat{\phi} = [\hat{L}_\mu, \hat{\phi}] = \hat{L}_\mu\,\hat{\phi} - \hat{\phi}\,\hat{L}_\mu. \tag{5.13}$$

Here the term $\hat{\phi}\,\hat{L}_\mu$ involves a right-acting $\hat{L}_\mu$ operator, which is awkward to implement. In order to avoid this difficulty, we rephrase the $N \times N$ matrix $\hat{\phi}$ as a vector $\vec{\phi}$ with N^2 elements, which allows for easy implementation of

Eq. (5.13). Precisely, if $\vec{\phi}$ is a N^2 vector, the $N^2 \times N^2$ operator $\hat{\partial}_\mu$ is given by

$$\hat{\partial}_\mu = \hat{L}_\mu \otimes \mathbb{1}_N - \mathbb{1}_N \otimes \hat{L}_\mu, \qquad \text{where } \hat{\partial}_\mu \text{ acts on } \vec{\phi}. \tag{5.14}$$

Once N is fixed, $\hat{\partial}_\mu$ is fixed as well.

Furthermore we have symmetrized the potential $V''(\phi)$

$$V''(\phi)_{\text{symm}} = \frac{1}{2}\Big(V''(\phi) \otimes \mathbb{1}_N + \mathbb{1}_N \otimes V''(\phi)\Big). \tag{5.15}$$

We found that with a symmetrized potential the eigenvalues of the Dirac operator are real positive, meaning that the statistical weights are positive as well. In the large N limit, which restores supersymmetry and commutativity, we recover the formulation (5.6).

We are now ready to put everything together in order to express the model in terms of matrices. The Dirac operator

$$D_\phi = \sigma_\mu \hat{\partial}_\mu + \mathbb{1}_2 + V''(\phi) \tag{5.16}$$

now turns into a $2N^2 \times 2N^2$ matrix given by

$$D_\phi = (\sigma_\mu \otimes \hat{\partial}_\mu) + (\mathbb{1}_2 \otimes V''_{\text{symm}}(\hat{\phi})) + \mathbb{1}_{2N^2}. \tag{5.17}$$

With the abbreviations

$$\hat{\partial}_+ = \hat{\partial}_1 + \mathrm{i}\,\hat{\partial}_2 \quad \text{and} \quad \hat{\partial}_- = \hat{\partial}_1 - \mathrm{i}\,\hat{\partial}_2 \tag{5.18}$$

we arrive at the form

$$D_\phi = \begin{pmatrix} \hat{\partial}_3 + V''_{\text{symm}} + \mathbb{1}_{N^2} & \hat{\partial}_- \\ \hat{\partial}_+ & -\hat{\partial}_3 + V''_{\text{symm}} + \mathbb{1}_{N^2} \end{pmatrix}. \tag{5.19}$$

Upon integrating out the fermionic degrees of freedom, we obtain the matrix model formulation

$$\begin{aligned} S[\phi] = \frac{4\pi}{N} \operatorname{Tr}\left(\frac{1}{2}\sum_{\mu=1}^{3}\left[\hat{\phi}\,[\hat{L}_\mu,[\hat{L}_\mu,\hat{\phi}]]\right] + \frac{m^2}{2}\,\hat{\phi}^2 + m\sqrt{\frac{\lambda}{12}}\,\hat{\phi}^3 + \frac{\lambda}{4!}\,\hat{\phi}^4\right) \\ - 2N^2 \ln\left(\frac{4\pi}{N}\right) + 2N^2 \ln(2) - \frac{1}{2}\ln(\det(D_\phi))\,. \end{aligned} \tag{5.20}$$

This is the model we have actually simulated.

phase	$\langle\|\phi\|^2\rangle$	$\langle\phi_0^2\rangle$
disordered	≈ 0	≈ 0
uniform ordered	$\gg 0$	$\gg 0$
nonuniform ordered	$\gg 0$	≈ 0

Table 5.1: *The phases of the SUSY model along with the respective magnitudes of the order parameters* $\langle|\phi|^2\rangle$ *and* $\langle\phi_0^2\rangle$.

5.2 The Phase Diagram

In order to investigate the phase diagram, we need to define an order parameter.

For this purpose it is natural to look at the coefficients c_{lm} in the expansion (2.112). These coefficients can be extracted from the field $\hat{\phi}$ by the relation

$$c_{lm} = \frac{4\pi}{N} \operatorname{Tr}\Big((\hat{Y}^{lm})^\dagger \, \hat{\phi}\Big) , \tag{5.21}$$

where $\hat{Y}^{lm}$ are the polarization tensors discussed in Section 2.6 and Appendix C. In particular we have

$$c_{00} = \frac{\sqrt{4\pi}}{N} \operatorname{Tr}\Big(\hat{\phi}\Big) . \tag{5.22}$$

We also define an auxiliary quantity

$$\phi_l^2 \equiv \sum_{m=-l}^{l} |c_{lm}|^2, \tag{5.23}$$

which is the base for

$$|\phi|^2 \equiv \sum_l \phi_l^2 = \frac{4\pi}{N} \operatorname{Tr}\Big(\hat{\phi}^2\Big) . \tag{5.24}$$

In order to explore the phase diagram we mainly rely on $\langle\phi_0^2\rangle$ and $\langle|\phi|^2\rangle$.

The quantity $|\phi|^2$ measures the invariance of $\hat{\phi}$ under rotation. A value of $\langle|\phi|^2\rangle \approx 0$ indicates rotational invariance. Such a phase is denoted as the *disordered phase*. It is an Ising type phase, since it resembles an Ising model in the phase of zero magnetization.

In the ordered regime, indicated by $\langle|\phi|^2\rangle \gg 0$, we distinguish two phases. In order to identify them, we use the value of $\langle\phi_0^2\rangle$. This quantity weighs the rotationally invariant components of the configuration. Thus we can detect

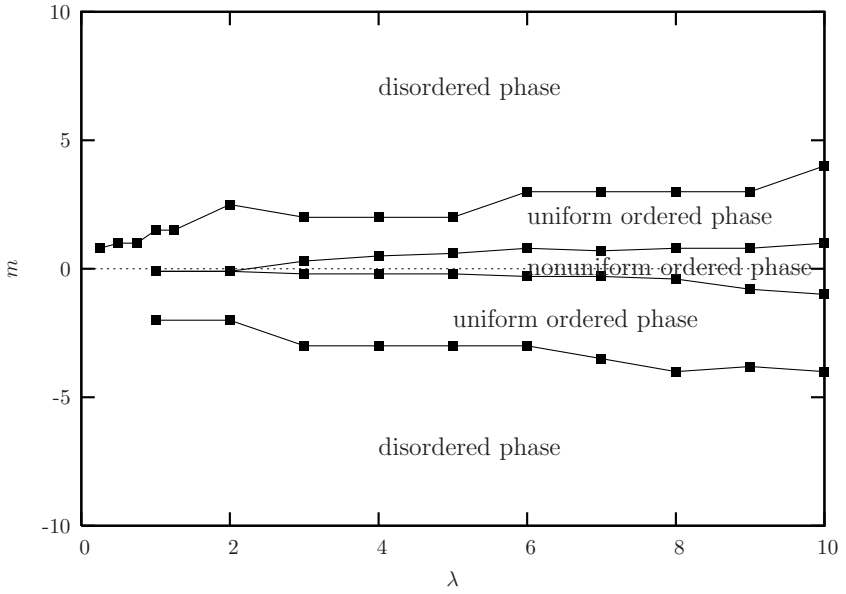

Figure 5.1: *The phase diagram of the SUSY theory obtained at $N = 6$. We see that for large $|m|$ the system is in the disordered phase. As the value of $|m|$ decreases, the model enters the uniform ordered phase. For λ values above some threshold, the lightest masses correspond to a theory in the nonuniform ordered phase.*

whether rotation invariance holds by comparing the values of $\langle|\phi|^2 - \phi_0^2\rangle$ and $\langle\phi_0^2\rangle$ in a specific sector of the phase diagram. If the rotational symmetry is broken, i.e.

$$\langle|\phi|^2\rangle \gg 0 \quad \text{as well as} \quad \langle|\phi|^2 - \phi_0^2\rangle \gg 0,$$

we are in the *nonuniform ordered phase*. On the other hand, if the rotational symmetry is maintained, indicated by $\langle|\phi|^2\rangle \approx \langle\phi_0^2\rangle \gg 0$ (i.e. the rotationally dependent contributions $\langle|\phi|^2 - \phi_0^2\rangle$ are negligible), we refer to the *uniform ordered phase*. For reference we list the phases along with their respective order parameters in Tab. 5.1.

5.3 Numerical Results

In order to investigate the phase structure we have simulated the theory at $N = 6$ and $N = 7$. The results for $N = 7$ are essentially the same as for $N = 6$. Here we focus on the $N = 6$ data. For gaining a first overview, the

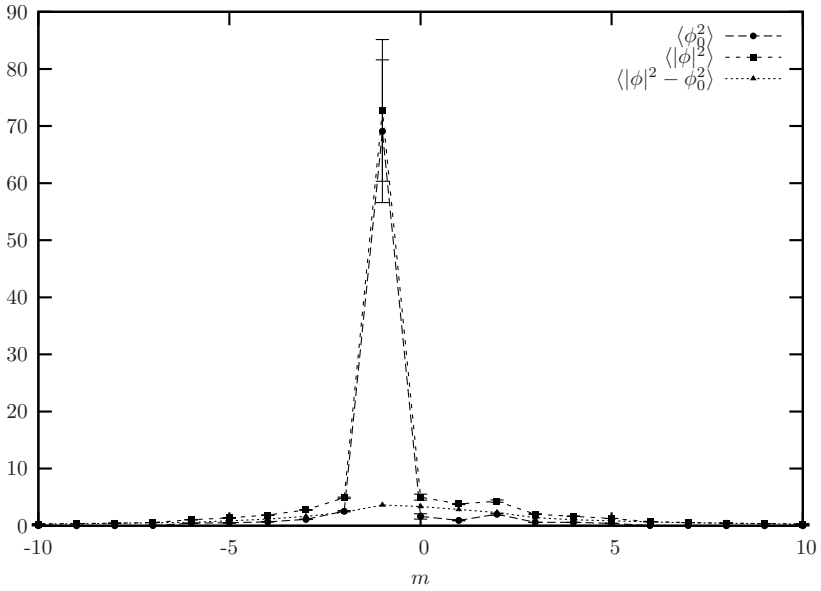

Figure 5.2: *The order parameters* $\langle|\phi|^2\rangle$ *and* $\langle\phi_0^2\rangle$ *as well as their difference at* $N = 6$ *and* $\lambda = 1$*. For large* $|m|$ *the theory is in the disordered phase, while it is in the uniform ordered phase for* $-2 < m < 0$*. A weak hint at a similar peak is seen at* $m = 2$*.*

chosen matrix sizes seem suitable. The overall phase structure is illustrated in Fig. 5.1.

This phase diagram shows that we are always in the disordered phase ($\langle|\phi|^2\rangle \approx \langle\phi_0^2\rangle \approx 0$) for large values of the mass $|m|$. This can be seen in Figs. 5.2, 5.3 and 5.4 as well. In these plots we show a cross cut of the phase space for $\lambda = 1$ (Fig. 5.2), $\lambda = 6$ (Fig. 5.3) and $\lambda = 9$ (Fig. 5.4). There we can see very well how all three order parameters $\langle|\phi|^2\rangle$, $\langle\phi_0^2\rangle$ and their difference decay towards zero as $|m|$ assumes large values.

As we decrease the value of $|m|$, we enter the uniform ordered phase ($\langle|\phi|^2\rangle \approx \langle\phi_0^2\rangle \gg 0$), regardless of whether we are coming from large positive m or strongly negative m. Apparently, this transition is not symmetric around the $m = 0$ line. As one can clearly see from Figs. 5.2 to 5.4, the order parameters indicating the uniform ordered phase occur in different intensities for different λ. In the $\lambda = 1$ example (Fig. 5.2) there is a clear peak characterized by $\langle|\phi|^2\rangle \approx \langle\phi_0^2\rangle \gg 0$, thus we are in the uniform ordered phase. To the right of this dominant peak there is a slight indication of another peak at $m \approx 2$. As λ increases the second peak becomes much more pronounced (see $\lambda = 6$ in Fig. 5.3). At $\lambda = 6$ one can also see a region characterized

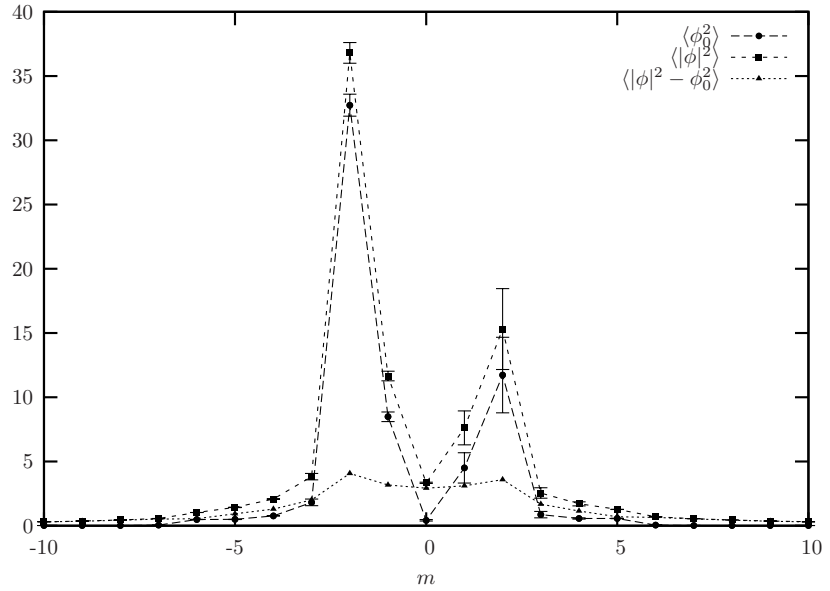

Figure 5.3: *The order parameters* $\langle|\phi|^2\rangle$ *and* $\langle\phi_0^2\rangle$ *and their difference at* $N = 6$ *and* $\lambda = 6$*. For large* $|m|$ *we are in the disordered phase. The two peaks are clearly in the uniform ordered phase, even though the peak at* $m < 0$ *is more pronounced. In-between the peaks the model is in the nonuniform ordered phase.*

by $\langle|\phi|^2\rangle \gg 0$ and $\langle\phi_0^2\rangle \approx 0$ in-between both peaks ($m \approx 0$), meaning we here deal with the nonuniform ordered phase. As λ increases even further (see Fig. 5.4 with $\lambda = 9$), the second peak becomes more pronounced. In fact, at $\lambda = 9$ both peaks are nearly symmetric around the $m = 0$ line. The nonuniform ordered phase occurs around vanishing masses, $|m| \approx 0$.

In summary, similarly to the $\lambda\phi^4$ model on the NC plane, we found three distinct phases. One of these, the nonuniform ordered phase, lacks an analogue in its commutative counterpart theory and thus represent a NC phenomenon. For the future the investigation of the different $N \to \infty$ limits certainly is a worthwhile target.

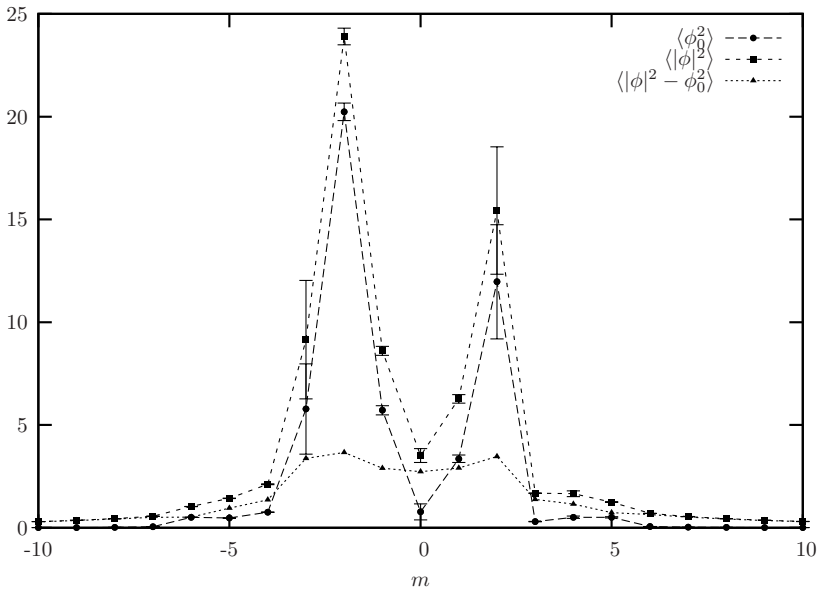

Figure 5.4: *The order parameters* $\langle|\phi|^2\rangle$ *and* $\langle\phi_0^2\rangle$ *as well as their difference at* $N = 6$ *and* $\lambda = 9$*. Again, at large* $|m|$ *the model is always in the disordered phase. There are two almost symmetric peaks indicating the uniform ordered phase. At vanishing mass the theory is in the nonuniform ordered phase.*

Chapter 6

Conclusions

In this work we have examined three quantum field theories (QFTs) situated on noncommutative (NC) spaces: a two-dimensional $\lambda\phi^4$ model, a four-dimensional U(1) gauge theory and a supersymmetric theory on a fuzzy sphere. Field theories on NC spaces are difficult to deal with perturbatively, in general only one-loop effects are under control. Here, however, we are able to investigate NCQFTs nonperturbatively by using equivalent matrix models, which are suitable for numerical simulations.

The $\lambda\phi^4$ model

The first theory under investigation was the scalar $\lambda\phi^4$ theory on a two-dimensional NC spacetime. Even though it is arguably the simplest model investigated here, it turned out to be numerically very demanding. This forced us to restrict the size of the matrices involved to $N \leq 25$.

The main focus of the work on the $\lambda\phi^4$ model was to establish the continuum limit at fixed noncommutativity while remaining in the vicinity of the striped phase. This limit is known as the double scaling limit (DSL). To this end we used the phase diagram provided by Ref. Hofheinz [2004] (see Fig. 3.2). In order to approach the DSL, we matched correlation functions at fixed coupling λ and different matrix sizes N by fine-tuning the parameter m^2.

From the tuned parameters m^2_{scaling} we determined the critical exponent σ, which in turn allowed us to determine the fate of the striped phase in the DSL. We found that the obtained σ values vary considerably. Therefore we conclude that the striped phase does not survive the continuum limit. This is in agreement with a conjecture by S. S. Gubser and S. L. Sondhi Gubser and Sondhi [2001], which is based on an extension of the Mermin-Wagner theorem to the (nonlocal) NC $\lambda\phi^4$ model.

The U(1) gauge theory

As the main project of this work we have simulated a U(1) gauge theory living on a four-dimensional spacetime. Two of the three spatial directions were chosen to be noncommutative. The remaining two directions are kept commutative in order to avoid problematic issues related to a NC time or a noninvertible NC tensor.

We investigated the phase structure of this gauge theory. Just like its commutative counterpart, the U(1) theory on the lattice with compact link variables features a strong and a weak coupling phase. In the NC case, however, an additional phase emerges in-between. This is what we called the broken phase, since it spontaneously breaks the translational invariance on the NC plane. The phase transition from weak to moderate couplings is of first order, since we found a clear hysteresis behavior.

We have examined the DSL of the theory as well. We found that the theory possesses a finite DSL, so renormalizability for this theory holds. In particular we showed the scaling for several observables, such as Wilson loops or eigenvalue densities of the involved matrices. We observed that when going to the continuum one ends up in the broken phase, regardless of whether one takes the planar limit or the DSL.

Another aspect we could clarify is the dispersion relation. It had been suggested by one-loop calculations that a class of theories — including the one studied here — features an infrared instability, thus ruling out a stable vacuum state Landsteiner et al. [2000], Martín and Ruiz Ruiz [2001], Ruiz Ruiz [2001], Landsteiner et al. [2001], Bassetto et al. [2001]. We have indeed found such a behavior in the symmetric phase at weak coupling. However, in the broken phase, this predicted instability seems to disappear, leaving us with a linear dispersion relation down to the smallest momenta probed. This dispersion relation corresponds to a massless particle.

The SUSY theory on the fuzzy sphere

We have also investigated a supersymmetric (SUSY) model first explored by Di Vecchia and Ferrara in 1977 Di Vecchia and Ferrara [1977]. In regard to the search for a numerically tractable regularization, the formulation on the fuzzy sphere might provide an alternative to corresponding attempts on the lattice. The fields involved in this theory are neutral scalar bosons and Majorana fermions. The fuzzy sphere formulation is a matrix model, which breaks the SUSY. Invariance under the SUSY transformation is restored in the limit of infinitely large matrices.

By scanning the parameter space we explored the phase structure of the

theory on a fuzzy sphere. The necessary simulations were carried out with matrices of size $N = 6$ and $N = 7$. We found three phases, a disordered phase, a nonuniform ordered phase and a uniform ordered phase and we were able to provide a phase diagram in Fig. 5.1.

For the future a first target will certainly be to determine the order of the phase transitions. Furthermore, it would be interesting to investigate the behavior — in particular the scaling — of the observables at larger matrix sizes, since in this limit SUSY is restored. In this vein we plan to measure the SUSY breaking in dependence of the matrix size N. One could also consider simulating the theory at large radius (see Eq. (2.5)), yielding a SUSY theory on a plane.

With this agenda we hope to provide the foundations for eventual numerical simulations of supersymmetric theories.

In summary we found that numerical simulations of NCQFTs are feasible. They allowed for many new insights in this modern field, which usually is hampered by weak analytical tools. In this work, however, we reached beyond the one-loop level barrier commonly encountered in NC perturbation theory calculations.

When extracting simulation results to the continuum, one has to be very careful. In particular, just like in the case of commutative QFTs, we first had to determine the phase structure of each theory. However, in NC theories the phase structure usually acquires an additional phase. In general this is due to the condensation of nonzero modes, a NC phenomenon related to UV/IR mixing.

Our nonperturbative studies were only possible by a reformulation of the theories as Morita equivalent matrix models. This break through the perturbation theory barrier should eventually allow for a confrontation of our theoretical results with experimental data.

The nonperturbative investigation of NCQFTs is still in its infancy and provides a rich playing field for future projects.

Appendix A

Noncommutativity from a Strong Magnetic Field

Here we show how an external background field can lead to an effectively noncommutative spacetime. As an example we consider the movement of a particle with mass m and charge q in a strong magnetic field $\vec{B}$. Here the movement of the particle is confined to the 1-2 plane. Another example employing NC coordinates in a similar fashion is given in Ref. Karabali and Nair [2006].

We set up the magnetic field to be perpendicular to the 1-2 plane,

$$\vec{B} = (0, 0, B). \tag{A.1}$$

Since we consider a magnetic field only (there is no electric field), the vector potential A_μ can be given by

$$A_\mu = -\frac{B}{2}\,\epsilon_{\mu\nu} x^\nu, \quad \mu = 1, 2, \qquad A_3 = 0. \tag{A.2}$$

The Lagrange function

$$L = \frac{m}{2}\,\dot{\vec{x}}^{\,2} - q\,\dot{\vec{x}} \cdot \vec{A} \tag{A.3}$$

yields the canonically conjugated momentum

$$\vec{p} = m\dot{\vec{x}} - q\vec{A}. \tag{A.4}$$

If we denote the mechanical momentum by $\vec{\pi}$, we obtain

$$\vec{\pi} = m\dot{\vec{x}} = \vec{p} + q\,\vec{A}. \tag{A.5}$$

The mechanical momentum $\vec{\pi}$ is a physical observable, thus it is gauge invariant. This, however, does not hold for the conjugate momentum $\vec{p}$.

We now quantize the above model by canonical quantization. If we combine Eqs. (A.2) and (A.5) and apply $[\hat{x}^\mu, \hat{p}_\nu] = \mathrm{i}\,\delta^\mu_\nu$, we obtain a nonvanishing commutator

$$[\hat{\pi}_1, \hat{\pi}_2] = -\mathrm{i}\,qB. \tag{A.6}$$

This means that we have established cells of smallest length in momentum space. It is impossible do determine the mechanical momentum (π_1, π_2) up to an arbitrarily high precision.

A consequence is that we effectively have imposed an IR cutoff in momentum space, since we now have $qB \leq \hat{\pi}_1^2 + \hat{\pi}_2^2$. In this manner the noncommutativity of the momentum space can cure certain types of integrals as well.

We now consider the limit of a strong magnetic field. This means that we can neglect the kinetic term in Eq. (A.3). Therefore the Lagrange function turns into

$$L_{B\text{ strong}} = -q\,\dot{\vec{x}} \cdot \vec{A} = -\frac{qB}{2}\dot{x}^\mu \epsilon_{\mu\nu} x^\nu. \tag{A.7}$$

From this we see that the coordinates x^1 and x^2 are canonically conjugated variables. If we now quantize again, we find the commutation relation

$$[\hat{x}^1, \hat{x}^2] = \mathrm{i}\,\frac{2}{qB}. \tag{A.8}$$

Effectively, the strong magnetic field induces a commutation relation in the position operators. The noncommutativity parameter $\theta = \Theta^{12}$ of this NC plane $\mathbb{R}^2_{\mathrm{NC}}$ is therefore

$$\theta = \frac{2}{qB}. \tag{A.9}$$

Appendix B

An Algorithm for Simulating a 4D U(1) NC Gauge Theory

In this appendix we are going to describe the heat bath algorithm we have used for simulating the 4D U(1) gauge theory described in Chapter 4. Using a heat bath method proved necessary, because the Metropolis algorithm turned out to be extremely inefficient. With a Metropolis version of our simulations we could not reach thermalized configurations in a sensible time. This difference in the performance of the Metropolis and the heat bath algorithm is typical for simulations of gauge theories.

Our algorithm is based on a generalization of the method described in Ref. Fabricius and Haan [1984]. This generalization is used in order to linearize the action (4.36), which allows us to use a heat bath procedure where the U(N) matrices $\hat{V}_\mu$ are updated by multiplication with SU(N) matrices Cabibbo and Marinari [1982].

Since we need to probe the whole U(N) space, the final step for proposing a new configuration is a multiplication with a phase factor $\mathrm{e}^{\mathrm{i}\alpha_\mu(x_3,x_4)}$. Here we employ a Metropolis algorithm.

Linearizing the action

As discussed in Section 4.4, the action of the model (4.36) is split into three qualitatively different parts. First, there is S_{NC}, which is the contribution to the action arising solely from the NC plane (4.37). The second contribution S_{mixed} is due to the planes extending in both a NC direction and a commutative direction (4.39). Finally we have S_{comm} from the commutative plane (4.40).

The contributions S_{NC} and S_{mixed} contain terms nonlinear in $\hat{V}_\mu(x_3, x_4)$, $\mu = 1, 2$. Therefore we cannot apply the regular heat bath method as de-

scribed in Ref. Creutz [1980]. Instead we generalize the technique introduced in Ref. Fabricius and Haan [1984], which has been devised for the simulation of TEK models (cf. Section 4.3). We briefly restate the gist of the idea here in order to discuss our own extension of it.

First an auxiliary matrix field $\hat{Q}_{12}(x_3, x_4)$ is introduced, which consists of general complex $N \times N$ matrices. In the simulations this field is generated by filling the real and imaginary part of the matrix elements with Gaussian distributed real numbers. This field is then used in the definition of a modified action S'_{NC},

$$\begin{aligned} S'_{\mathrm{NC}} = N\beta \sum_{x_3,x_4} \Big[& \mathrm{Tr}_N\Big(\hat{Q}^\dagger_{12}(x_3,x_4)\,\hat{Q}_{12}(x_3,x_4)\Big) \\ & - 2\,\mathrm{Re}\,\mathrm{Tr}_N\Big(\hat{Q}^\dagger_{12}[t\,\hat{V}_1(x_3,x_4)\,\hat{V}_2(x_3,x_4) + t^*\,\hat{V}_2(x_3,x_4)\,\hat{V}_1(x_3,x_4)]\Big)\Big]. \end{aligned} \tag{B.1}$$

Here t is a square root of the twist $\mathcal{Z}_{12}$ from Eq. (4.38). Upon completing the square and integrating out $\hat{Q}_{12}(x_3, x_4)$, Eq. (B.1) yields the desired S_{NC} from Eq. (4.37).

This method has been generalized by us in order to accommodate for the mixed action (4.39) Bietenholz et al. [2006]. Again, auxiliary fields consisting of general complex $N \times N$ matrices are introduced. They are labeled in the same vein as above, $\hat{Q}_{13}(x_3, x_4)$, $\hat{Q}_{14}(x_3, x_4)$, $\hat{Q}_{23}(x_3, x_4)$ and $\hat{Q}_{24}(x_3, x_4)$. The modified action S'_{mixed} is now given by

$$\begin{aligned} S'_{\mathrm{mixed}} = & N\beta \sum_{x_3,x_4} \sum_{\mu=1}^{2} \sum_{\nu=3}^{4} \Big[\mathrm{Tr}_N\Big(\hat{Q}^\dagger_{\mu\nu}(x_3,x_4)\,\hat{Q}_{\mu\nu}(x_3,x_4)\Big) \\ & - 2\,\mathrm{Re}\,\mathrm{Tr}_N\Big(\hat{Q}^\dagger_{\mu\nu}[t\,\hat{V}_\mu(x_3,x_4)\,\hat{V}_\nu(x_3,x_4) + t^*\,\hat{V}_\nu(x_3,x_4)\,\hat{V}_\mu((x_3,x_4)+a\hat{\nu})]\Big)\Big], \end{aligned} \tag{B.2}$$

which contains a shift in one of its terms. The notation $\hat{\nu}$ represents the unit vector in the ν-direction here as well. If one takes Eq. (B.2), completes the square and integrates out the fields $\hat{Q}_{\mu\nu}(x_3, x_4)$, the action S_{mixed} (4.39) is recovered.

The new action

$$S' = S'_{\mathrm{NC}} + S'_{\mathrm{mixed}} + S_{\mathrm{comm}} \tag{B.3}$$

is linear in the $\hat{V}_\mu(x_3, x_4)$ fields, so the heat bath algorithm Creutz [1980] can now be used.

In practice we update the $\hat{V}_\mu(x_3, x_4)$ matrices by multiplying them with a matrix from one of the $N(N-1)/2$ SU(2) subgroups of SU(N) Cabibbo and Marinari [1982]. This is repeated for all independent SU(2) subgroups.

Multiplying a phase factor through a Metropolis update

With the above steps we are still not scanning the whole space of U(N) matrices. This can be accomplished by multiplying a phase factor to each matrix $\hat{V}_\mu(x_3, x_4)$. To this end we introduce a field $\alpha_\mu(x_3, x_4)$, $\alpha_\mu \in \mathbb{R}$.

Besides multiplying a phase to the $\hat{V}_\mu(x_3, x_4)$ matrices, it turns out that doing the same covariantly with the $\hat{Q}_{\mu\nu}(x_3, x_4)$ matrices increases our acceptance rate. Thus a phase is multiplied to the $\hat{Q}_{\mu\nu}(x_3, x_4)$ entries as well.

To be specific, the phase rotations we used are

$$\begin{cases} \hat{V}_\mu(x_3, x_4) & \to & \mathrm{e}^{\mathrm{i}\alpha_\mu(x_3,x_4)}\, \hat{V}_\mu(x_3, x_4) \\ \hat{Q}_{12}(x_3, x_4) & \to & \mathrm{e}^{\mathrm{i}\alpha_\mu(x_3,x_4)}\, \hat{Q}_{12}(x_3, x_4) \end{cases}, \quad \mu = 1, 2 \tag{B.4}$$

and

$$\begin{cases} \hat{V}_\nu(x_3, x_4) & \to & \mathrm{e}^{\mathrm{i}\alpha_\nu(x_3,x_4)}\, \hat{V}_\nu(x_3, x_4) \\ \hat{Q}_{\mu\nu}(x_3, x_4) & \to & \mathrm{e}^{\mathrm{i}\alpha_\nu(x_3,x_4)}\, \hat{Q}_{\mu\nu}(x_3, x_4) \end{cases}, \quad \mu = 1, 2, \quad \nu = 3, 4. \tag{B.5}$$

In both cases there is no summation over any index.

In our simulations the value of $\alpha_\mu(x_3, x_4)$ was taken randomly (uniformly distributed) from the interval $[0, \frac{2\pi\varepsilon}{N}]$. The parameter ε was tuned such that the acceptance rate was reasonably high, i.e. 60% to 80%. This typically required $\varepsilon \approx 0.1$.

Appendix C

Polarization Tensors and Angular Momentum Operators

Here we want to review the polarization tensors $\hat{Y}^{lm}$ introduced in Section 2.6. This overview is similar to the one in Ref. Medina [2006]. An extensive compendium on these objects can be found in Ref. Varshalovich et al. [1998].

The polarization tensors $\hat{Y}^{lm}$ form a complete orthogonal system, thus we can parametrize the field configurations $\hat{\phi}$ on the fuzzy sphere S_F^2 by expanding as in Eq. (2.112). In essence, the polarization tensors $\hat{Y}^{lm}$ are the matrix analogue to the spherical harmonics $\mathcal{Y}^{lm}(\phi, \vartheta)$.

General properties of the polarization tensors

The spherical harmonics $\mathcal{Y}^{lm}(\phi, \vartheta)$ are characterized by being eigenfunctions to the squared angular momentum operator $\hat{L}^2$, as well as to one of the $\hat{L}_\mu$ operators, usually $\hat{L}_3$.

In our case of a finite representation, the $\hat{L}^2$ operator is given by

$$\hat{L}^2 \cdot = \sum_{\mu=1}^{3} [\hat{L}_\mu, [\hat{L}_\mu, \cdot]]. \tag{C.1}$$

The $\hat{L}_\mu$ operators are $N \times N$ matrices, which represent the three SU(2) angular momentum operators. The $\hat{Y}^{lm}$ are $N \times N$ matrices as well, and form a set $\{\hat{Y}^{lm}\}$, where l runs from 0 to $N-1$ and m from $-l$ to l.

We require the following relations to hold, which strongly resemble rela-

tions known from the spherical harmonics $\mathcal{Y}^{lm}(\phi, \vartheta)$,

$$\hat{L}^2\,\hat{Y}^{lm} = \sum_{\mu=1}^{3}[\hat{L}_\mu,[\hat{L}_\mu,\hat{Y}^{lm}]] = l(l+1)\,\hat{Y}^{lm}, \tag{C.2}$$

$$\hat{L}_3\,\hat{Y}^{lm} = m\,\hat{Y}^{lm}, \tag{C.3}$$

$$(\hat{Y}^{l,m})^\dagger = (-1)^m\,\hat{Y}^{l,-m}. \tag{C.4}$$

The normalization of the polarization tensors in our case is given by

$$\frac{4\pi}{N}\,\mathrm{Tr}_N\Big((\hat{Y}^{lm})^\dagger \hat{Y}^{l'm'}\Big) = \delta_{ll'}\delta_{mm'}. \tag{C.5}$$

Another relation that is very useful when one needs to do actual calculations is the algebra

$$\hat{Y}^{l_1m_1}\hat{Y}^{l_2m_2} = \sqrt{\frac{N}{4\pi}}\sum_{l'=|l_1-l_2|}^{l_1+l_2}\sum_{m'=-l'}^{l'}(-1)^{N+l'-1}\sqrt{(2l_1+1)(2l_2+1)} \tag{C.6}$$
$$\times \left\{ \begin{array}{ccc} l_1 & l_2 & l' \\ (N-1)/2 & (N-1)/2 & (N-1)/2 \end{array} \right\} C^{l'm'}_{l_1m_1l_2m_2}\,\hat{Y}^{l'm'}.$$

The symbol $C^{l'm'}_{l_1m_1l_2m_2}$ denotes the Clebsch-Gordon coefficients. The expression in the curly brackets represents the Wigner 3j symbol Messiah [2000], Lai and Chiu [2000].

Explicit construction of the polarization tensors

Here we will show how to explicitly construct the $\hat{Y}^{lm}$ tensors in the $l = 0$ and $l = 1$ case. The matrices $\hat{Y}^{lm}$ can be constructed from polynomials of order l of the operators $\hat{L}_\mu$. This leads e.g. to $\hat{Y}^{00} \propto \mathbb{1}_N$. The normalization (C.5) implies $\frac{4\pi}{N}\,\mathrm{Tr}_N\Big((\hat{Y}^{00})^\dagger\,\hat{Y}^{00}\Big) = 1$. Combining these two requirements yields

$$\hat{Y}^{00} = \frac{1}{\sqrt{4\pi}}\,\mathbb{1}_N. \tag{C.7}$$

Of course, other normalizations are possible. An example using a different normalization is Ref. Varshalovich et al. [1998].

In the $N > 1$ case we have $\hat{Y}^{1,0} \propto \hat{L}_3$, $\hat{Y}^{1,1} \propto \hat{L}_+ = \hat{L}_1 + \mathrm{i}\,\hat{L}_2$ and $\hat{Y}^{1,-1} \propto \hat{L}_- = \hat{L}_1 - \mathrm{i}\,\hat{L}_2$. The factors yielding the correct normalization can be found from

$$\mathrm{Tr}_N\Big(\hat{L}_3^\dagger\,\hat{L}_3\Big) = \frac{N\,(N-1)\,(N+1)}{12} \quad \text{and} \tag{C.8}$$

$$\mathrm{Tr}_N\Big(\hat{L}_+^\dagger\,\hat{L}_+\Big) = \mathrm{Tr}_N\Big(\hat{L}_-^\dagger\,\hat{L}_-\Big) = 2\,\mathrm{Tr}_N\Big(\hat{L}_3^\dagger\,\hat{L}_3\Big). \tag{C.9}$$

The above expressions still leave us with the freedom of an arbitrary phase factor in the $\hat{Y}^{1m}$ construction. This phase factor is fixed such that the constraint (C.4) is fulfilled. This train of thought finally leads to an explicit form of the $\hat{Y}^{1m}$ matrices,

$$\begin{aligned}
\hat{Y}^{1,1} &= \sqrt{\frac{3}{2\pi}} \frac{\mathrm{i}}{\sqrt{(N-1)(N+1)}} \hat{L}_+, \\
\hat{Y}^{1,0} &= \sqrt{\frac{3}{\pi}} \frac{1}{\sqrt{(N-1)(N+1)}} \hat{L}_3, \\
\hat{Y}^{1,-1} &= \sqrt{\frac{3}{2\pi}} \frac{-\mathrm{i}}{\sqrt{(N-1)(N+1)}} \hat{L}_-.
\end{aligned} \tag{C.10}$$

Explicit angular momentum operators and the Casimir operator

Here we briefly state the explicit matrix formulation of the angular momentum operators $\hat{L}_3$ and $\hat{L}_\pm$, since they show up frequently in this work,

$$\begin{aligned}
(\hat{L}_3)_{ij} &= \begin{cases} \frac{1}{2}(N+1-2i) & \text{if } i=j \\ 0 & \text{otherwise} \end{cases}, \\
(\hat{L}_+)_{ij} &= \begin{cases} \sqrt{i(N-i)} & \text{if } i+1=j \\ 0 & \text{otherwise} \end{cases}, \\
(\hat{L}_-)_{ij} &= \begin{cases} \sqrt{j(N-j)} & \text{if } i-1=j \\ 0 & \text{otherwise} \end{cases}.
\end{aligned} \tag{C.11}$$

From this $\hat{L}_1$ and $\hat{L}_2$ are easily obtained. As required, these matrices fulfill

$$\begin{aligned}
(\hat{L}_+)^\dagger &= \hat{L}_-, \\
[\hat{L}_3, \hat{L}_+] &= \hat{L}_+, \\
[\hat{L}_3, \hat{L}_-] &= -\hat{L}_-, \\
[\hat{L}_+, \hat{L}_-] &= 2\hat{L}_3.
\end{aligned} \tag{C.12}$$

Finally, the Casimir operator for the SU(2) group is given by

$$\hat{C}^2_{\mathrm{SU}(2)} = \sum_{\mu=1}^{3} \hat{L}_\mu \hat{L}_\mu = \frac{1}{4}(N^2-1)\,\mathbb{1}_N. \tag{C.13}$$

Bibliography

Euclid. *The Thirteen Books of Euclids Elements, Vol. I-III.* Dover, New York, 1956.

B. Riemann. Über die hypothesen, welche der geometrie zu grunde liegen. *Abhandlungen der Königlichen Gesellschaft der Wissenschaften zu Göttingen*, XIII, 1854.

D. J. Struik. *A Concise History of Mathematics.* Dover, New York, 1987.

A. Einstein. On the general theory of relativity. *Sitzungsber. Preuß. Akad. Wiss. Berlin (Math. Phys.)*, page 778, 1915.

H. S. Snyder. Quantized space-time. *Phys. Rev.*, 71:38, 1947a.

H. S. Snyder. The electromagnetic field in quantized space-time. *Phys. Rev.*, 72:68, 1947b.

C. N. Yang. On quantized space-time. *Phys. Rev.*, 72:874, 1947.

A. Connes. *Noncommutative Geometry.* Academic Press, San Diego, 1994.

G. Veneziano. A stringy nature needs just two constants. *Europhys. Lett.*, 2: 199, 1986.

D. J Gross and P. F. Mende. String theory beyond the planck scale. *Nucl. Phys.*, B303:407, 1988.

D. V. Amati, M. Ciafaloni, and G. Veneziano. Can spacetime be probed below the string size? *Phys. Lett.*, B216:4, 1989.

A. Connes. Noncommutative differential geometry. *Inst. Hautes Études Sci. Publ. Math.*, 62:257, 1986.

A. H. Chamsedinne, G. Felder, and J. Fröhlich. Gravity in noncommutative geometry. *Commun. Math. Phys.*, 155:205, 1993.

G. Landi and C. Rovelli. General relativity in terms of dirac eigenvalues. *Phys. Rev. Lett.*, 78:3051, 1997.

J. L. F. Barbón. Introduction to noncommutative field theory. *Trieste 2001, Particle physics*, page 185, 2001. ICTP Summer School in Particle Physics, Trieste, Italy.

M. R. Douglas and N. A. Nekrasov. Noncommutative field theory. *Rev. Mod. Phys.*, 73:977, 2001.

R. J. Szabo. Quantum field theory on noncommutative spaces. *Phys. Rept.*, 378:207, 2003.

A. Connes and M. Rieffel. Yang–mills for noncommutative two–tori. *Contemp. Math. Oper. Algebra. Math. Phys.*, 62:237, 1987.

J. Madore. *An Introduction to Noncommutative Geometry and its Physical Applications.* Cambridge University Press, Cambridge, 1999.

S. Minwalla, M. van Raamsdonk, and N. Seiberg. Noncommutative perturbative dynamics. *JHEP*, 02:020, 2000.

T. Filk. Divergencies in a field theory on quantum space. *Phys. Lett.*, B376: 53, 1996.

G. Landi. *An Introduction to Noncommutative Spaces and their Geometries.* Springer Verlag, Berlin Heidelberg, 1997.

J. M. Gracia-Bondía, J. C. Várilly, and H. Figueroa. *Elements of Noncommutative Geometry.* Birkhäuser, Boston, 2000.

J. Ambjørn, Y. M. Makeenko, J. Nishimura, and R. J. Szabo. Lattice gauge fields and discrete noncommutative yang-mills theory. *JHEP*, 05: 023, 2000a.

J. Ambjørn, Y. M. Makeenko, J. Nishimura, and R. J. Szabo. Finite n matrix models of noncommutative gauge theory. *JHEP*, 11:029, 1999.

P. van Baal and B. van Geemen. A simple construction of twist eating solutions. *J. Math. Phys.*, 27:455, 1986.

J. Madore. The fuzzy sphere. *Class. Quant. Grav.*, 9:69, 1992.

A. P. Balachandran, S. Kürkçüoğlu, and S. Vaidya. Lectures on fuzzy and fuzzy susy physics. 2005.

V.P. Nair. Noncommutative mechanics, landau levels, twistors and yang-mills amplitudes. 2005.

A. H. Chamsedinne and A. Connes. The spectral action principle. *Commun. Math. Phys.*, 186:731, 1997.

G. Amelino-Camelia, J. Ellis, N. E. Mavromatos, D. V. Nanopoulos, and S. Sarkar. Potential sensitivity of gamma-ray burster observations to wave dispersion in vacuo. *Nature*, 393:763, 1998.

J. R. Ellis, N. E. Mavromatos, D. V. Nanopoulos, A. S. Sakharov, and E. K. G. Sarkisyan. Robust limits on lorentz violation from gamma-ray bursts. *Astropart. Phys.*, 25:402, 2006.

S.E. Boggs, C.B. Wunderer, K. Hurley, and W. Coburn. Testing lorentz non-invariance with grb021206. *Astrophys. J.*, 611:L77, 2004.

K. Shinozaki. Agasa results. *Nucl. Phys. Proc. Suppl.*, 151:3, 2006.

F. W. Stecker. Cosmic physics: The high energy frontier. *J. Phys.*, G29:R47, 2003.

K. Greisen. End to the cosmic ray spectrum? *Phys. Rev. Lett.*, 16:748, 1966.

G. Zatsepin and V. Kuzmin. Upper limit of the spectrum of cosmic rays. *JETP Lett.*, 4:78, 1966.

R. J. Protheroe and H. Meyer. An infrared background tev gamma ray crisis? *Phys. Lett.*, B493:1, 2000.

A. J. Nikishov. Pogloshchenie fotonov bolshikh energiy vo vselennoy. *Zh. Eksperim. i Teor. Fiz.*, 41:549, 1961.

P. Goldreich and P. Morrison. O pogloshchenii γ-luchey v mezhgalaktich-eskom prostranstve. *Zh. Eksperim. i Teor. Fiz.*, 45:344, 1963.

F. W. Stecker and O. C. de Jager. New upper limits on intergalactic infrared radiation from high-energy astrophysics. *Astrophys. J.*, 415:L71, 1993.

S. R. Coleman and S. L. Glashow. High-energy tests of lorentz invariance. *Phys. Rev.*, D59:116008, 1999.

G. Amelino-Camelia and T. Piran. Planck-scale deformation of lorentz symmetry as a solution to the uhecr and the tev-gamma paradoxes. *Phys. Rev.*, D64:036005, 2001.

R. Aloisio, P. Blasi, A. Galante, and A. F. Grillo. Planck scale kinematics and the pierre auger observatory. *Lect. Notes Phys.*, 669:1, 2005.

M. Hayakawa. Perturbative analysis on infrared and ultraviolet aspects of noncommutative qed on r^4. *Phys. Lett.*, B478:394, 2000.

J. L. Hewett, Frank J. Petriello, and T.G. Rizzo. Signals for non-commutative interactions at linear colliders. *Phys. Rev.*, D64:075012, 2001.

P. Mathews. Compton scattering in noncommutative space-time at the nlc. *Phys. Rev.*, D63:075007, 2001.

M. Chaichian, M. M. Sheikh-Jabbari, and A. Tureanu. Hydrogen atom spectrum and the lamb shift in noncommutative qed. *Phys. Rev. Lett.*, 86: 2716, 2001.

H. Falomir, J. Gamboa, M. Loewe, F. Mendez, and J. C. Rojas. Testing spatial noncommutativity via the aharonov-bohm effect. *Phys. Rev.*, D66: 045018, 2002.

S. M. Carroll, J. A. Harvey, V. A. Kostelecky, C. D. Lane, and T. Okamoto. Noncommutative field theory and lorentz violation. *Phys. Rev. Lett.*, 87: 141601, 2001.

J. D. Prestage, J. J. Bollinger, W. M. Itano, and D. J. Wineland. Limits for spatial anisotrophy by use of nuclear spin polarized be-9+ ions. *Phys. Rev. Lett.*, 54:2387, 1985.

S. K. Lamoreaux, J. P. Jacobs, B. R. Heckel, F. J. Raab, and E. N. Fortson. New limits on spatial anisotrophy from optically pumped he-201 and hg-199. *Phys. Rev. Lett.*, 57:3125, 1986.

A. Alboteanu, T. Ohl, and R. Rückl. Collider tests of the non-commutative standard model. *PoS*, HEP2005:322, 2006.

K. Osterwalder and R. Schrader. Feynman-kac formula for euclidean fermi and bose fields. *Phys. Rev. Lett.*, 29:1423, 1972.

S. S. Gubser and S. L. Sondhi. Phase structure of non-commutative scalar field theories. *Nucl. Phys.*, B605:395, 2001.

S. A. Brazovskii. Phase transition of an isotropic system to a nonuniform state. *Zh. Eksp. Teor. Fiz*, 68:175, 1975.

F. Hofheinz. Field theory on a non-commutative plane: A non-perturbative study. *Fortsch. Phys.*, 52:391, 2004. Ph.D. thesis, Humboldt University, Berlin.

W. Bietenholz, F. Hofheinz, and J. Nishimura. Phase diagram and dispersion relation of the non-commutative $\lambda\phi^4$ model in d = 3. *JHEP*, 06:042, 2004a.

J. Ambjørn and S. Catterall. Stripes from (noncommutative) stars. *Phys. Lett.*, B549:253, 2002.

N. D. Mermin and H. Wagner. Absence of ferromagnetism or antiferromagnetism in one-dimensional or two-dimensional isotropic heisenberg models. *Phys. Rev. Lett.*, 17:1133, 1966.

P. C. Hohenberg. Existence of long-range order in one and two dimensions. *Phys. Rev.*, 158:383, 1967.

S. R. Coleman. There are no goldstone bosons in two-dimensions. *Commun. Math. Phys.*, 31:259, 1973.

E. Brezin, C. Itzykson, G. Parisi, and J. B. Zuber. Planar diagrams. *Commun. Math. Phys.*, 59:35, 1978.

F. Garcia Flores, D. O'Connor, and X. Martin. Simulating the scalar field on the fuzzy sphere. *PoS*, LAT2005:262, 2006.

X. Martin. A matrix phase for the ϕ^4 scalar field on the fuzzy sphere. *JHEP*, 04:077, 2004.

M. Panero. Numerical simulations of a non-commutative theory: The scalar model on the fuzzy sphere. 2006.

B. Jurco, L. Möller, S. Schraml, P. Schupp, and J. Wess. Construction of non-abelian gauge theories on noncommutative spaces. *Eur. Phys. J.*, C21: 383, 2001.

C. E. Carlson, C. D. Carone, and R. F. Lebed. Bounding noncommutative qcd. *Phys. Lett.*, B518:201, 2001.

X. Calmet, B. Jurco, P. Schupp, J. Wess, and M. Wohlgenannt. Noncommutative standard model. *Paris 2002, Physical and mathematical aspects of symmetries*, page 477, 2002. 24th International Colloquium on Group Theoretical Methods in Physics, Paris, France.

C. P. Martín and D. Sanchez-Ruiz. The one-loop uv divergent structure of u(1) yang-mills theory on noncommutative r^4. *Phys. Rev. Lett.*, 83:476, 1999.

A. H. Fatollahi and A. Jafari. On the bound states of photons in noncommutative quantum electrodynamics. *Eur. Phys. J.*, 3:2, 2003.

T. Eguchi and H. Kawai. Reduction of dynamical degrees of freedom in the large-n gauge theory. *Phys. Rev. Lett.*, 48:1063, 1982.

G. Bhanot, U. M. Heller, and H. Neuberger. The quenched eguchi-kawai model. *Phys. Lett.*, B113:47, 1982.

A. González-Arroyo and M. Okawa. A twisted model for large n lattice gauge theories. *Phys. Lett.*, B120:174, 1983.

A. González-Arroyo and C. P. Korthals Altes. Reduced model for large n continuum field theories. *Phys. Lett.*, B131:396, 1983.

D. J Gross and E. Witten. Possible third-order phase transition in the large-n lattice gauge theory. *Phys. Rev.*, D21:446, 1980.

H. Aoki, N. Ishibashi, S. Iso, H. Kawai, Y. Kitazawa, and Tsukasa T. Noncommutative yang-mills in iib matrix model. *Nucl. Phys.*, B565:176, 2000.

J. Ambjørn, Y. M. Makeenko, J. Nishimura, and R. J. Szabo. Nonperturbative dynamics of non-commutative gauge theory. *Phys. Lett.*, B480:399, 2000b.

D. Bahns, S. Doplicher, K. Fredenhagen, and G. Piacitelli. On the unitarity problem in space/time noncommutative theories. *Phys. Lett.*, B533:178, 2002.

W. Bietenholz, F. Hofheinz, and J. Nishimura. On the relation between noncommutative field theories at $\theta = \infty$ and large n matrix field theories. *JHEP*, 05:047, 2004b.

W. Bietenholz, F. Hofheinz, and J. Nishimura. A non-perturbative study of gauge theory on a non-commutative plane. *JHEP*, 09:009, 2002.

W. Bietenholz, J. Nishimura, Y. Susaki, and J. Volkholz. A non-perturbative study of 4d u(1) non-commutative gauge theory: The fate of one-loop instability. *JHEP*, 10:042, 2006.

M. Creutz. Phase transition in su(5) lattice gauge theory. *Phys. Rev. Lett.*, 46:1441, 1981.

N. Seiberg and E. Witten. String theory and noncommutative geometry. *JHEP*, 09:032, 1999.

H. Kawai, S. Kawamoto, T. Kuroki, T. Matsuo, and S. Shinohara. Mean field approximation of iib matrix model and emergence of four dimensional space-time. *Nucl. Phys.*, B647:153, 2002.

H. Aoki, S. Iso, H. Kawai, Y. Kitazawa, and T. Tada. Space-time structures from iib matrix model. *Prog. Theor. Phys.*, 99:713, 1998.

M. van Raamsdonk. The meaning of infrared singularities in noncommutative gauge theories. *JHEP*, 11:006, 2001.

K. Landsteiner, E. Lopez, and M. H. G. Tytgat. Excitations in hot noncommutative theories. *JHEP*, 09:027, 2000.

C. P. Martín and F. Ruiz Ruiz. Paramagnetic dominance, the sign of the beta function and uv/ir mixing in non-commutative u(1). *Nucl. Phys.*, B597:197, 2001.

F. Ruiz Ruiz. Gauge-fixing independence of ir divergences in non- commutative u(1), perturbative tachyonic instabilities and supersymmetry. *Phys. Lett.*, B502:274, 2001.

K. Landsteiner, E. Lopez, and M. H. G. Tytgat. Instability of noncommutative sym theories at finite temperature. *JHEP*, 06:055, 2001.

A. Bassetto, L. Griguolo, G. Nardelli, and F. Vian. On the unitarity of quantum gauge theories on noncommutative spaces. *JHEP*, 07:008, 2001.

H. Liu and J. Michelson. *-trek: The one-loop n = 4 noncommutative sym action. *Nucl. Phys.*, B614:279, 2001.

A. Armoni and E. Lopez. Uv/ir mixing via closed strings and tachyonic instabilities. *Nucl. Phys.*, B632:240, 2002.

N. Ishibashi, S. Iso, H. Kawai, and Y. Kitazawa. Wilson loops in noncommutative yang-mills. *Nucl. Phys.*, B573:573, 2000.

A. Matusis, L. Susskind, and N. Toumbas. The ir/uv connection in the non-commutative gauge theories. *JHEP*, 12:002, 2000.

P. Di Vecchia and S. Ferrara. Classical solutions in two-dimensional supersymmetric field theories. *Nucl. Phys.*, B130:93, 1977.

W. Bietenholz. Exact supersymmetry on the lattice. *Mod. Phys. Lett.*, A14: 51, 1999.

T. Aoyama and Y. Kikukawa. Overlap formula for the chiral multiplet. *Phys. Rev.*, D59:054507, 1999.

S. Catterall and S. Karamov. Exact lattice supersymmetry: The two-dimensional $n = 2$ wess-zumino model. *Phys. Rev.*, D65:094501, 2002.

D.B. Kaplan, E. Katz, and M. Unsal. Supersymmetry on a spatial lattice. *JHEP*, 0305:037, 2003.

M. Harada and S. Pinsky. $\mathcal{N} = (1, 1)$ superyang-mills on a (2+1)-dimensional transverse lattice with one exact supersymmetry. *Phys. Lett.*, B567:277, 2003.

F. Sugino. Superyang-mills theories on the two-dimensional lattice with exact supersymmetry. *JHEP*, 0403:067, 2004.

S. Catterall and S. Ghadab. Lattice sigma models with exact supersymmetry. *JHEP*, 0405:044, 2004.

M. Bonini and A. Feo. Wess-zumino model with exact supersymmetry on the lattice. *JHEP*, 09:011, 2004.

A. D'Adda, I. Kanamori, N. Kawamoto, and K. Nagata. Exact extended supersymmetry on a lattice: Twisted n = 2 super yang-mills in two dimensions. *Phys. Lett.*, B633:645, 2006.

D. Karabali and V. P. Nair. Quantum hall effect in higher dimensions, matrix models and fuzzy geometry. *J. Phys.*, A39:12735, 2006.

K. Fabricius and O. Haan. Heat bath method for the twisted eguchi-kawai model. *Phys. Lett.*, 143B:459, 1984.

N. Cabibbo and E. Marinari. A new method for updating su(n) matrices in computer simulations of gauge theories. *Phys. Lett.*, 119B:387, 1982.

M. Creutz. Monte carlo study of quantized su(2) gauge theory. *Phys. Rev.*, D21:2308, 1980.

J. Medina. Fuzzy scalar field theories: Numerical and analytical investigations. *Ph.D. Thesis, CINVESTAV-IPN, México D.F., Mexico*, 2006.

D. A. Varshalovich, A. N. Moskalev, and V. K. Khersonky. *Quantum Theory of Angular Momentum: Irreducible Tensors, Spherical Harmonics, Vector Coupling Coefficients, 3nj Symbols*. World Scientific, Singapore, 1998.

A. Messiah. *Quantum Mechanics*. Dover, New York, 2000.

S. T. Lai and Y. N. Chiu. Exact computation of the 3j and 6j symbols. *Comput. Phys. Comm.*, page 350, 2000.

Acknowledgement

There were many people involved in working on the projects of this thesis, but first and foremost I would like to thank Prof. Michael Müller-Preußker, the chair of our department, and Wolfgang Bietenholz, my Ph.D. supervisor, for shedding light onto my ignorance. The fruitful discussions and their illuminating insights and endless patience proved invaluable to me. I would also like to acknowledge my collaborators, in particular Antonio Bigarini, Frank Hofheinz, Jun Nishimura and Yoshiaki Susaki, who worked with us on the NC $\lambda\phi^4$ and the NC U(1) model, and Denjoe O'Connor and Marco Panero, who are our collaborators on the fuzzy sphere SUSY model.

I am also deeply indebted to "Deutsche Forschungsgemeinschaft" (DFG), who funded my work under the project Bi 793/2-1 "Simulation der nicht kommutativen Feldtheorie". The machines and technical advise were provided by "Norddeutscher Verbund für Hoch- und Höchstleistungsrechnen" (HLRN). Especially Hinnerk Stüben provided valuable advise and assistance when dealing with these machines.

I would also like to thank our whole phenomenology department at the physics institute at Humboldt-Universität, in particular I would like to mention Sylvia Richter, Stanislav Shcheredin and André Sternbeck for providing a pleasant working environment and all necessary facilities.

Selbständigkeitserklärung

Hiermit erkläre ich, die vorliegende Arbeit selbständig, ohne fremde Hilfe und Hilfsmittel und nur mit der angegebenen Literatur verfasst zu haben.

Jan Volkholz